Title

Gas phase formation of cyclopentanaphthalene (benzindene) isomers via reactions of 5- and 6-indenyl radicals with vinylacetylene

Journal
Physical Chemistry Chemical Physics, 22(39)

ISSN
0956-5000

Authors
Zhao, Long
Kaiser, Ralf I
Lu, Wenchao
et al.

Publication Date
2020-10-15

DOI
10.1039/d0cp03846f

Peer reviewed

Gas Phase Formation of Cyclopentanaphthalene (Benzindene) Isomers via Reactions of 5- and 6-Indenyl Radicals with Vinylacetylene

Long Zhao[1], Ralf I. Kaiser[1*]
[1] Department of Chemistry, University of Hawaii at Manoa, Honolulu, Hawaii, 96822 (USA)

Wenchao Lu[2], Oleg Kostko[2], Musahid Ahmed[2*]
[2] Chemical Sciences Division, Lawrence Berkeley National Laboratory, Berkeley, CA 94720 (USA)

Mikhail M. Evseev,[3] Eugene K. Bashkirov[3]
[3]Samara National Research University, Samara 443086, Russian Federation

Artem D. Oleinikov[3,4], Valeriy N. Azyazov[3,4]
[3]Samara National Research University, Samara 443086, Russian Federation
[4]Lebedev Physical Institute, Samara 443011

Alexander M. Mebel[3,5]* A. Hasan Howlader,[5] Stanislaw F. Wnuk[5]
[3]Samara National Research University, Samara 443086
(Russian Federation)
[5]Department of Chemistry and Biochemistry, Florida International University, Miami, FL 33199 (USA)

[*] Corresponding author:
Ralf I. Kaiser <ralfk@hawaii.edu>
Musahid Ahmed <mahmed@lbl.gov>
Alexander M. Mebel <mebela@fiu.edu>

Abstract:

The tricyclic polycyclic aromatic hydrocarbons (PAHs) 3*H*-cyclopenta[*a*]naphthalene ($C_{13}H_{10}$), 1*H*-cyclopenta[*b*]naphthalene ($C_{13}H_{10}$) and 1*H*-cyclopenta[*a*]naphthalene ($C_{13}H_{10}$) along with their indene-based bicyclic isomers (*E*)-5-(but-1-en-3-yn-1-yl)-1*H*-indene, (*E*)-6-(but-1-en-3-yn-1-yl)-1*H*-indene, 5-(but-3-ene-1-yn-1-yl)-1*H*-in-dene, and 6-(but-3-ene-1-yn-1-yl)-1*H*-indene were formed via a "directed synthesis" in a high-temperature chemical micro reactor at the temperature of 1300 ± 10 K through the reactions of the 5- and 6-indenyl radicals ($C_9H_7^{\bullet}$) with vinylacetylene (C_4H_4). The isomer distributions were probed utilizing tunable vacuum ultraviolet light by recording the photoionization efficiency curves at mass-to-charge of *m/z* = 166 ($C_{13}H_{10}$) and 167 ($^{13}CC_{12}H_{10}$) of the products in a supersonic molecular beam. The underlying reaction mechanisms involve the initial formation of van-der-Waals complexes followed by addition of the 5- and 6-indenyl radicals to vinylacetylene via submerged barriers, followed by isomerization (hydrogen shifts, ring closures), and termination via atomic hydrogen elimination accompanied by aromatization. All the barriers involved in the formation of 3*H*-cyclopenta[*a*]naphthalene, 1*H*-cyclopenta[*b*]naphthalene and 1*H*-cyclopenta[*a*]naphthalene are submerged with respect to the reactants indicating that the mechanisms are in fact barrierless, potentially forming PAHs via the hydrogen abstraction – vinylacetylene addition (HAVA) pathway in the cold molecular clouds such as Taurus Molecular Cloud-1 (TMC-1) at temperatures as low as 10 K.

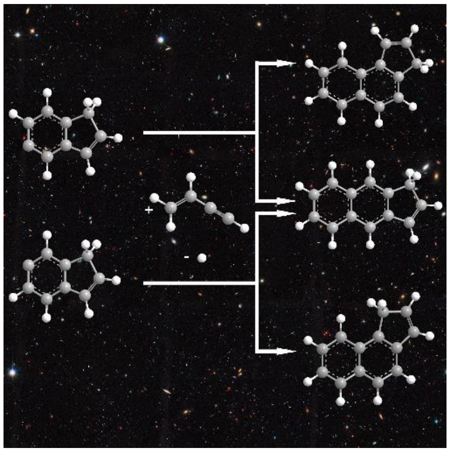

The reaction of indenyl radicals with vinylacetylene leads to cyclopentanaphthalene at low temperature.

1. INTRODUCTION

Polycyclic aromatic hydrocarbons (PAHs) carrying five membered rings such as fluorene ($C_{13}H_{10}$) and cyclopentanaphthalenes ($C_{13}H_{10}$) represent fundamental molecular building blocks of non-planar PAHs like corannulene ($C_{20}H_{10}$) along with fullerenes (C_{60}, C_{70}) (Scheme 1).[1-5] These species necessitate five-membered rings in the carbon backbone of the PAH to 'curve' planar PAHs out of the plane. An intimate knowledge of the elementary mechanisms forming PAHs carrying five-membered ring(s) is therefore critical in aiding our understanding of the early stage chemistry in combustion systems as to how precursor PAHs lead to three dimensional (bowl-shaped) carbonaceous structures and ultimately soot particles. However, the elementary steps, chemical dynamics, and reaction mechanisms to form PAHs carrying five-membered ring(s) on the molecular level are largely elusive as detailed synthetic routes have not been investigated comprehensively to date. The presence of five-membered rings in PAHs is also important from the viewpoint of molecular mass growth processes and ring expansion pathways.[6] In combustion flames, ubiquitous open shell reactants such as atomic hydrogen can easily abstract a hydrogen atom from the CH_2 moiety of, e.g. the five-membered ring of indene resulting in the 1-indenyl radical. The radical-radical reaction with a methyl radical has been revealed to lead via ring expansion from a five- to a six-membered ring thus effectively converting molecular building blocks relevant to the formation of three-dimensional carbonaceous nanostructures to those of critical importance to graphene-type two-dimensional nano-sheets at elevated temperatures.[6]

Previously, the simplest prototype of a PAH carrying a single six and five membered ring – indene (C_9H_8) (Scheme 1) has been synthesized under single collision conditions exploiting a crossed molecular beams machine via the reactions of phenyl radicals ($C_6H_5^\bullet$) with allene (H_2CCCH_2) and methylacetylene (CH_3CCH) along with their (partially) deuterated counterparts (Scheme 2).[7-11] After overcoming barriers to addition of the phenyl radical to the π-electron density of methylacetylene or allene of 1 to 26 kJ mol^{-1}, the initial collision complexes isomerize predominantly via hydrogen shifts and ring closures followed ultimately by atomic hydrogen loss accompanied by aromatization and indene formation (Scheme 2).[12] These findings were confirmed in recent studies exploiting a micro reactor coupled with vacuum ultraviolet (VUV) photoionization of the neutral reaction products leading to the isomer-selective identification of indene along with its phenylallene, 1-phenyl-1-propyne, and 3-phenyl-1-propyne isomers.[10]

Alternatively, chemical micro reactor studies revealed that indene can also be synthesized at elevated temperatures of 600 ± 100 K exclusively through the reaction of the resonantly stabilized, aromatic benzyl radical ($C_7H_7^{\bullet}$) with acetylene (C_2H_2) after overcoming a significant barrier to addition of 51 kJ mol^{-1} followed by ring closure and hydrogen atom elimination, [13] i.e. a derivative of the Hydrogen-Abstraction-aCetylene-Addition (HACA) mechanism. These C6-C3 and C7-C2 pathways effectively lead to ring annulation to an existing C6-benzene-type ring.[12]

HACA is also implicated in the reaction of the 2-naphthyl radical ($C_{10}H_7^{\bullet}$) with allene (H_2CCCH_2) and methylacetylene (CH_3CCH) leading to 3*H*-cyclopenta[*a*]naphthalene ($C_{13}H_{10}$) and 1*H*-cyclopenta[*b*]naphthalene ($C_{13}H_{10}$) (Scheme 2).[14] However, 1*H*-cyclopenta [*a*]naphthalene was not reported in the study due to low yields. Previous experimental and theoretical investigations also suggested that 3*H*-cyclopenta[*a*]naphthalene can be synthesized from 1-methylnaphthalene ($C_{11}H_{10}$) via hydrogen abstraction from the methyl group followed by acetylene addition reaction, isomerization, and hydrogen elimination (HACA).[2, 15-25] However, these molecular mass growth processes operate only at elevated temperatures as found in combustion systems and in circumstellar envelopes of Asymptotic Giant Branch (AGB) carbon stars close to the photosphere; entrance barriers to addition of 8 to 11 kJ mol^{-1} would effectively block these reactions at low temperatures such as in molecular clouds, e.g., Taurus Molecular Cloud -1 (TMC-1) (10 K), and in hydrocarbon rich atmospheres of planets and their moons like Saturn's satellite Titan (70 – 200 K).[26] Therefore, as of now, ring annulation sequences resulting in an efficient addition of a five-membered ring to an existing benzene moiety have only been exposed to operate at high temperatures; pathways leading to molecular mass growth processes involving five-membered rings at ultralow temperatures are still elusive.

The elucidation of the hydrogen abstraction – vinylacetylene addition (HAVA) reaction mechanisms has opened up barrier-less low temperature pathways to form PAHs even at temperatures as low at 10 K.[27] In the prototype phenyl ($C_6H_5^{\bullet}$) – vinylacetylene (C_4H_4) system, Parker et al. and Zhao et al. provided compelling evidence via crossed molecular beams and chemical micro reactor studies coupled with electronic structure calculations on the formation of naphthalene ($C_{10}H_8$) plus atomic hydrogen.[28, 29] The reaction is initiated by the formation of a van-der-Waals complex followed by addition of the phenyl radical to the CH_2 moiety of the vinylacetylene reactant leading to a resonantly stabilized radical intermediate ($C_{14}H_{11}$). Although a barrier to addition of 9 kJ mol^{-1} does exist, the transition state is located below the energy of the separated reactants, and hence the barrier to addition is 'submerged'. The existence of submerged barriers is also important in the formation of methyl-substituted naphthalenes such as 1-methylnaphthalene ($C_{11}H_{10}$) and 2-methylnaphthalene ($C_{11}H_{10}$) as demonstrated through the reactions of *m*- and *p*-tolyl radicals ($C_7H_7^{\bullet}$) with vinylacetylene.[30]

Considering that the HAVA mechanism operates at ultralow temperatures and the fact that substituted phenyl-type radicals such as tolyl also react with vinylacetylene barrierlessly leading to ring annulation of a benzene ring, we explore to what extent the reactions of the 5- and 6-indenyl radicals ($C_9H_7^{\bullet}$) with vinylacetylene lead to effective (barrierless) ring annulation of a benzene ring ultimately leading to prototype tricyclic polycyclic aromatic hydrocarbons (PAHs) carrying two six membered and one five membered ring ($C_{13}H_{10}$) in the gas phase (Scheme 2). The 5- and 6-indenyl radicals ($C_9H_7^{\bullet}$) can be rationalized as 'disubstituted' phenyl radicals, in which the five-membered ring acts as a spectator moiety leading to PAH growth in low temperature environments from aromatic radical reactions with key hydrocarbon molecules (vinylacetylene).[31]

2. EXPERIMENTAL

The experiments were carried out at the Advanced Light Source (ALS), Lawrence Berkeley National Laboratory. A detailed description of the experimental set-up was provided previously.[6, 10, 13, 27, 32-36] Briefly, by studying the reactions of the 5- and 6-indenyl radicals ($C_9H_7^{\bullet}$) with vinylacetylene (C_4H_4; Applied Gas; 5% C_4H_4 seeded in 95 % He) under simulated combustion conditions, we deliver experimental and computational evidence of the molecular growth processes to benzindene ($C_{13}H_{10}$) isomers. In separate experiments, a continuous beam of 5- and 6-indenyl radicals ($C_9H_7^{\bullet}$) was prepared *in situ* through the pyrolysis of the corresponding 5- and 6-iodoindene (C_9H_7I) precursors. The in-house synthesis of both iodoindene precursors is described in the Supplementary Information.[37] In separate experiments, the precursors were seeded in the vinylacetylene/helium carrier gas at an inlet pressure of 300 ± 5 Torr. Control experiments were also performed by just replacing the vinylacetylene/helium gases with pure helium while all the other settings (temperature, pressure) remained identical. The gas mixture was expanded through a 0.1 mm diameter orifice into the high-temperature pyrolytic reactor, i.e.

a resistively heated silicon carbide (SiC) tube with 1.0 mm inner diameter and 20 mm heating length. The SiC tube was held at 1300 ± 10 K as monitored by a Type-C thermocouple attached to the center of the heating area. The residence time in the reactor tube under our experimental condition are up to a few tens of μs,[38, 39] with the number of collisions up to a few hundreds.[39] The products formed in the reactor were expanded supersonically, passed through a 2 mm diameter skimmer located 10 mm downstream of the pyrolytic reactor, and entered into the photoionization chamber housing the Wiley–McLaren reflectron time-of-flight mass spectrometer (ReTOF-MS), which was kept at 10^{-6} Torr during the experiment. The quasi-continuous tunable synchrotron VUV light from ALS intersected the neutral molecular beam perpendicularly in the extraction region of the ReTOF-MS. VUV single photon ionization is essentially a fragment-free ionization technique, which would preserve the original information of the target molecules.[40] The ions of the photoionized molecules were accelerated to the field-free TOF region and then collected by a microchannel plate (MCP) detector in the ReTOF mode. The time-dependent ion signal was amplified by a fast preamplifier and convoluted by a multichannel digitizer card.

Photoionization efficiency (PIE) curves, which report the ion count as a function of photon energy with a step interval of 0.05 eV at a well-defined mass-to-charge ratio (*m/z*), were produced by integrating the signal recorded at the specific *m/z* for the species of interest from 7.30 eV to 10.00 eV and normalized by photon fluxes. Experimentally measured PIE curves are usually used for species identification by fitting the calibration PIE curve(s) of the species of interest linearly. To fit the PIE curve and identify the target products lied at *m/z* = 166 ($C_{13}H_{10}$), the calibration curves of the individual isomers were newly obtained at the photoionization energy from 7.3 to 10.0 eV with the 0.05 eV step interval, as presented in the Supporting Information (Figure S1). Among these isomers, 1*H*-cyclopenta[*a*]naphthalene **(P3)** and the branched molecules [(*E*)-5-(but-1-en-3-yn-1-yl)-1*H*-indene **(P4)**, 5-(but-3-ene-1-yn-1-yl)-1*H*-indene **(P5)**, (*E*)-6-(but-1-en-3-yn-1-yl)-1*H*-indene **(P6)** and 6-(but-3-ene-1-yn-1-yl)-1*H*-indene **(P7)**] were synthesized for the current work,[37] while the PIE calibration curves for 3*H*-cyclopenta[*a*]naphthalene **(P1)**, and 1*H*-cyclopenta[*b*]naphthalene **(P2)** were already measured and taken from our previous study.[14]

3. COMPUTATIONAL

The calculations of the energies and molecular parameters of various intermediates and transition states for the reactions of 5- and 6-indenyl with vinylacetylene occurring on the $C_{13}H_{11}$ potential energy surface (PES), as well as of the reactants and possible products were carried out at the G3(MP2,CC)//B3LYP/6-311G(d,p) level of theory. Within this theoretical scheme, geometries were optimized and vibrational frequencies were calculated using the density functional B3LYP method with the 6-311G(d,p) basis set. Then, single-point total energies were improved using a series of coupled clusters CCSD(T) and second-order Møller-Plesset perturbation theory MP2 calculations, and the final energy was computed as

E[G3(MP2,CC)] = E[CCSD(T)/6-311G(d,p)] + E[MP2/G3Large)] – E[MP2/6-311G(d,p)] + ZPE [B3LYP/6-311G(d,p)][41-43]

The G3(MP2,CC) model chemistry approach normally provides chemical accuracy of 0.01–0.02 Å for bond lengths, 1–2º for bond angles, and 3–6 kJ mol^{-1} for relative energies of hydrocarbons, their radicals, reaction energies, and barrier heights in terms of average absolute deviations.[42] The GAUSSIAN 09[44] and MOLPRO 2010[45] program packages were employed for the ab initio calculations.

4. RESULTS & DISCUSSION

Illustrative mass spectra collected at a photoionization energy of 9.50 eV are presented in Figure 1 for the reactions of 5-indenyl and 6-indenyl with vinylacetylene (Figs. 1b and d) to extract the molecular formulae of the reaction products connected to the formation of benzindene isomers. An analysis of these data discloses the formation of $C_{13}H_{10}$ molecules (166 amu) along with their ^{13}C isotopologues at *m/z* = 167 in both systems. Considering the molecular weight of the reactants and the products, the $C_{13}H_{10}$ isomer(s) are products of the reaction of the 5-/6-indenyl radical with vinylacetylene followed by hydrogen atom elimination. The ion counts at mass-to-charge ratios (*m/z*) of 242 ($C_9H_7I^+$), 115 ($C_9H_7^+$), and 116 ($C_8{}^{13}CH_7^+$, $C_9H_8^+$) are detectable in the control experiments as well and hence cannot be linked to the reaction of 5- or 6-indenyl radicals with vinylacetylene. These species are associated with the 5- and 6-iodoindene precursors (242 amu), 5-/6-indenyl radicals (115 amu), and indene (116 amu) with the indene likely formed through recombination of 5- or 6-indenyl with a hydrogen atom in the reactor.

The investigation of the mass spectra delivered convincing evidence on the formation of $C_{13}H_9$ (165 amu) and $C_{13}H_{10}$ (166 amu) isomer(s) along with their ^{13}C substituted species $C_{12}{}^{13}CH_{10}$ (167 amu) via the reaction of 5-/6-indenyl radicals with vinylacetylene. It is our goal not only to identify the molecular formulae of the reaction products, but also to unravel which isomers are contributing to these mass-to-charge ratios. Thus, an in-depth analysis of the underlying PIE curves of the *m/z* ratios of interest (Fig. 2) is necessary to reveal the isomers produced. PIE curves for other *m/z* ratios are provided in the Supporting Information (Figures S2 and S3). Each PIE curve reports the ion counts at a well-defined *m/z* ratio as a function of the photon energy ranging from 7.30 eV to 10.00 eV (Fig. 2). The shapes of the PIE curves of different $C_{13}H_{10}$ isomers are distinct and therefore unique; these calibration curves were recorded in separate experiments reported in previous works and here.[14] A linear combination of these base functions is used to fit the experimental PIE curves shown for *m/z* = 165, 166, and 167 (Fig. 2). Even after scaling, these calibrated PIE curves are not superimposable suggesting that *m/z* = 165 does not represent a photoionization fragment of *m/z* = 166, but rather distinct isomer(s). Due to the lack of reference PIE curves of any $C_{13}H_9$ isomer, it is not feasible to elucidate its structure(s). Considering a 1.1% natural abundance of ^{13}C, 14.3 % of the ion signal of *m/z* = 165 ($C_{13}H_9^+$) could contribute to ion counts of *m/z* = 166 ($C_{12}{}^{13}CH_9^+$) (Fig. 2). Fitting of the PIE curves at *m/z* = 166 ($C_{12}{}^{13}CH_9^+/C_{13}H_{10}^+$) reveals the formation of seven $C_{13}H_{10}$ isomers: 3*H*-cyclopenta[*a*]naphthalene **(P1)**, 1*H*-cyclopenta[*b*]naphthalene **(P2)**, 1*H*-cyclopenta[*a*]naphthalene **(P3)**, (*E*)-5-(but-1-en-3-yn-1-yl)-1*H*-indene **(P4)**, 5-(but-3-ene-1-yn-1-yl)-1*H*-indene **(P5)**, (*E*)-6-(but-1-en-3-yn-1-yl)-1*H*-indene **(P6),** and 6-(but-3-ene-1-yn-1-yl)-1*H*-indene **(P7)**. The corresponding PIE curves of *m/z* = 167 ($C_{12}{}^{13}CH_{10}^+$) match the linear fit of the aforementioned seven PAH isomers and reveal that ion signal at *m/z* = 167 originate from their ^{13}C-isotoplogue PAHs ($C_{13}H_{10}$). It should be noticed that for the PIE calibration experiments of the branched indene isomers **P4, P5, P6,** and **P7**, only calibration mixtures of (*E*)-5-(but-1-en-3-yn-1-yl)-1*H*-indene **(P4)** and (*E*)-6-(but-1-en-3-yn-1-yl)-1*H*-indene **(P6)** (40:60) as well as 5-(but-3-ene-1-yn-1-yl)-1*H*-indene **(P5)** and 6-(but-3-ene-1-yn-1-yl)-1*H*-indene **(P7)** (40:60) has been synthesized and hence exploited for the calibration curve (Supporting Information). Note that actual product branching ratios could not be derived due to unknown photoionization cross sections for any of the $C_{13}H_{10}$ isomers formed and hence only mechanistic information for five membered PAH ring formation is reported here. For the calibration PIE curves of the tricyclic isomers cyclopentanaphthalenes (Fig. S1a-S1c), their ionization energies (IEs) lie in the range of 7.5-7.6 eV, which match the onsets of the experimental PIE measurement (7.55 ± 0.05 eV, Fig. 2). While for the branched indene isomers (Fig. S1d-S1e), their IEs are around 7.70 eV. As the photoionization thresholds are specific for individual species,[46] the cyclopentanaphthalene isomers are critical for the fit in the lower photon energy range, especially at the onsets of PIE curves. Moreover, the experimental PIE curves cannot be fit without the calibration curves of the branched isomers at photon energies higher than 7.70 eV. With the fit presented in Fig. 2, it is clear that all the isomers are necessary for the overall fit. However, due to the two component cis/trans mixtures of the branched isomers, it might not be concluded that all branched isomers were detected. As a conclusion, it is tentative to claim that all the four branched indene isomers are produced in this work. But for the tricyclic isomers, they are critical to replicate the experimentally determined PIE curve.

To extract the underlying reaction pathways, the experimental data are corroborated with electronic structure calculations (Figs. 3 and 4). Figure 3 reveals the potential energy surface (PES) for the reaction of 5-indenyl with vinylacetylene. The approach of 5-indenyl to the C4 and C1 carbon atoms of vinylacetylene is dictated by an attractive long range potential and leads to the barrierless formation of van der-Waals-complexes **[i0a]** and **[i0b]** located 10 kJ mol^{-1} and 7 kJ mol^{-1} below the energy of the separated reactants. By overcoming a barrier of 6 kJ mol^{-1} to addition, **[i0a]** isomerizes to intermediate **[i1]**; this complex represents the key intermediate leading to the formation of the benzindene molecules. It should be stressed that a barrier to addition does exist, but this barrier lies below the energy of the separated reactants and hence is called 'submerged barrier'. Therefore, the formation of **[i1]** from the reactants represents essentially a barrierless entrance process. With a hydrogen shift from C4 and C6 of the indenyl moiety to the β position of the branched C4 chain, **[i1]** can isomerize to **[i3]** and **[i6]**, respectively, followed by cyclization processes to intermediates **[i4]** and **[i7]**. Further [1,2]-type hydrogen shifts from CH_2 to the bare carbon atom in the newly formed six-membered ring lead to intermediates [**i5**] and [**i8**], which contain the carbon backbones of the benzindene isomers. Distinct hydrogen atom losses accompanied by aromatization forms 3*H*-cyclopenta [*a*]naphthalene **(P1)** (from **[i5]**) and 1*H*-cyclopenta[*b*]naphthalene **(P2)** (from **[i8]**). Besides the reaction sequences leading to **P1** and **P2**, intermediate **[i1]** can also undergo an immediate hydrogen atom loss to produce (*E*)-5-(but-1-en-3-yn-1-yl)-1*H*-indene **(P4)** by overcoming a barrier of 168 kJ mol^{-1}. All the barriers in the routes initiated by the van der-Waals complex **[i0a]** lie below the separate reactants. On the other hand, **[i0b]** isomerizes to intermediate **[i2]**, followed by hydrogen atom loss yielding 5-(but-3-ene-1-yn-1-yl)-1*H*-indene **(P5)**. The barrier in the process from **[i0b]** to **[i2]** is 3 kJ mol^{-1} above the separated reactants indicating that this is not a barrierless route thus requiring somewhat elevated temperatures to proceed.

Figure 4 exhibits the PES for the 6-indenyl - vinylacetylene system. The reaction mechanisms are similar to those described in the aforementioned system of 5-indenyl reacting with vinylacetylene. First, two van der-Waals complexes **[i'0a]** (-11 kJ mol^{-1}) and **[i'0b]** (-7 kJ mol^{-1}) are produced via the approach of 5-indenyl to the C4 and C1 atoms of vinylacetylene, respectively. **[i'0a]** isomerizes to intermediate **[i'1]** by overcoming a submerged barrier of 7 kJ mol^{-1}. Followed by isomerization (hydrogen shifts, cyclization) and hydrogen atom elimination, 1*H*-cyclo-penta[*a*]naphthalene **(P3)** and 1*H*-cyclopenta[*b*]naphthalene **(P2)** can be produced via the reaction sequences **[i'1]** → **[i'3]** → **[i'4]** → **[i'5]** → **P5** and **[i'1]** → **[i'6]** → **[i'7]** → **[i'8]** → **P2**, respectively. Alternatively, a hydrogen atom elimination leads **[i'1]** to (*E*)-6-(but-1-en-3-yn-1-yl)-1*H*-indene **(P6)**. In addition, the van der-Waals complex **[i'0b]** may isomerize to **[i'2]** through a barrier of 11 kJ mol^{-1}, followed by hydrogen atom loss leading to 6-(but-3-ene-1-yn-1-yl)-1*H*-indene **(P7)**. This pathway does not represent a barrierless entrance process since the barrier from **[i'0b]** to **[i'2]** lies 4 kJ mol^{-1} above the energy of the separated reactants.

As the experiments were conducted under combustion-like condition at 1300 $\pm$ 10 K, the barriers of 3 and 4 kJ mol^{-1} can be easily overcome. Thus, even 5-(but-3-ene-1-yn-1-yl)-1*H*-indene **(P5)** and 6-(but-3-ene-1-yn-1-yl)-1*H*-indene **(P7)**, can be produced. Recall that due to the isomer mixture of (*E*)-5-(but-1-en-3-yn-1-yl)-1*H*-indene **(P4)** and (*E*)-6-(but-1-en-3-yn-1-yl)-1*H*-indene **(P6)** as well as 5-(but-3-ene-1-yn-1-yl)-1*H*-indene **(P5)** and 6-(but-3-ene-1-yn-1-yl)-1*H*-indene **(P7)**, four branched indene molecules are involved in the fits of the PIE curves of the $C_{13}H_{10}$ isomers in both systems. However, based on the theoretical calculations, we may conclude that **P4** and **P5** are only accessible in the 5-indenyl – vinylacetylene system, while **P6** and **P7** may only be formed in the reaction of 6-indenyl with vinylacetylene.

5. CONCLUSION

Our combined experimental and computational studies revealed critical mass growth processes from aromatic aryl radicals (5-indenyl and 6-indenyl) leading to distinct tricyclic PAHs carrying two six- and one five-membered rings: 3*H*-cyclopenta[*a*]naphthalene, 1*H*-cyclopenta[*b*] naphthalene, and 1*H*-cyclopenta[*a*]naphthalene. The underlying reaction mechanisms involve the formation of van-der-Waals complexes and the de-facto barrier-less addition of the carbon-centered radicals of the 5- and 6-indenyl species to the π-electron density of vinylacetylene reactant at the terminal carbon atoms. The resonantly stabilized free radical intermediates formed further isomerize through hydrogen shifts and ring closure; these processes are terminated by atomic hydrogen elimination accompanied by aromatization leading to the tricyclic PAHs in an overall exoergic reaction. The reaction mechanisms essentially mirror the formation of the naphthalene molecule ($C_{10}H_8$) in the phenyl-vinylacetylene system[12, 28, 29] and suggest that the five-membered ring in the indenyl radicals acts as a spectator. These overall routes to these PAHs are essentially barrierless since all the transition states involved are located below the energy of the separated reactants. The submerged barriers represent a crucial prerequisite for a bimolecular reaction to proceed at low temperatures, since any transition state located above the energy of the separated reactants cannot be overcome at low temperatures in cold molecular clouds such as TMC-1 at temperatures as low as 10 K. Here, the hydrogen abstraction – vinylacetylene addition (HAVA) pathway signifies a versatile reaction mechanism to generate benzindene molecules through barrierless, stepwise ring expansion via elementary gas-phase reactions of an aryl radical with vinylacetylene. The aryl radical can be formed inside molecular clouds from the corresponding aromatic precursor via photolysis by an internal ultraviolet field. In circumstellar envelopes of carbon stars and even under combustion conditions with temperatures of up to a few 1,000 K, molecular mass growth processes could also be triggered by HAVA as a facile key mechanism propelling molecular mass growth processes of PAHs. This study potentially suggests that the five-member-ring contained PAHs can lead, via a low-temperature propagation mechanism, to more complex 3D-structured PAHs such as corannulene and even fullerenes observed in the galaxy.

Acknowledgments

This work was supported by the US Department of Energy, Basic Energy Sciences DE-FG02-03ER15411 (experimental studies) and DE-FG02-04ER15570 (computational studies; synthesis of the $C_{13}H_{10}$ isomers) to the University of Hawaii (UH) and Florida International University (FIU), respectively. W.L., O.K., and M.A. are supported by the Director, Office of Science, Office of Basic Energy Sciences, of the U.S. Department of Energy under Contract No. DE-AC02-05CH11231, through the Gas Phase Chemical Physics program of the Chemical Sciences Division. The ALS is supported under the same contract. Ab initio calculations at Samara University were supported by the Ministry of Science and Higher Education of the Russian Federation under Grant No. 14.Y26.31.0020.

Author Contributions

R.I.K. designed the experiment; L.Z., W.L. and O.K. carried out the experimental measurements; M.A. supervised the experiment; L.Z. performed the data analysis; M.M.E., E.K.B., A.D.O., V.N.A. and A.M.M. carried out the theoretical analysis; A.H.H. and S.F.W. synthesized the compounds, A.M.M., and M.A. discussed the data; R.I.K., A.M.M. and L.Z. wrote the manuscript.

References

1. D. Josa, L. Azevedo dos Santos, I. Gonzalez-Veloso, J. Rodriguez-Otero, E. M. Cabaleiro-Lago and T. de Castro Ramalho, *RSC Adv.*, 2014, **4**, 29826-29833.
2. H. Richter, W. J. Grieco and J. B. Howard, *Combust. Flame*, 1999, **119**, 1-22.
3. H. Richter, W. J. Grieco and J. B. Howard, *Chem. Phys. Processes Combust.*, 1997, 135-138.
4. L. Becker and T. E. Bunch, *Meteorit. Planet. Sci.*, 1997, **32**, 479-487.
5. G. Devi, M. Buragohain and A. Pathak, *Planet. Space Sci.*, 2020, **183**, 104593.
6. L. Zhao, R. I. Kaiser, W. Lu, B. Xu, M. Ahmed, A. N. Morozov, A. M. Mebel, A. H. Howlader and S. F. Wnuk, *Nat. Commun.*, 2019, **10**, 1-7.
7. T. Yang, D. S. N. Parker, B. B. Dangi, R. I. Kaiser and A. M. Mebel, *Phys. Chem. Chem. Phys.*, 2015, **17**, 10510-10519.
8. L. Vereecken, H. F. Bettinger and J. Peeters, *Phys. Chem. Chem. Phys.*, 2002, **4**, 2019-2027.
9. L. Vereecken, J. Peeters, H. F. Bettinger, R. I. Kaiser, P. v. R. Schleyer and H. F. Schaefer, III, *J. Am. Chem. Soc.*, 2002, **124**, 2781-2789.
10. F. Zhang, R. I. Kaiser, V. V. Kislov, A. M. Mebel, A. Golan and M. Ahmed, *J. Phys. Chem. Lett.*, 2011, **2**, 1731-1735.
11. D. S. N. Parker, F. Zhang, R. I. Kaiser, V. V. Kislov and A. M. Mebel, *Chem. - Asian J.*, 2011, **6**, 3035-3047.
12. A. M. Mebel, A. Landera and R. I. Kaiser, *J. Phys. Chem. A*, 2017, **121**, 901-926.
13. D. S. N. Parker, R. I. Kaiser, O. Kostko and M. Ahmed, *ChemPhysChem*, 2015, **16**, 2091-2093.
14. L. Zhao, M. Prendergast, R. I. Kaiser, B. Xu, U. Ablikim, W. Lu, M. Ahmed, A. D. Oleinikov, V. N. Azyazov, A. H. Howlader, S. F. Wnuk and A. M. Mebel, *Phys. Chem. Chem. Phys.*, 2019, **21**, 16737-16750.
15. A. Kitajima, T. Hatanaka, M. Takeuchi, H. Torikai and T. Miyadera, *Combust. Flame*, 2005, **142**, 72-88.
16. C. S. McEnally and L. D. Pfefferle, *Combust. Flame*, 2007, **148**, 210-222.
17. V. Kislov and A. Mebel, *J. Phys. Chem.*, 2008, **112**, 700-716.
18. L. Vereecken and J. Peeters, *Phys. Chem. Chem. Phys.*, 2003, **5**, 2807-2817.
19. J. Bittner and J. Howard, *Proc. Combust. Inst.*, 1981, **18**, 1105-1116.
20. J. DeCoster, A. Ergut, Y. A. Levendis, H. Richter, J. B. Howard and J. B. Carlson, *Proc. Combust. Inst.*, 2007, **31**, 491-499.
21. F. Zhang, X. Gu and R. I. Kaiser, *J. Chem. Phys.*, 2008, **128**, 084315.
22. R. Sivaramakrishnan, R. S. Tranter and K. Brezinsky, *J. Phys. Chem.*, 2006, **110**, 9400-9404.
23. M. Frenklach, D. W. Clary, W. C. Gardiner Jr and S. E. Stein, *Proc. Combust. Inst.*, 1988, **21**, 1067-1076.
24. M. Frenklach, T. Yuan and M. Ramachandra, *Energy Fuels*, 1988, **2**, 462-480.
25. V. Kislov and A. Mebel, *J. Phys. Chem.*, 2007, **111**, 3922-3931.
26. R. D. Lorenz and J. I. Lunine, *Planet. Space Sci.*, 1997, **45**, 981-992.
27. L. Zhao, R. I. Kaiser, B. Xu, U. Ablikim, M. Ahmed, M. M. Evseev, E. K. Bashkirov, V. N. Azyazov and A. M. Mebel, *Nat. Astron.*, 2018, **2**, 973.
28. D. S. Parker, F. Zhang, Y. S. Kim, R. I. Kaiser, A. Landera, V. V. Kislov, A. M. Mebel and A. Tielens, *Proc. Natl. Acad. Sci. USA*, 2012, **109**, 53-58.

29. L. Zhao, R. I. Kaiser, B. Xu, U. Ablikim, M. Ahmed, M. V. Zagidullin, V. N. Azyazov, A. H. Howlader, S. F. Wnuk and A. M. Mebel, *J. Phys. Chem. Lett.*, 2018, **9**, 2620-2626.
30. T. Yang, L. Muzangwa, R. I. Kaiser, A. Jamal and K. Morokuma, *Phys. Chem. Chem. Phys.*, 2015, **17**, 21564-21575.
31. F. Zhang, Y. S. Kim, R. I. Kaiser, S. P. Krishtal and A. M. Mebel, *J. Phys. Chem.*, 2009, **113**, 11167-11173.
32. F. Zhang, R. I. Kaiser, A. Golan, M. Ahmed and N. Hansen, *J. Phys. Chem. A*, 2012, **116**, 3541-3546.
33. A. Golan, M. Ahmed, A. M. Mebel and R. I. Kaiser, *Phys. Chem. Chem. Phys.*, 2013, **15**, 341-347.
34. T. Yang, T. P. Troy, B. Xu, O. Kostko, M. Ahmed, A. M. Mebel and R. I. Kaiser, *Angew. Chem. Int. Ed.*, 2016, **55**, 14983-14987.
35. L. Zhao, R. I. Kaiser, B. Xu, U. Ablikim, M. Ahmed, D. Joshi, G. Veber, F. R. Fischer and A. M. Mebel, *Nat. Astron.*, 2018, **2**, 413-419.
36. L. Zhao, R. I. Kaiser, B. Xu, U. Ablikim, W. Lu, M. Ahmed, M. M. Evseev, E. K. Bashkirov, V. N. Azyazov, M. V. Zagidullin, A. N. Morozov, A. H. Howlader, S. F. Wnuk, A. M. Mebel, D. Joshi, G. Veber and F. R. Fischer, *Nat. Commun.*, 2019, **10**, 1510.
37. A. Hasan Howlader, K. Diaz, A. M. Mebel, R. I. Kaiser and S. F. Wnuk, *Tetrahedron Letters*, 2020, DOI: https://doi.org/10.1016/j.tetlet.2020.152427, 152427.
38. Q. Guan, K. N. Urness, T. K. Ormond, D. E. David, G. Barney Ellison and J. W. Daily, *Int. Rev. Phys. Chem.*, 2014, **33**, 447-487.
39. M. V. Zagidullin, R. I. Kaiser, D. P. Porfiriev, I. P. Zavershinskiy, M. Ahmed, V. N. Azyazov and A. M. Mebel, *J. Phys. Chem. A*, 2018, **122**, 8819-8827.
40. F. Qi, *Proc. Combust. Inst.*, 2013, **34**, 33-63.
41. L. A. Curtiss, K. Raghavachari, P. C. Redfern, V. Rassolov and J. A. Pople, *J. Chem. Phys.*, 1998, **109**, 7764-7776.
42. L. A. Curtiss, K. Raghavachari, P. C. Redfern, A. G. Baboul and J. A. Pople, *Chem. Phys. Lett.*, 1999, **314**, 101-107.
43. A. G. Baboul, L. A. Curtiss, P. C. Redfern and K. Raghavachari, *J. Chem. Phys.*, 1999, **110**, 7650-7657.
44. M. J. Frisch, G. W. Trucks, H. B. Schlegel, G. E. Scuseria, M. A. Robb, J. R. Cheeseman, G. Scalmani, V. Barone, B. Mennucci, G. A. Petersson, H. Nakatsuji, M. Caricato, X. Li, H. P. Hratchian, A. F. Izmaylov, J. Bloino, G. Zheng, J. L. Sonnenberg, M. Hada, M. Ehara, K. Toyota, R. Fukuda, J. Hasegawa, M. Ishida, T. Nakajima, Y. Honda, O. Kitao, H. Nakai, T. Vreven, J. A. Montgomery, Jr., J. E. Peralta, F. Ogliaro, M. Bearpark, J. J. Heyd, E. Brothers, K. N. Kudin, V. N. Staroverov, T. Keith, R. Kobayashi, J. Normand, K. Raghavachari, A. Rendell, J. C. Burant, S. S. Iyengar, J. Tomasi, M. Cossi, N. Rega, J. M. Millam, M. Klene, J. E. Knox, J. B. Cross, V. Bakken, C. Adamo, J. Jaramillo, R. Gomperts, R. E. Stratmann, O. Yazyev, A. J. Austin, R. Cammi, C. Pomelli, J. W. Ochterski, R. L. Martin, K. Morokuma, V. G. Zakrzewski, G. A. Voth, P. Salvador, J. J. Dannenberg, S. Dapprich, A. D. Daniels, O. Farkas, J. B. Foresman, J. V. Ortiz, J. Cioslowski and D. J. Fox, Gaussian 09, revision A.02, (Gaussian Inc., CT), 2009.
45. H. J. Werner, P. J. Knowles, G. Knizia, F. R. Manby, M. Schütz, P. Celani, W. Györffy, D. Kats, T. Korona, R. Lindh, A. Mitrushenkov, G. Rauhut, K. R. Shamasundar, T. B. Adler, R. D. Amos, A. Bernhardsson, A. Berning, D. L. Cooper, M. J. O. Deegan, A. J. Dobbyn, F. Eckert, E. Goll, C. Hampel, A. Hesselmann, G. Hetzer, T. Hrenar, G. Jansen,

C. Köppl, Y. Liu, A. W. Lloyd, R. A. Mata, A. J. May, S. J. McNicholas, W. Meyer, M. E. Mura, A. Nicklaß, D. P. O'Neill, P. Palmieri, D. Peng, K. Pflüger, R. Pitzer, M. Reiher, T. Shiozaki, H. Stoll, A. J. Stone, R. Tarroni, T. Thorsteinsson and M. Wang, MOLPRO, version 2010.1, http://www.molpro.net, (University College Cardiff Consultants Ltd, United Kingdom), 2010.

46. T. A. Cool, J. Wang, K. Nakajima, C. A. Taatjes and A. Mcllroy, *International Journal of Mass Spectrometry*, 2005, **247**, 18-27.

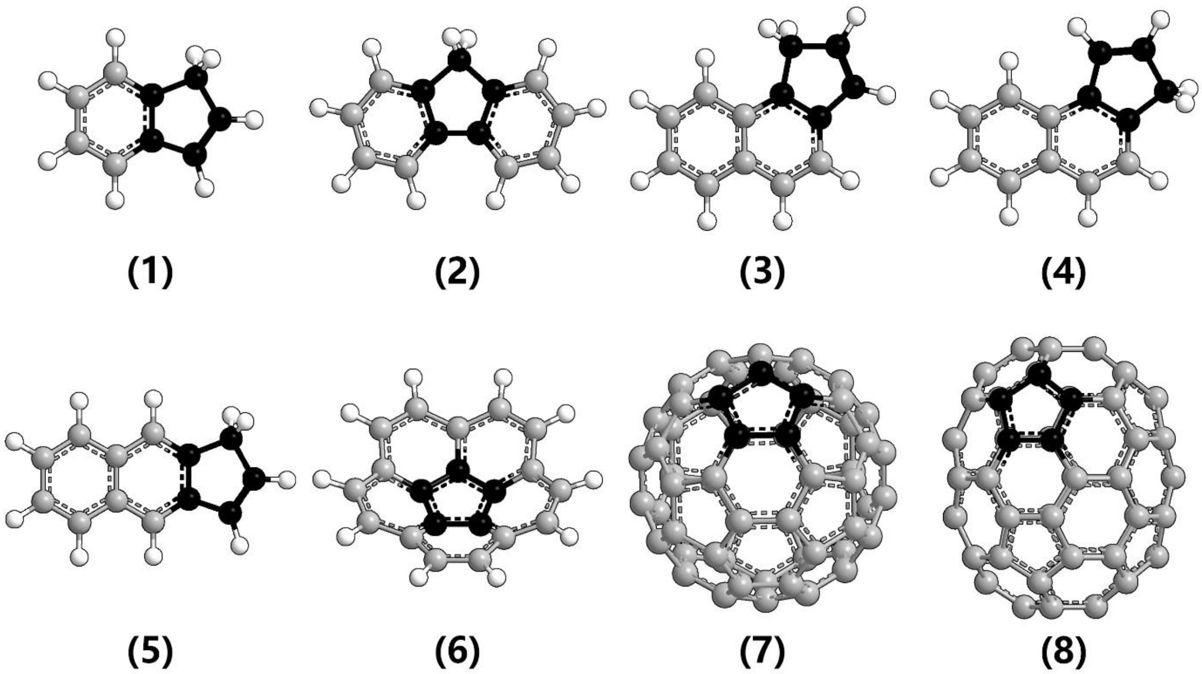

Scheme 1. Molecular building blocks of the 5-member-ring carbon skeleton (black) in indene **(1)**, fluorene **(2)**, 1*H*-cyclopenta[*a*]naphthalene **(3)**, 3*H*-cyclopenta[*a*]naphthalene **(4)**, 1*H*-cyclopenta[*b*]naphthalene **(5)**, corannulene **(6)**, C_{60}-fullerene **(7)** and C_{70}-fullerene **(8)**.

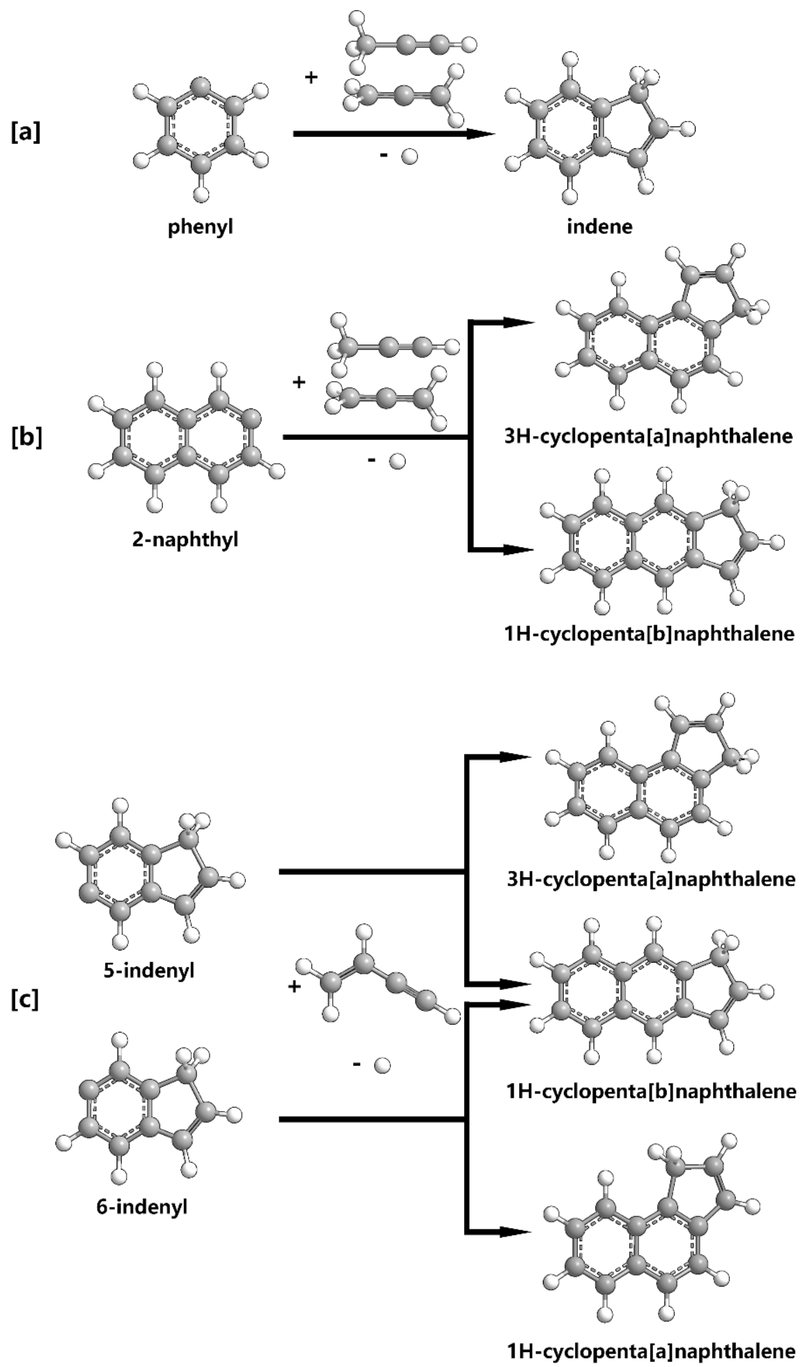

Scheme 2. Reaction schemes: [a] phenyl ($C_6H_5^\bullet$) reacts with allene/methylacetylene (C_3H_4) and yields indene;[11] [b] 2-naphthyl ($C_{10}H_7^\bullet$) reacts with allene/methylacetylene (C_3H_4) leading to the formation of 3*H*-cyclopenta[*a*]naphthalene/1*H*-cyclopenta[*b*]naphthalene ($C_{13}H_{10}$);[14] [c] 5-/6-indenyl radicals ($C_9H_7^\bullet$) is proposed to react with vinylacetylene (C_4H_4) to produce 3*H*-cyclopenta[*a*]naphthalene, 1*H*-cyclopenta[*b*]naphthalene, and 1*H*-cyclopenta[*a*]naphthalene ($C_{13}H_{10}$).

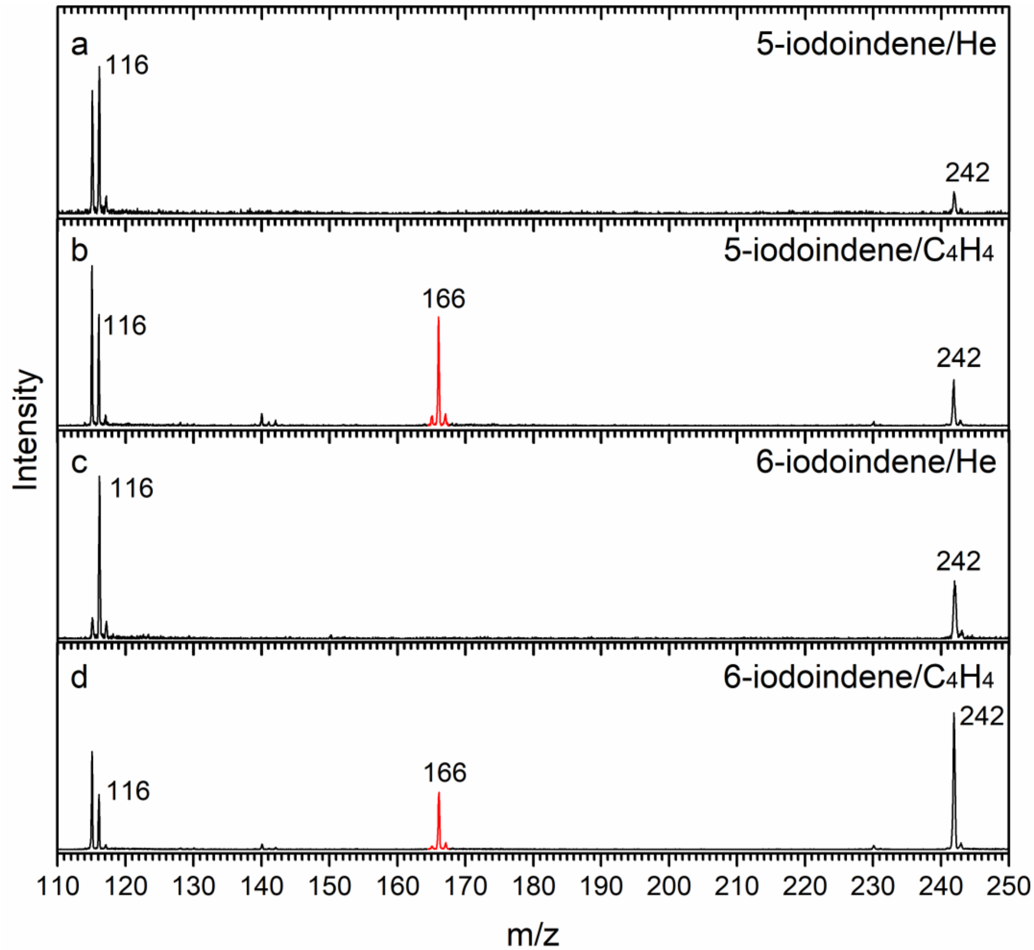

Figure 1. Comparison of photoionization mass spectra recorded at a photon energy of 9.50 eV with the reaction temperature at 1300 ± 10 K. (a) 5-iodoindene (C_9H_7I) – helium (He) system; (b) 5-iodoindene (C_9H_7I) – vinylacetylene (C_4H_4) system; (c) 6-iodoindene (C_9H_7I) – helium (He) system; and (d) 6-iodoindene (C_9H_7I) – vinylacetylene (C_4H_4) system. The mass peaks of the newly formed species along with the ^{13}C-counterparts are highlighted in red.

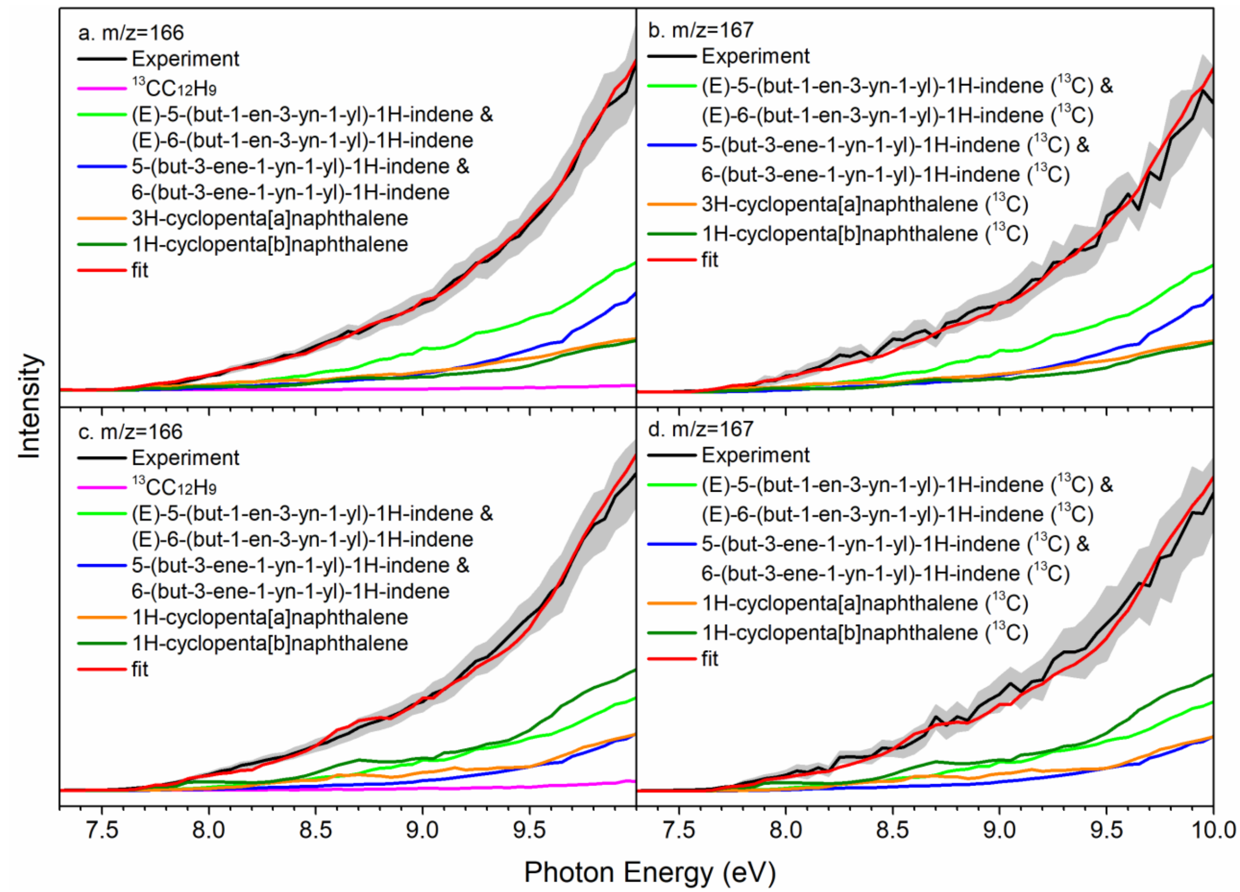

Figure 2. Photoionization efficiency (PIE) curves for signal at *m/z* = 166 and 167 in the reactions of indenyl radicals with vinylacetylene. Upper panels (a and b): 5-indenyl ($C_9H_7^•$) + vinylacetylene (C_4H_4); Lower panels (c and d): 6-indenyl ($C_9H_7^•$) + vinylacetylene (C_4H_4). Black lines present experimentally derived PIE curves along with the error bars indicated in gray; colored lines (green, blue, olive and orange) present the reference PIE curves; and red lines are the overall fit. The overall error bars consist of two parts: ±10% based on the accuracy of the photodiode and a 1 σ error of the PIE curve averaged over the individual scans.

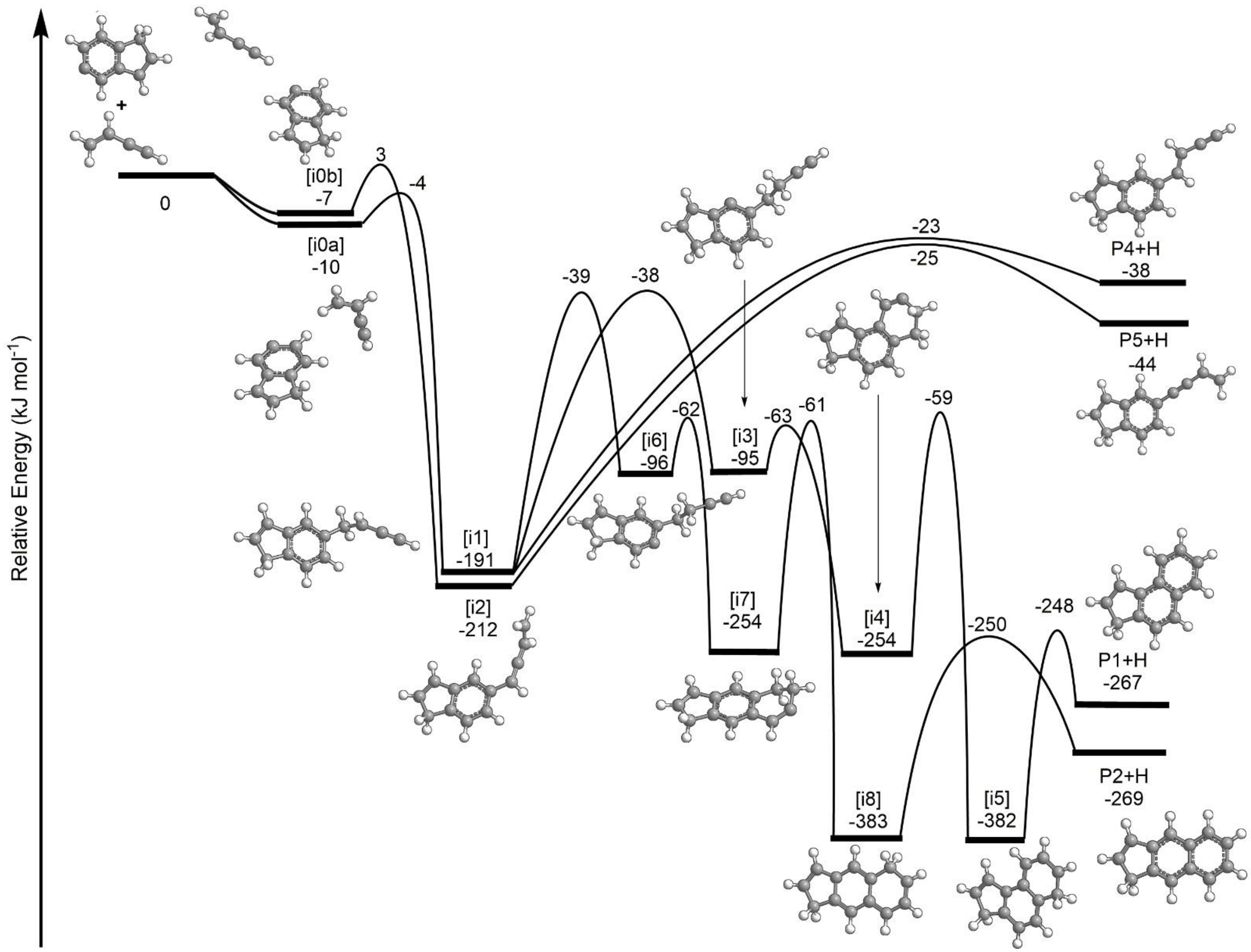

Figure 3. Potential energy surface (PES) for the 5-indenyl ($C_9H_7^{\bullet}$) reaction with vinylacetylene (C_4H_4) leading to the formation of 3*H*-cyclopenta[*a*]naphthalene (**P1**), 1*H*-cyclopenta[*b*]naphthalene (**P2**), (*E*)-5-(but-1-en-3-yn-1-yl)-1*H*-indene (**P4**), and 5-(but-3-ene-1-yn-1-yl)-1*H*-indene (**P5**). The relative energies are given in kJ mol^{-1}.

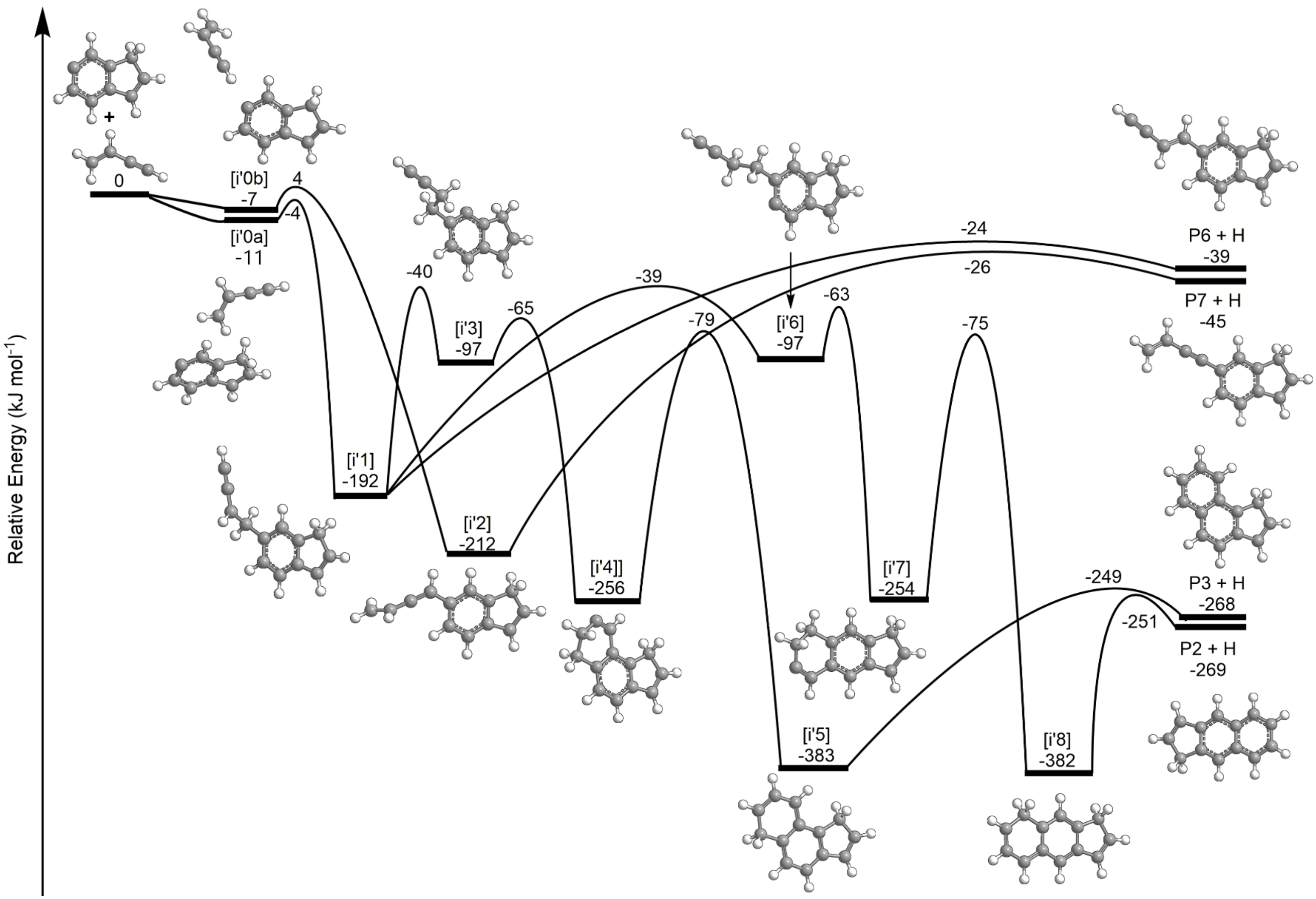

Figure 4. Potential energy surface (PES) for the 6-indenyl ($C_9H_7^\bullet$) reaction with vinylacetylene (C_4H_4) leading to the formation of 1*H*-cyclopenta[*b*]naphthalene (**P2**), 1*H*-cyclopenta[*a*]naphthalene (**P3**), (*E*)-6-(but-1-en-3-yn-1-yl)-1*H*-indene (**P6**), and 6-(but-3-ene-1-yn-1-yl)-1*H*-indene (**P7**). The relative energies are given in kJ mol^{-1}.

Supporting Information

Gas Phase Formation of Cyclopentanaphthalene (Benzindene) Isomers via Reactions of 5- and 6-Indenyl Radicals with Vinylacetylene

Long Zhao[1], Ralf I. Kaiser[1*]

[1] *Department of Chemistry, University of Hawaii at Manoa, Honolulu, Hawaii, 96822 (USA)*

Wenchao Lu[2], Oleg Kostko[2], Musahid Ahmed[2*]

[2] *Chemical Sciences Division, Lawrence Berkeley National Laboratory, Berkeley, CA 94720* (USA)

Mikhail M. Evseev,[3] Eugene K. Bashkirov[3]

[3]*Samara National Research University, Samara 443086, Russian Federation*

Artem D. Oleinikov[3,4], Valeriy N. Azyazov[3,4]

[3]*Samara National Research University, Samara 443086, Russian Federation*

[4]*Lebedev Physical Institute, Samara 443011*

Alexander M. Mebel[3,5*], A. Hasan Howlader,[5] Stanislaw F. Wnuk[5]

[3]*Samara National Research University, Samara 443086*
(Russian Federation)

[5]*Department of Chemistry and Biochemistry, Florida International University, Miami, FL 33199* (USA)

[*] Corresponding author:

Ralf I. Kaiser <ralfk@hawaii.edu>

Musahid Ahmed <mahmed@lbl.gov>

Alexander M. Mebel <mebela@fiu.edu>

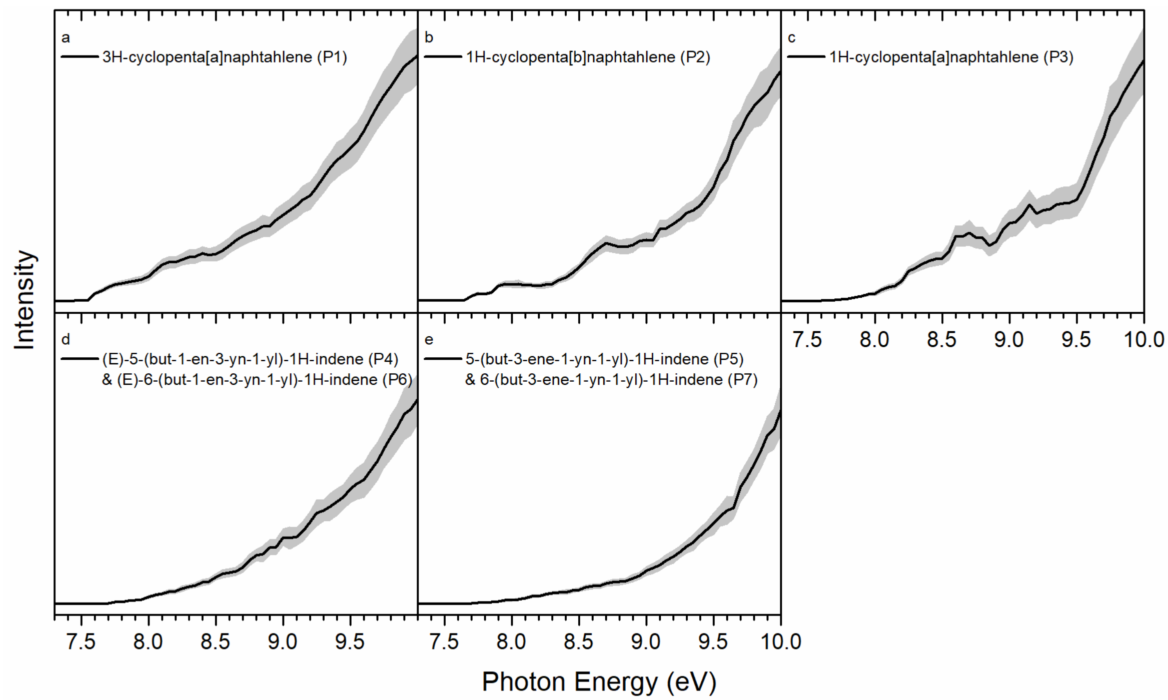

Figure S1. PIE calibration curves for distinct $C_{13}H_{10}$ isomers: a. 3*H*-cyclopenta[*a*]naphthalene (**P1**); b. 1*H*-cyclopenta[*b*]naphthalene (**P2**); c. 1*H*-cyclopenta[*a*]naphthalene (**P3**); d. (*E*)-5-(but-1-en-3-yn-1-yl)-1*H*-indene **(P4)** and (*E*)-6-(but-1-en-3-yn-1-yl)-1*H*-indene **(P6)** (as a 40:60 inseparable mixture); and e. 5-(but-3-ene-1-yn-1-yl)-1*H*-indene **(P5)** and 6-(but-3-ene-1-yn-1-yl)-1*H*-indene **(P7)** (as a 40:60 inseparable mixture). The values in the parenthesis indicates the ionization energies. The overall error bars (grey area) consist of two parts: ±10% based on the accuracy of the photodiode and a 1 σ error of the PIE curve averaged over the individual scans.

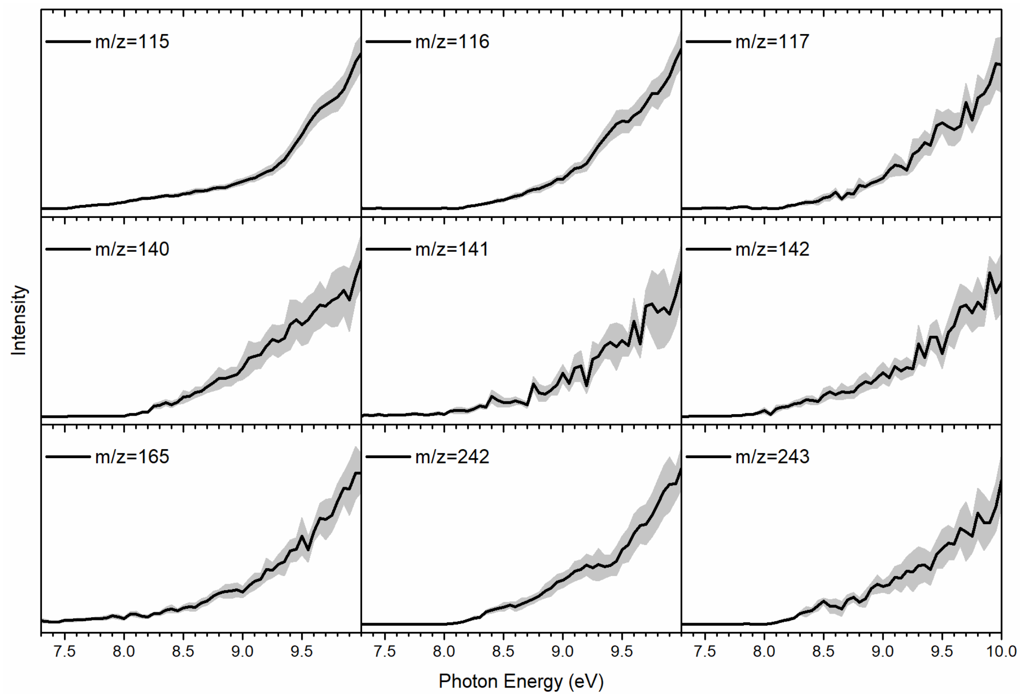

Figure S2. Photoionization efficiency (PIE) curves in the reaction of 5-indenyl ($C_9H_7^{\bullet}$) and vinylacetylene (C_4H_4) along with the experimental errors (gray area). Signal at *m/z* = 115 is 5-indenyl radical produced from the C-I bond scission of the precursor. The H-addition to this radical leads to the formation of indene (*m/z* = 116), along with its ^{13}C-isotopologue at *m/z* = 117. In the high temperature condition, acetylene (C_2H_2) is produced in the pyrolysis process of vinylacetylene, reacting with 5-indenyl radical to produce 5-ethynylindene (*m/z* = 140) after H-elimination. And signal at *m/z* = 141 and 142 might be related to the ^{13}C- and doubly ^{13}C-counterpart. Signal at *m/z* = 165 should be the $C_{13}H_9^{\bullet}$ radical from the H-loss of $C_{13}H_{10}$. Species at *m/z* = 242 and 243 are the precursor and the ^{13}C counterparts.

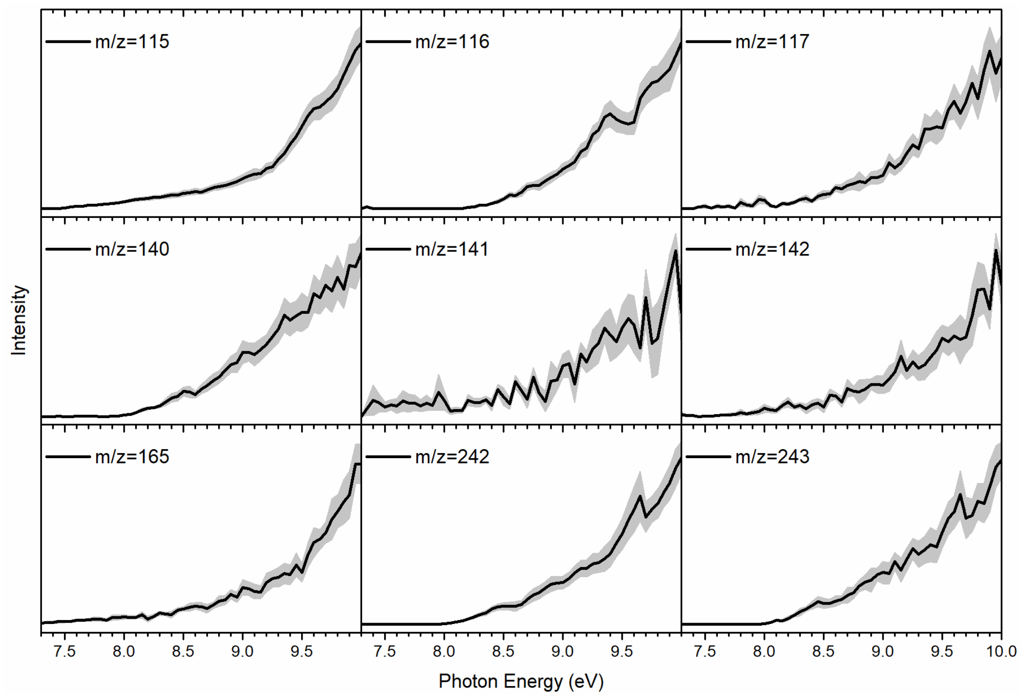

Figure S3. Photoionization efficiency (PIE) curves in the reaction of 6-indenyl ($C_9H_7^•$) and vinylacetylene (C_4H_4) along with the experimental errors (gray area). Signal at *m/z* = 115 is 6-indenyl radical produced from the C-I bond scission of the precursor. The H-addition to this radical leads to the formation of indene (*m/z* = 116), along with its ^{13}C-isotopologue at *m/z* = 117. In the high temperature condition, acetylene (C_2H_2) is produced in the pyrolysis process of vinylacetylene, reacting with 5-indenyl radical to produce 5-ethynylindene (*m/z* = 140) after H-elimination. And signal at *m/z* = 141 and 142 might be related to the ^{13}C- and doubly ^{13}C-counterpart. Signal at *m/z* = 165 should be the $C_{13}H_9^•$ radical from the H-loss of $C_{13}H_{10}$. Species at *m/z* = 242 and 243 are the precursor and the ^{13}C counterparts.

Synthesis of 5- and 6-iodoindene and calibration compounds P4, P5, P6, and P7.

The 5- and 6-iodoindene have been synthesized from 6- and 5-aminoindanone-1 by improving reported protocol.[1] The detailed synthesis and characterization have been published elsewhere.[2] The calibration compounds (*E*)-5-(but-1-en-3-yn-1-yl)-1*H*-indene **(P4)** and (*E*)-6-(but-1-en-3-yn-1-yl)-1*H*-indene **(P6)** (as a 40:60 inseparable mixture) have been synthesized from 5-iodoindene employing Stille and Sonogashira couplings. Similarly, 5-(but-3-ene-1-yn-1-yl)-1*H*-indene **(P5)**, and 6-(but-3-ene-1-yn-1-yl)-1*H*-indene **(P7)** (as a 40:60 inseparable mixture) have been synthesized from 6-iodoindene utilizing Sonogashira couplings (Figure S4). The detailed synthesis and characterization of **P4**, **P5**, **P6**, and **P7** have been recently published.[2]

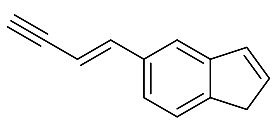

P4

(*E*)-5-(but-1-en-3-yn-1-yl)-1*H*-indene

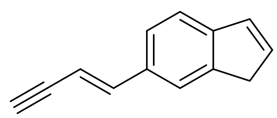

P6

(*E*)-6-(but-1-en-3-yn-1-yl)-1*H*-indene

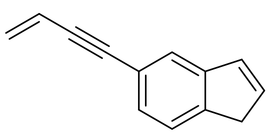

P5

5-(but-3-ene-1-yn-1-yl)-1*H*-indene

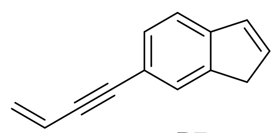

P7

6-(but-3-ene-1-yn-1-yl)-1*H*-indene

Figure S4. Structure of calibration compounds **P4**, **P5**, **P6**, and **P7.**

Synthesis of 1*H*-cyclopenta[a]naphthalene P3

Acylation of 3-(naphthalen-1-yl)propanoic acid[3] with $SOCl_2$ and cyclization with $AlCl_3$ provided perinaphthanone-7 **A** (75%) and 1,2-dihydro-3*H*-cyclopenta[a]naphthalene-1-one **B** (11%). Reduction of ketone **B** with $NaBH_4$ and dehydration of the resulting **C** with HCl gave 1*H*-cyclopenta(a)naphthalene **P3** (**Scheme S1**).

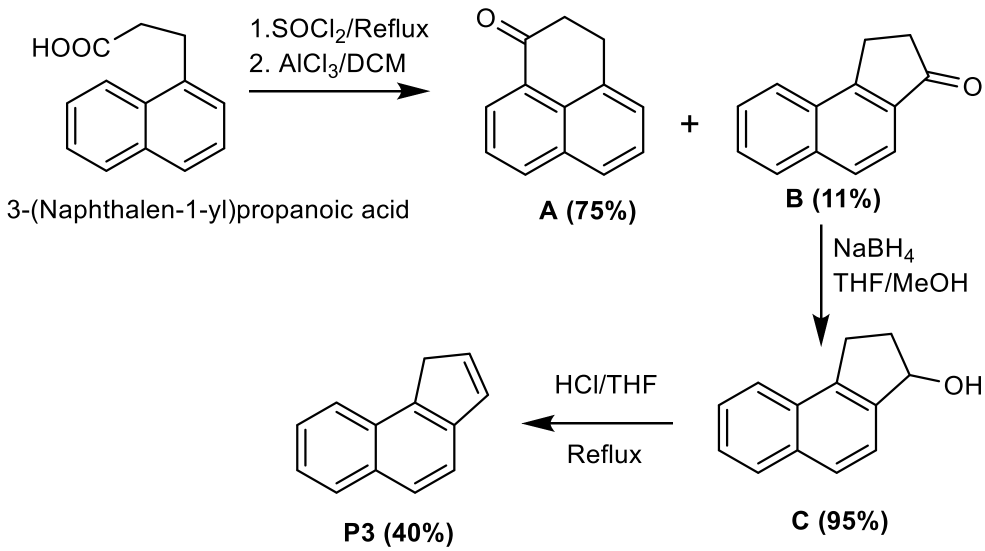

Scheme S1. Synthesis of 1*H*-cyclopenta[a]naphthalene

1,2-Dihydro-3*H*-cyclopenta[a]naphthalene-3-one; B.

3-(Naphthalen-1-yl)propanoic acid[3] (1.0 g, 4.99 mmol) was dissolved in $SOCl_2$ (15 mL) and the solution was refluxed at 85 ^oC for 1 h. The $SOCl_2$ was distilled off under reduced pressure. The resulted acid chloride was dissolved in 5 mL of dry dichloromethane and then added dropwise to a cold (-10°C) solution of 1.6 g (12.0 mmol) of aluminum chloride in 30 mL of dry dichloromethane. After stirring for 30 min at 0 ^oC, the mixture was poured into 100 mL of ice/water and the resulting solution was extracted with dichloromethane. The organic layer was separated, dried over anhydrous Na_2SO_4, filtered, and evaporated. The residue was column chromatographed (5 → 10 % EtOAc/hexane) to give 2,3-dihydro-1*H*-phenalen-1-one[3] **A** (682 mg, 75%) as off-white solid and **B** (100 mg, 11%) as pale yellow solid: ^{1}H NMR (400 MHz, $CDCl_3$) δ 8.06 (ddd, *J* = 8.0, 2.0, 0.8 Hz, 1H), 7.95 (dd, *J* = 7.2, 1.6 Hz, 1H), 7.81 (d, *J* = 8.4 Hz, 1H), 7.75 (d, *J* = 8.4 Hz, 1H), 7.71-7.62 (m, 2H), 3.47-3.43 (m, 2H), 2.87 – 2.83 (m, 2H); ^{13}C NMR (101 MHz, $CDCl_3$) δ 206.96, 156.56, 136.69, 134.83, 130.70, 129.33, 129.06, 128.65, 127.21, 124.55, 119.65, 36.30, 24.48.

2,3-Dihydro-1*H*-cyclopenta[a]naphthalene-3-ol; C

$NaBH_4$ (74 mg, 1.96 mmol) was added to a stirred solution of **B** (90 mg, 0.49 mmol) in dry MeOH/THF (10 mL, 2;1) at 0 ^{o}C (ice-bath). After 5 min, the reaction mixture was allowed to warm to rt and stirring was continued for 1 h. Water (2 mL) was then added to quench the reaction. The mixture was concentrated under reduced pressure and extracted with EtOAc. The organic phase was separated, dried over anhydrous Na_2SO_4, filtered, and evaporated. The residue was column chromatographed (EtOAc in hexane 20 → 30%) to give **C** (85 mg, 94%) as an off-white solid: ^{1}H NMR (400 MHz, $CDCl_3$) δ 7.88 (dd, *J* = 7.6, 2.0 Hz, 1H), 7.85 (ddd, *J* = 7.6, 2.0, 0.8 Hz, 1H), 7.77 (dd, *J* = 8.4, 0.8 Hz, 1H), 7.56 (d, *J* = 8.4 Hz, 1H), 7.54 – 7.46 (m, 2H), 5.45 (t, *J* = 6.4 Hz, 1H), 3.43 (ddd, *J* = 16.0, 8.8, 4.8 Hz, 1H), 3.17-3.09 (m, 1H), 2.71 (dddd, *J* = 15.6, 11.6, 6.8, 4.4 Hz, 1H), 2.12 (dddd, *J* = 14.8, 10.4, 6.0, 4.8 Hz, 1H), 1.83 (s, 1H); ^{13}C NMR (101 MHz, $CDCl_3$) δ 141.68, 139.78, 133.85, 130.48, 128.65, 127.84, 126.35, 125.97, 124.66, 122.40, 77.57, 35.63, 28.36.

1*H*-Cyclopenta[a]naphthalene; P3

The secondary alcohol **C (**75 mg, 0.41 mmol) was dissolved in the mixture of THF/H_2O (6 mL, 1:1). Aqueous 4 N HCl (1.0 mL, 4 mmol) was then added and the reaction mixture was refluxed at 105 ^{o}C for 12 h. The reaction mixture was transferred to a separatory funnel and extracted with EtOAc. The organic phase was separated, dried over anhydrous Na_2SO_4, filtered, and evaporated. The residue was column chromatographed (*n*-hexane) to give **P3** (27 mg, 40%) as a light yellow solid: ^{1}H NMR (400 MHz, $CDCl_3$) δ 7.97 (d, *J* = 8.0 Hz, 1H), 7.88 (d, *J* = 8.4 Hz, 1H), 7.78 (d, *J* = 8.0 Hz, 1H), 7.60 (d, *J* = 8.0 Hz, 1H), 7.49 (t, *J* = 7.2 Hz, 1H), 7.40 (t, *J* = 7.2 Hz, 1H), 7.03 – 7.01 (m, 1H), 6.68 – 6.66 (m, 1H), 3.73 (s, 2H); ^{13}C NMR (101 MHz, $CDCl_3$) δ 142.39, 140.35, 133.80, 132.79, 131.63, 130.24, 128.97, 127.25, 126.29, 124.62, 123.66, 120.65, 38.19.

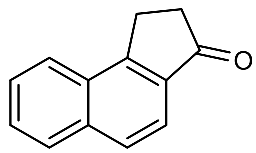

O

B

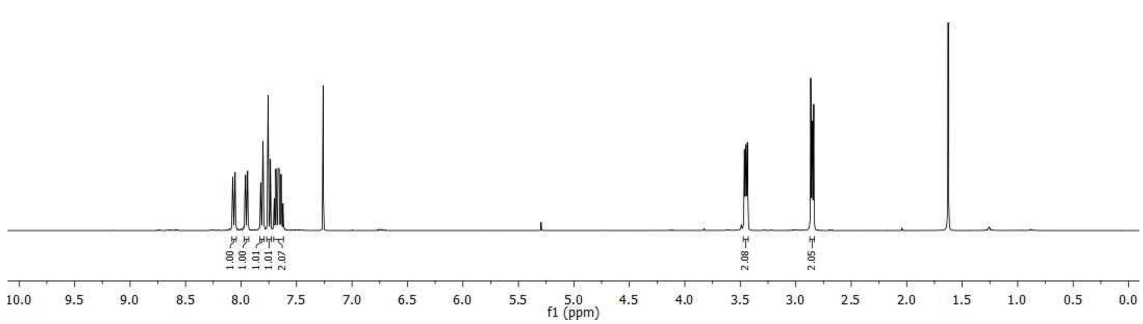

8.076
8.074
8.071
8.056
8.054
8.052
7.963
7.959
7.945
7.941
7.823
7.802
7.757
7.736
7.700
7.686
7.683
7.667
7.663
7.660
7.656
7.639
7.636
7.260 CDCl3
3.463
3.449
3.436
2.865
2.860
2.857
2.852
2.847
2.843
2.838
1.626 HDO
1.00
1.00
1.01
1.01
2.07
2.08
2.05
f1 (ppm)

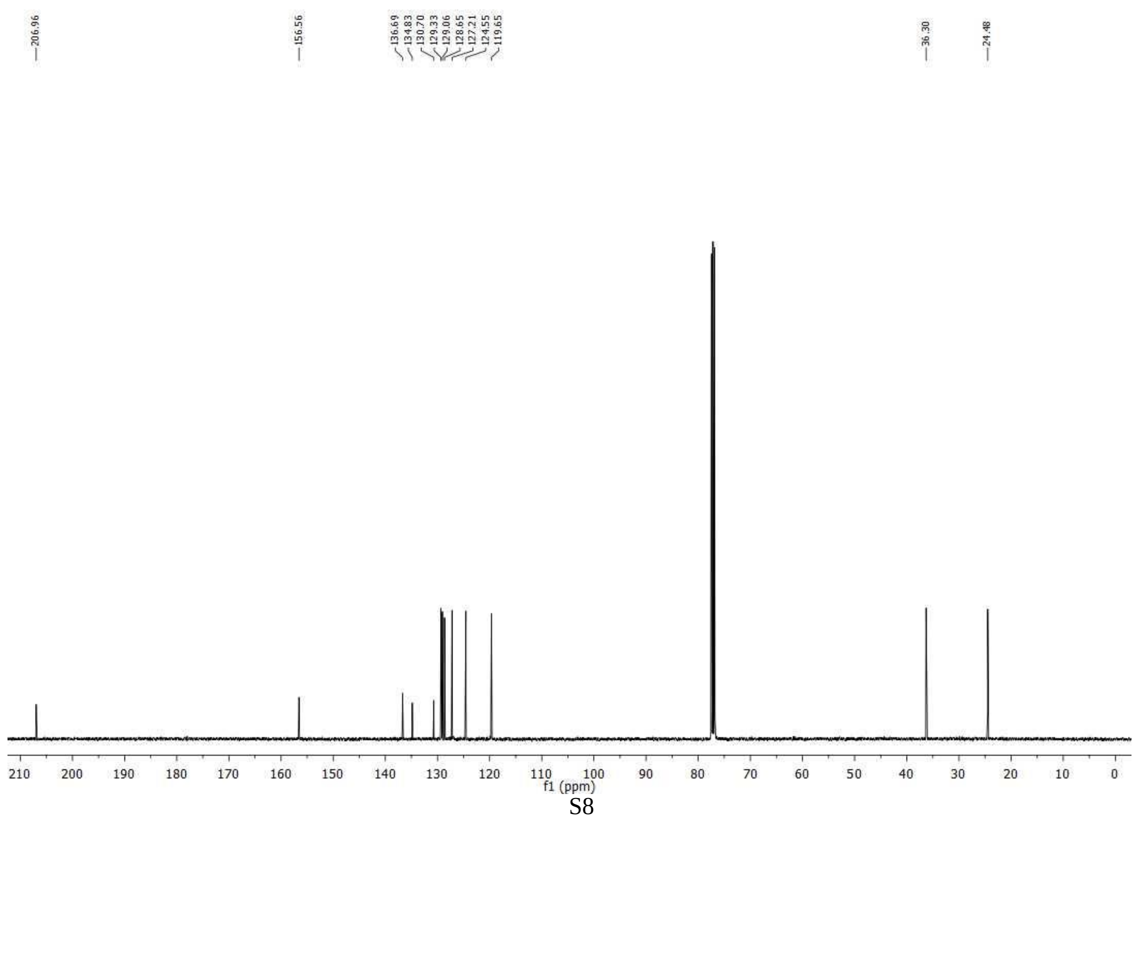

206.96
156.56
136.69
134.83
130.70
129.33
129.06
128.65
127.21
124.55
119.65
36.30
24.48
f1 (ppm)

Figure S5. ^{1}H NMR and ^{13}C NMR spectra of compound **B** in $CDCl_3$.

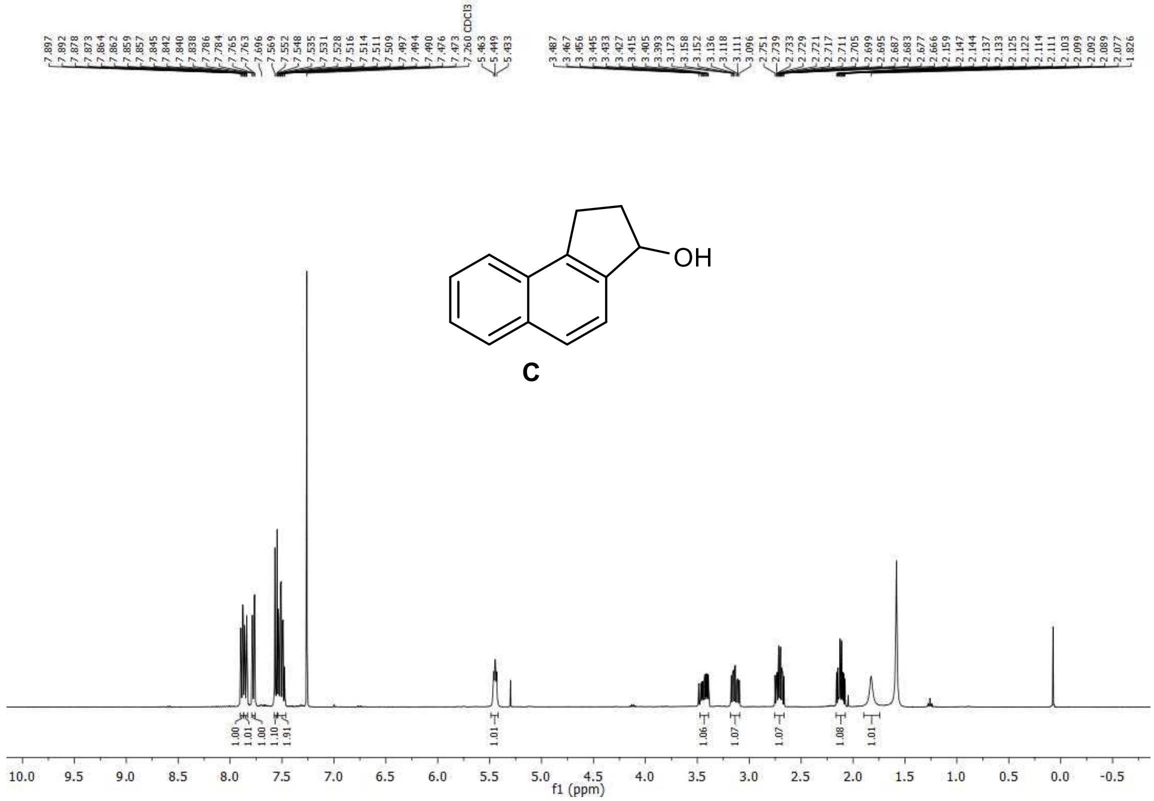

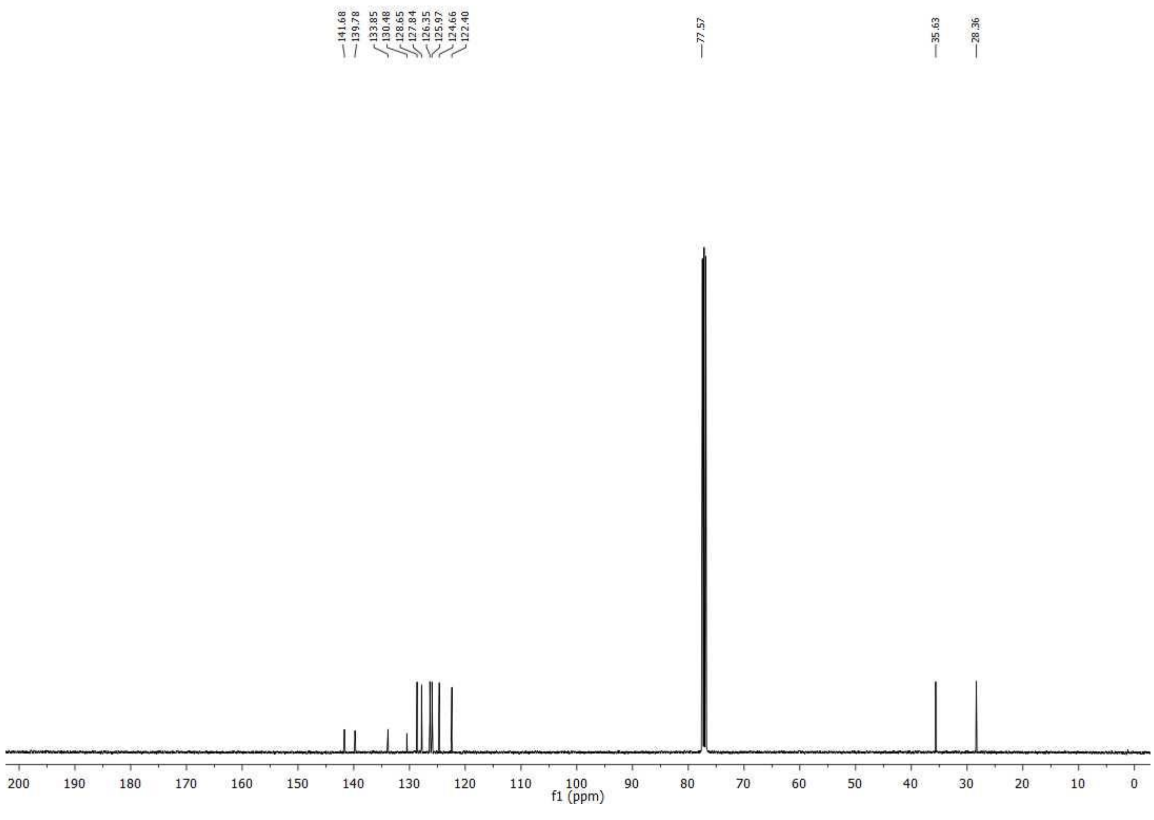

Figure S6. ^{1}H NMR and ^{13}C NMR spectra of compound **C** in $CDCl_3$

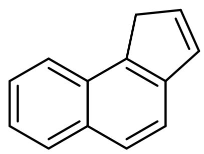

P3

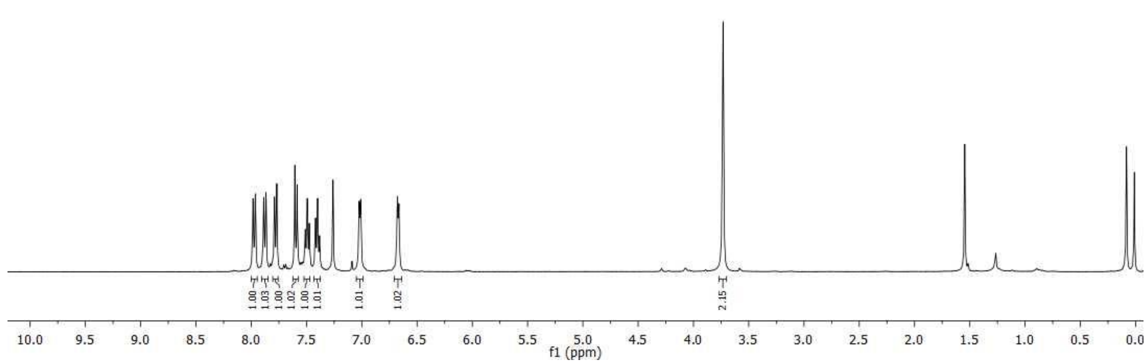

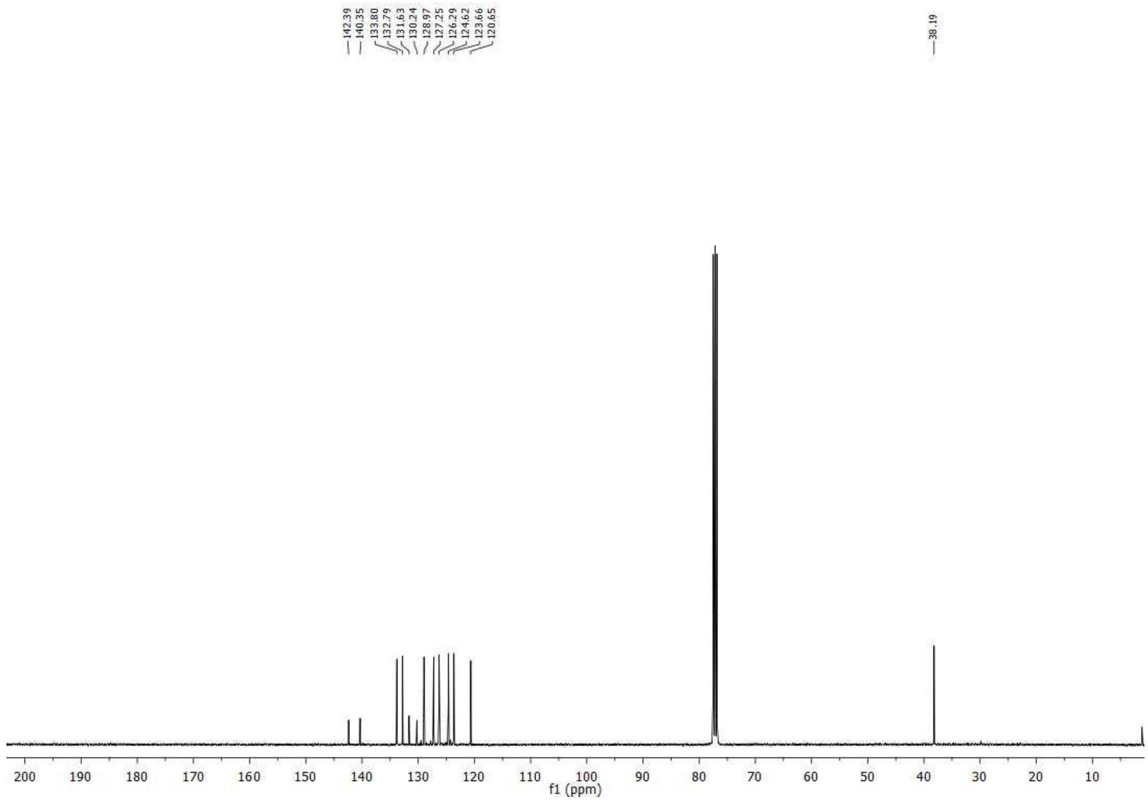

Figure S7. ^{1}H NMR and ^{13}C NMR spectra of compound **P3** in $CDCl_3$.

Optimized Cartesian Coordinates (Å) and Calculated Vibrational Frequencies (cm^{-1}) for the 5-Indenyl + Vinylacetylene System

Reactants

Vinylacetylene C_4H_4, C_s, $^{1}A'$

6	0	0.121125	-1.700404	0.000000
6	0	-0.579921	-0.557132	0.000000
6	0	0.000000	0.743992	0.000000
6	0	0.453986	1.866353	0.000000
1	0	1.206897	-1.705189	0.000000
1	0	-0.382460	-2.662132	0.000000
1	0	-1.669070	-0.596050	0.000000
1	0	0.873491	2.846518	0.000000

Frequencies

229.5891	339.4361	558.9958
588.1117	631.2114	714.7025
899.2819	944.5974	1013.3805
1122.3708	1335.8813	1463.2716
1690.9964	2223.9797	3158.4122
3178.0551	3263.9634	3495.5663

5-1H-indenyl C_9H_7, C_s, $^{2}A'$

6	0	-0.340876	-0.684507	0.000000
6	0	0.000000	0.685392	0.000000
6	0	1.325254	1.095426	0.000000
6	0	2.342318	0.123184	0.000000
6	0	1.950136	-1.195996	0.000000
6	0	0.658505	-1.668764	0.000000
6	0	-1.802274	-0.794823	0.000000
6	0	-2.347930	0.433727	0.000000
6	0	-1.275313	1.496181	0.000000
1	0	1.586154	2.149465	0.000000
1	0	3.386931	0.413175	0.000000
1	0	0.419882	-2.726900	0.000000
1	0	-2.343252	-1.732589	0.000000
1	0	-3.406242	0.659317	0.000000
1	0	-1.351195	2.149305	0.878439
1	0	-1.351195	2.149305	-0.878439

Frequencies

193.0636	221.9687	390.3952
391.4342	419.3922	532.9600
546.9856	603.7417	695.8004
734.6857	738.9651	781.4171
827.7034	858.4912	865.7767
928.0563	956.3110	956.3483
964.2426	1041.1762	1086.0045
1124.6772	1148.9166	1170.5416
1205.3139	1238.7476	1287.2114
1320.6399	1376.0584	1417.5719
1438.0175	1458.8385	1564.1300
1620.1414	1633.3490	3015.3295
3038.1201	3152.6851	3164.7501
3174.5852	3190.8419	3213.4939

Intermediates

[i0a] $C_{13}H_{11}$, C_1, ^2A

6	0	-2.413803	0.473979	0.152369
6	0	-1.394140	-0.405553	-0.271135
6	0	-0.117763	0.057977	-0.556227
6	0	0.157350	1.431766	-0.418521
6	0	-0.875500	2.240951	-0.001904
6	0	-2.158958	1.846114	0.295972
6	0	-3.633788	-0.307793	0.372200
6	0	-3.394977	-1.602963	0.102358
6	0	-1.962959	-1.804384	-0.331149
6	0	4.260536	-0.518160	0.830946
6	0	3.396277	-0.252923	1.816116
6	0	3.826817	-0.120138	-1.730197
6	0	4.003282	-0.294555	-0.550864
1	0	0.669654	-0.614756	-0.881557
1	0	1.145962	1.818890	-0.637541
1	0	-2.927261	2.539988	0.619931
1	0	-4.575972	0.111415	0.701899
1	0	-4.111652	-2.410340	0.176577
1	0	-1.900667	-2.233919	-1.338914
1	0	-1.430826	-2.497090	0.332860
1	0	5.237101	-0.933306	1.067952
1	0	2.414668	0.160879	1.618233

1	0	3.659157	-0.447416	2.848826
1	0	3.665595	0.039752	-2.768061

Frequencies

7.9503	14.0869	15.0599
27.9534	40.5263	43.3326
195.1020	222.4223	228.3440
319.3288	390.4235	392.3506
421.5745	532.6202	548.3044
559.3361	604.0084	646.1855
681.8311	696.0756	704.4418
735.0659	738.5748	793.2958
827.8719	858.1796	865.4396
891.9652	934.0723	956.2115
960.6860	964.4556	969.7989
1010.5092	1040.6757	1085.6784
1112.4783	1124.6234	1148.7042
1170.3438	1204.7077	1238.2372
1287.1256	1319.8954	1322.5491
1375.8913	1415.8596	1437.8725
1445.8026	1458.4111	1562.7481
1619.1952	1632.5605	1668.1787
2201.4000	3015.6658	3038.2534
3135.6727	3146.9947	3158.6992
3164.0422	3176.7023	3190.2502
3212.9811	3236.6107	3475.6129

[i0b] $C_{13}H_{11}$, C_1, ^2A

6	0	1.956554	-0.594057	-0.101893
6	0	2.926697	0.412771	0.092960
6	0	2.569518	1.751326	0.162833
6	0	1.213590	2.105650	0.036311
6	0	0.315959	1.080064	-0.151125
6	0	0.599369	-0.263177	-0.230547
6	0	2.637908	-1.891067	-0.130980
6	0	3.959412	-1.709792	0.035809
6	0	4.283792	-0.244003	0.194417
6	0	-3.367705	0.630730	-0.164410
6	0	-4.484900	0.183954	-0.230916
6	0	-5.802952	-0.336074	-0.355905
6	0	-6.534200	-0.804186	0.661030

1	0	3.316744	2.524683	0.312436
1	0	0.903514	3.143106	0.085761
1	0	-0.164296	-1.018456	-0.381070
1	0	2.136211	-2.840576	-0.267124
1	0	4.709988	-2.488898	0.057549
1	0	4.972551	0.105968	-0.584701
1	0	4.772757	-0.038080	1.154834
1	0	-2.379542	1.021590	-0.094003
1	0	-6.218269	-0.339751	-1.360933
1	0	-6.153799	-0.815656	1.675499
1	0	-7.534106	-1.186771	0.496238

Frequencies

4.1975	6.2751	10.2151
20.3332	37.0028	50.2474
193.2095	222.3959	226.3791
321.0334	391.1724	391.3840
419.3702	532.4940	543.9750
557.2327	604.7971	693.0024
694.5777	702.9853	709.0506
734.5147	738.9394	777.7118
828.0454	859.4834	866.0302
892.5266	927.2492	951.9828
956.0291	956.5659	965.0345
1010.4641	1042.4906	1086.0790
1111.7345	1124.9486	1149.4485
1170.7252	1205.9217	1239.4749
1287.7240	1320.1117	1321.0168
1376.3105	1417.8115	1437.7179
1443.2442	1458.8706	1563.8833
1619.4625	1633.3771	1668.0570
2200.4372	3016.0109	3038.9804
3133.4321	3146.0366	3154.5878
3167.8927	3177.0800	3192.2166
3214.5148	3234.8585	3436.0646

[i1] $C_{13}H_{11}$, C_1, ^2A

6	0	1.709350	-0.631600	-0.031487
6	0	1.907258	0.761988	-0.013615
6	0	0.833326	1.620914	-0.193702
6	0	-0.439666	1.082355	-0.390551

6	0	-0.649950	-0.303698	-0.414497
6	0	0.436073	-1.164395	-0.231046
6	0	3.006643	-1.279969	0.180494
6	0	3.962579	-0.345520	0.323494
6	0	3.373695	1.041143	0.216450
6	0	-2.967770	-0.573553	0.536329
6	0	-2.052173	-0.854287	-0.626320
6	0	-5.286082	0.562651	0.289041
6	0	-4.194865	0.026438	0.411503
1	0	0.970561	2.697495	-0.183876
1	0	0.284693	-2.239439	-0.249538
1	0	3.155440	-2.352036	0.214354
1	0	5.014897	-0.532038	0.492700
1	0	3.821449	1.611227	-0.607426
1	0	3.546003	1.628355	1.127360
1	0	-2.629070	-0.864208	1.526341
1	0	-2.488451	-0.438342	-1.538475
1	0	-1.983717	-1.939563	-0.779087
1	0	-6.235767	1.027191	0.188302
1	0	-1.286545	1.746563	-0.527216

Frequencies

19.1898	24.6641	99.5756
167.2659	195.6223	208.6313
273.1625	333.5220	388.2351
398.2869	412.9301	437.4730
440.4372	487.7944	553.5826
594.2484	607.5389	644.1581
650.9059	715.1717	751.2293
752.6254	775.4405	832.9936
856.0138	875.1782	896.5276
939.6754	945.5221	960.5454
961.9726	968.1893	1024.0670
1091.6673	1138.3501	1143.7370
1147.2101	1156.1514	1187.5556
1204.0527	1239.4310	1258.6515
1294.5096	1313.8051	1344.5907
1379.6060	1401.4142	1436.8149
1463.2378	1474.8897	1501.7280
1601.9483	1629.7418	1653.8693
2013.3749	2995.7770	3014.0799

3036.5019	3065.8727	3150.2805
3154.3204	3155.5169	3172.9620
3188.7274	3212.7094	3469.3721

[i2] $C_{13}H_{11}$, C_1, ^2A

6	0	1.293982	-0.620372	-0.063401
6	0	2.182098	0.468893	0.071297
6	0	1.690722	1.761556	0.139692
6	0	0.310112	1.965227	0.073051
6	0	-0.583625	0.891814	-0.061390
6	0	-0.078190	-0.416865	-0.129518
6	0	2.089505	-1.851272	-0.108185
6	0	3.395852	-1.551864	-0.007991
6	0	3.596094	-0.059628	0.115903
6	0	-2.033744	1.173306	-0.128051
6	0	-2.999540	0.302277	-0.260839
6	0	-4.013282	-0.575132	-0.408303
6	0	-4.706204	-1.202113	0.625856
1	0	2.358783	2.610470	0.243531
1	0	-0.084661	2.974514	0.125522
1	0	-0.762115	-1.252711	-0.231317
1	0	1.670380	-2.844688	-0.207459
1	0	4.213083	-2.261106	-0.012503
1	0	4.213410	0.337924	-0.699723
1	0	4.109056	0.206594	1.048839
1	0	-2.302941	2.230169	-0.056224
1	0	-4.310233	-0.810025	-1.431229
1	0	-4.459367	-1.010604	1.662222
1	0	-5.508072	-1.895493	0.409626

Frequencies

37.3302	51.9800	115.4053
156.1684	198.8267	227.4695
239.2652	333.8724	361.0310
397.6764	434.2973	445.3417
515.2342	544.0238	583.0848
600.9403	611.4748	711.4759
746.3576	748.3893	749.6278
785.5882	796.2849	850.2891
852.7829	908.9120	919.6846
936.0838	940.6584	953.4673

961.9971	965.9968	968.5694
1082.3080	1094.4621	1140.2472
1148.0051	1156.9634	1191.1496
1202.9389	1236.0820	1252.4510
1278.8366	1327.0621	1346.8922
1376.1227	1417.9304	1438.2388
1465.3835	1490.4663	1497.5140
1603.1148	1628.0953	1654.1083
1888.4606	3012.8439	3034.8010
3057.3787	3093.6820	3149.1097
3154.7445	3168.0359	3171.6106
3189.5679	3212.7673	3249.7519

[i3] $C_{13}H_{11}$, C_1, ^2A

6	0	1.571703	-0.668259	-0.170905
6	0	2.148314	0.599564	0.101288
6	0	1.359030	1.738704	0.120656
6	0	-0.013317	1.633497	-0.129517
6	0	-0.621653	0.393707	-0.404915
6	0	0.219896	-0.701367	-0.406476
6	0	2.633158	-1.677657	-0.130378
6	0	3.805834	-1.084261	0.150399
6	0	3.630275	0.405410	0.325708
6	0	-2.109133	0.275618	-0.653059
6	0	-2.862071	-0.307481	0.569100
6	0	-4.299738	-0.425118	0.345242
6	0	-5.480210	-0.510267	0.136319
1	0	1.794645	2.711297	0.324378
1	0	-0.630986	2.526716	-0.120181
1	0	2.472883	-2.733395	-0.303405
1	0	4.761627	-1.582470	0.243980
1	0	4.233292	0.973818	-0.393553
1	0	3.942737	0.737781	1.323703
1	0	-2.523915	1.257968	-0.891614
1	0	-2.293606	-0.368788	-1.516381
1	0	-2.445950	-1.291656	0.809123
1	0	-2.678758	0.326704	1.443300
1	0	-6.524505	-0.590508	-0.040127

Frequencies

26.3390	58.1487	60.8122

152.2198	191.6722	197.5596
270.7359	329.4724	352.8966
397.2419	421.7177	439.5967
478.8960	546.6679	594.4029
620.8555	663.9575	674.7589
697.0232	747.3365	750.8051
767.7881	784.2304	816.9490
852.7346	928.7575	944.6726
954.4810	958.5765	963.0623
974.1759	1011.2260	1027.1384
1079.1923	1136.2829	1146.4051
1160.0811	1180.4798	1219.9485
1252.5205	1262.8411	1292.1092
1310.5651	1331.9455	1360.1402
1371.6427	1434.5292	1446.8275
1454.0743	1476.7182	1497.7769
1565.2409	1615.3197	1646.6747
2220.2512	3014.5055	3023.6031
3037.9630	3048.1293	3052.3756
3091.6110	3148.8040	3169.9316
3197.7203	3219.5324	3478.1161

[i4] $C_{13}H_{11}$, C_1, ^2A

6	0	-0.940202	-0.465611	0.050457
6	0	-1.683552	0.730445	-0.034588
6	0	-1.044084	1.956753	-0.057570
6	0	0.354395	1.987868	0.013452
6	0	1.106435	0.818648	0.103415
6	0	0.458258	-0.438655	0.118220
6	0	-1.885571	-1.586874	0.037801
6	0	-3.144187	-1.121516	-0.043986
6	0	-3.153271	0.386491	-0.098985
6	0	2.613736	0.866150	0.273815
6	0	3.338402	-0.327765	-0.398614
6	0	2.579314	-1.558119	-0.079203
6	0	1.286190	-1.664589	0.169653
1	0	-1.606101	2.882051	-0.129621
1	0	0.866851	2.944681	0.003861
1	0	-1.605820	-2.631104	0.085320
1	0	-4.043196	-1.723099	-0.069460
1	0	-3.717318	0.822119	0.735535

1	0	-3.624890	0.757678	-1.017644
1	0	3.014785	1.808764	-0.108644
1	0	2.839934	0.835444	1.347864
1	0	3.379445	-0.198968	-1.488969
1	0	4.373272	-0.378062	-0.047512
1	0	0.807862	-2.618863	0.366070

Frequencies

100.8064	122.8722	191.6841
221.0765	239.8362	320.7981
362.9138	398.3263	420.6233
466.0411	487.5212	525.2545
552.7059	616.9461	626.6907
708.0155	718.5461	756.8742
766.9664	819.3274	831.3602
842.7495	874.6128	904.9534
934.4935	950.4602	954.1875
959.8006	961.7809	977.4639
1020.0962	1043.2416	1125.3655
1147.6095	1159.7515	1175.7962
1197.9630	1214.9531	1229.3850
1244.5555	1267.4100	1291.2724
1323.8411	1340.6771	1358.0440
1395.5525	1435.6760	1450.7272
1465.2809	1475.1137	1479.3824
1604.0711	1624.1568	1640.5093
1683.2755	2992.5872	3002.0328
3013.4345	3035.6397	3055.3536
3064.8116	3152.2334	3153.6689
3170.3515	3193.1758	3215.2857

[i5] $C_{13}H_{11}$, C_s, $^2A''$

6	0	0.962260	-0.405998	0.000000
6	0	0.578094	-1.755926	0.000000
6	0	-0.763742	-2.110416	0.000000
6	0	-1.724899	-1.094570	0.000000
6	0	-1.372350	0.253468	0.000000
6	0	0.000000	0.632552	0.000000
6	0	2.426113	-0.351308	0.000000
6	0	2.929986	-1.599008	0.000000
6	0	1.817978	-2.617982	0.000000

6	0	-2.459318	1.312404	0.000000
6	0	0.357674	2.018229	0.000000
6	0	-0.627422	3.022483	0.000000
6	0	-1.961741	2.724719	0.000000
1	0	-1.069703	-3.151280	0.000000
1	0	-2.777713	-1.361093	0.000000
1	0	3.011483	0.558680	0.000000
1	0	3.979605	-1.861394	0.000000
1	0	1.865237	-3.274119	0.878406
1	0	1.865237	-3.274119	-0.878406
1	0	-3.119421	1.157344	-0.868423
1	0	-3.119421	1.157344	0.868423
1	0	1.403869	2.296540	0.000000
1	0	-0.314070	4.061737	0.000000
1	0	-2.700903	3.518479	0.000000

Frequencies

79.2257	111.2371	165.6439
237.3644	240.0496	304.3759
399.3095	418.5838	457.8222
461.7358	495.9142	529.2433
599.3024	600.9960	659.8510
662.9974	698.9020	730.9872
744.9458	798.9261	809.5701
833.4705	874.7439	925.1218
936.0879	942.7873	953.8186
954.5730	956.3344	964.7983
966.3135	1033.2506	1099.3012
1132.2813	1145.2536	1167.5734
1177.2311	1203.1482	1219.5623
1233.4672	1255.8415	1271.1454
1306.0796	1342.4045	1384.1335
1402.8621	1430.0805	1436.8785
1439.1890	1448.2143	1488.9798
1562.1478	1595.2184	1613.4987
1624.2574	2950.8735	2951.1885
3013.6398	3036.0542	3147.6114
3151.3053	3169.6435	3171.2872
3189.9296	3196.0160	3216.3533

[i6] $C_{13}H_{11}$, C_1, ^2A

6	0	1.640915	-0.642017	-0.100144
6	0	2.107443	0.680929	0.042607
6	0	1.221489	1.753411	-0.058059
6	0	-0.092378	1.417606	-0.296795
6	0	-0.623971	0.151450	-0.451231
6	0	0.293564	-0.909937	-0.343437
6	0	2.787718	-1.543814	0.048278
6	0	3.904074	-0.829599	0.271416
6	0	3.597375	0.649434	0.291937
6	0	-2.098080	-0.087695	-0.689845
6	0	-2.934974	0.077789	0.603698
6	0	-4.359928	-0.156224	0.390086
6	0	-5.527803	-0.355283	0.188030
1	0	1.548659	2.783228	0.043148
1	0	-0.056299	-1.932199	-0.458704
1	0	2.726110	-2.622961	-0.015168
1	0	4.898063	-1.230534	0.419220
1	0	4.156584	1.193533	-0.479457
1	0	3.865244	1.109336	1.251418
1	0	-2.473649	0.612243	-1.440416
1	0	-2.250030	-1.094904	-1.085669
1	0	-2.561432	-0.613131	1.367330
1	0	-2.783925	1.087299	1.000455
1	0	-6.561983	-0.528204	0.018605

Frequencies

25.4125	58.5970	62.0210
152.5493	197.6583	206.4384
266.5540	326.6006	352.5619
400.4553	409.9303	430.0956
458.5614	541.9977	601.9792
636.6865	664.1884	675.0781
702.6663	743.0876	745.4636
770.0182	778.4355	847.1947
854.4484	886.0556	921.2584
946.6530	955.3004	961.6237
966.8069	1013.0825	1019.5340
1092.4480	1141.7706	1146.2568
1163.1230	1179.9113	1233.5662
1254.7443	1263.5073	1290.7891
1306.3146	1331.3049	1361.2946

1369.2691	1424.7420	1436.1169
1460.9959	1476.8013	1497.7355
1567.1408	1611.5006	1640.6182
2220.3563	3016.1417	3023.6769
3039.2244	3048.3474	3052.4401
3091.8024	3146.7371	3158.6879
3190.0836	3213.6753	3478.1275

[i7] $C_{13}H_{11}$, C_1, ^2A

6	0	-1.458342	-0.726582	0.005456
6	0	-1.512287	0.679683	0.008386
6	0	-0.346567	1.425305	0.062222
6	0	0.892588	0.769751	0.115608
6	0	0.949878	-0.644243	0.124359
6	0	-0.228392	-1.384604	0.065503
6	0	-2.828699	-1.237062	-0.064409
6	0	-3.695349	-0.209130	-0.102417
6	0	-2.959271	1.109425	-0.060749
6	0	2.298058	-1.321738	0.288521
6	0	3.453244	-0.559556	-0.410096
6	0	3.288078	0.883275	-0.120756
6	0	2.162632	1.529107	0.126801
1	0	-0.375620	2.510953	0.054840
1	0	-0.184497	-2.469681	0.073081
1	0	-3.089028	-2.288119	-0.081434
1	0	-4.773277	-0.286106	-0.155135
1	0	-3.253567	1.713053	0.807158
1	0	-3.168323	1.720931	-0.947573
1	0	2.528069	-1.371668	1.361025
1	0	2.257412	-2.351967	-0.075882
1	0	4.415040	-0.944593	-0.058843
1	0	3.426531	-0.717380	-1.497119
1	0	2.123835	2.602797	0.289300

Frequencies

92.2730	125.5395	187.1191
253.3751	256.8313	317.0229
367.2295	392.2872	414.0118
432.0562	441.8394	519.1787
560.8412	638.9912	700.5585
718.6662	737.2266	755.0903

761.1461	779.8554	828.2434
865.1479	891.4462	894.0891
897.0562	927.1677	950.4545
954.9695	960.4073	973.8320
1021.0725	1066.5038	1112.5173
1146.7393	1171.0745	1180.5467
1196.2513	1212.9779	1232.5584
1246.0069	1278.7382	1292.8437
1323.7607	1327.8382	1356.3870
1381.2511	1436.6238	1455.7690
1467.5598	1476.9355	1499.8780
1574.0832	1624.8854	1649.5160
1685.2828	2992.0443	3001.7825
3014.1254	3036.6400	3055.4043
3064.1101	3140.1302	3151.5972
3153.5449	3188.1796	3212.7715

[i8] $C_{13}H_{11}$, C_s, $^2A''$

6	0	1.469071	-0.759783	0.000000
6	0	0.350461	-1.625977	0.000000
6	0	-0.926193	-1.114347	0.000000
6	0	-1.130087	0.289727	0.000000
6	0	0.000000	1.157229	0.000000
6	0	1.286041	0.622449	0.000000
6	0	2.678448	-1.577148	0.000000
6	0	2.348170	-2.882850	0.000000
6	0	0.846992	-3.054326	0.000000
6	0	-0.190609	2.662649	0.000000
6	0	-2.448736	0.840891	0.000000
6	0	-1.617947	3.117347	0.000000
6	0	-2.659370	2.232408	0.000000
1	0	-1.793058	-1.768642	0.000000
1	0	2.144565	1.288396	0.000000
1	0	3.685302	-1.178285	0.000000
1	0	3.040769	-3.714094	0.000000
1	0	0.500437	-3.613050	0.878429
1	0	0.500437	-3.613050	-0.878429
1	0	0.331467	3.095317	0.868482
1	0	0.331467	3.095317	-0.868482
1	0	-3.296117	0.164824	0.000000
1	0	-1.804949	4.185688	0.000000

1	0	-3.677772	2.607959	0.000000

Frequencies

70.4352	120.7611	159.2442
255.1103	266.9734	307.6414
398.2054	408.3799	414.8067
429.6699	495.9819	558.6225
585.5938	631.3007	664.7430
706.6247	724.0272	746.1902
747.9620	782.7334	783.8659
863.2247	883.1577	885.2209
899.5266	946.6566	950.1786
952.1518	954.1532	959.5561
964.6461	1048.3517	1100.4563
1124.4145	1148.8423	1166.1281
1180.9999	1203.7761	1227.6961
1241.9142	1253.3917	1272.7095
1311.9502	1331.2744	1367.7929
1392.6479	1434.8241	1440.4195
1447.3931	1464.9132	1493.8426
1561.3115	1576.4664	1614.8079
1641.0103	2950.2364	2950.6348
3014.2562	3036.5516	3146.4447
3150.5680	3152.1584	3168.7983
3179.8973	3188.0434	3212.4721

Products

3H-cyclopenta[a]naphthalene [P1] $C_{13}H_{10}$, C_s, $^1A'$

6	0	0.924373	-0.413419	0.000000
6	0	0.483046	-1.732947	0.000000
6	0	-0.887360	-2.042206	0.000000
6	0	-1.807157	-1.016884	0.000000
6	0	-1.397836	0.344203	0.000000
6	0	0.000000	0.667509	0.000000
6	0	2.390825	-0.418136	0.000000
6	0	2.839112	-1.686514	0.000000
6	0	1.680062	-2.650712	0.000000
6	0	0.386186	2.032362	0.000000
6	0	-0.556046	3.032961	0.000000
6	0	-1.933972	2.716786	0.000000
6	0	-2.341373	1.405165	0.000000

1	0	-1.219072	-3.075382	0.000000
1	0	-2.869477	-1.237091	0.000000
1	0	3.013043	0.467065	0.000000
1	0	3.875258	-1.997286	0.000000
1	0	1.695725	-3.308892	0.878281
1	0	1.695725	-3.308892	-0.878281
1	0	1.440453	2.284459	0.000000
1	0	-0.244318	4.071476	0.000000
1	0	-2.667798	3.514960	0.000000
1	0	-3.398687	1.160579	0.000000

Frequencies

114.2372	132.0570	229.1156
242.3782	268.5622	387.5335
433.0191	439.3947	463.9684
506.3711	519.7729	565.1862
613.0959	666.4571	682.1473
723.5469	748.9623	753.2205
798.5637	818.1915	841.1685
879.3718	882.5764	933.2719
950.4223	955.5959	959.0772
967.2270	969.3689	992.6970
1044.1496	1074.2564	1126.8287
1141.8636	1167.2558	1178.6990
1191.9635	1216.4784	1236.8079
1283.6730	1293.2675	1352.2697
1378.6488	1389.4194	1430.2038
1431.5527	1469.4414	1486.5783
1555.3473	1585.0322	1619.0469
1634.2600	1664.4750	3013.2641
3035.9395	3155.0041	3156.8946
3164.8202	3173.8559	3176.9878
3187.3411	3195.5485	3217.5782

1H-cyclopenta[b]naphthalene [P2] $C_{13}H_{10}$, C_s, $^1A'$

6	0	-0.274495	-1.600869	0.000000
6	0	-1.428382	-0.755109	0.000000
6	0	-1.297784	0.604896	0.000000
6	0	0.000000	1.192878	0.000000
6	0	1.157970	0.345205	0.000000
6	0	0.991533	-1.065552	0.000000

6	0	-0.739094	-2.988790	0.000000
6	0	-2.082493	-3.023472	0.000000
6	0	-2.664072	-1.628432	0.000000
6	0	2.442505	0.949854	0.000000
6	0	0.184026	2.598751	0.000000
6	0	2.584192	2.316613	0.000000
6	0	1.443138	3.150646	0.000000
1	0	-2.167492	1.255386	0.000000
1	0	1.870386	-1.702573	0.000000
1	0	-0.082590	-3.849851	0.000000
1	0	-2.692519	-3.917436	0.000000
1	0	-3.297001	-1.450501	0.878396
1	0	-3.297001	-1.450501	-0.878396
1	0	3.318424	0.309101	0.000000
1	0	-0.692984	3.238165	0.000000
1	0	3.573446	2.760523	0.000000
1	0	1.565067	4.227980	0.000000

Frequencies

101.6939	135.6973	251.2229
263.6581	278.7787	393.8545
406.0427	417.1045	426.3078
485.8694	560.0141	577.9544
628.7414	686.3422	732.7069
737.9740	751.3041	764.3906
782.9561	806.1093	856.7377
857.4651	888.3833	900.8895
913.7686	955.7244	957.3809
962.2859	970.1595	991.2861
1043.3698	1077.5211	1121.5879
1154.8071	1169.1007	1174.4976
1180.5263	1244.3719	1251.1493
1268.1191	1282.2110	1348.0689
1373.3486	1387.6188	1434.8920
1446.7381	1470.2751	1486.6068
1537.3062	1611.9868	1627.0489
1654.9286	1677.6559	3012.8723
3034.3514	3151.7288	3154.3238
3157.7318	3161.0250	3172.2271
3185.5638	3188.8036	3211.4998

5-((E)-but-1-en-3-ynyl)-1H-indene [P4] $C_{13}H_{10}$, C_s, $^1A'$

6	0	-1.383771	-0.816307	0.000000
6	0	-2.201038	0.335263	0.000000
6	0	-1.626000	1.595005	0.000000
6	0	-0.234456	1.701523	0.000000
6	0	0.597423	0.566598	0.000000
6	0	0.000000	-0.708454	0.000000
6	0	-2.258334	-1.993120	0.000000
6	0	-3.544230	-1.602736	0.000000
6	0	-3.647800	-0.095741	0.000000
6	0	2.046048	0.772235	0.000000
6	0	3.005191	-0.175064	0.000000
6	0	4.392769	0.111153	0.000000
6	0	5.580868	0.318742	0.000000
1	0	-2.238065	2.490951	0.000000
1	0	0.224720	2.684297	0.000000
1	0	0.611902	-1.603194	0.000000
1	0	-1.904273	-3.016311	0.000000
1	0	-4.406924	-2.255799	0.000000
1	0	-4.190590	0.276330	0.878190
1	0	-4.190590	0.276330	-0.878190
1	0	2.368040	1.809940	0.000000
1	0	2.740544	-1.228788	0.000000
1	0	6.625213	0.511659	0.000000

Frequencies

41.3854	76.2752	88.7572
168.4440	199.8460	207.9519
315.0984	326.0922	395.6476
412.6149	419.9192	476.7744
495.1764	562.1622	615.5683
624.2264	626.0156	679.6003
715.0217	745.3753	755.6125
809.7724	820.0342	855.1418
871.4554	891.8096	938.0962
952.7129	962.0506	967.4890
970.9169	990.9841	1035.1887
1094.4578	1141.3337	1148.6789
1158.1166	1208.3136	1238.6626
1262.5411	1288.6255	1318.6665
1341.8769	1349.1121	1384.2579

1437.0368	1465.5309	1501.3434
1599.7722	1625.6737	1649.1397
1669.6653	2194.1225	3013.9382
3036.0703	3141.2986	3151.6874
3158.5500	3174.4784	3175.7091
3190.6567	3213.9080	3477.9449

5-(but-3-en-1-ynyl)-1H-indene [P5] $C_{13}H_{10}$, C_s, $^1A'$

6	0	0.303343	-1.795813	0.000000
6	0	-1.095489	-1.975727	0.000000
6	0	-1.943454	-0.878223	0.000000
6	0	-1.395967	0.403623	0.000000
6	0	0.000000	0.597514	0.000000
6	0	0.856020	-0.521038	0.000000
6	0	0.933153	-3.119804	0.000000
6	0	-0.015056	-4.072134	0.000000
6	0	-1.393805	-3.455595	0.000000
6	0	0.539274	1.914721	0.000000
6	0	0.988472	3.039716	0.000000
6	0	1.556166	4.338110	0.000000
6	0	0.858632	5.482000	0.000000
1	0	-3.021162	-1.004356	0.000000
1	0	-2.042768	1.272314	0.000000
1	0	1.929423	-0.372552	0.000000
1	0	2.002903	-3.286240	0.000000
1	0	0.156406	-5.140435	0.000000
1	0	-1.977354	-3.759841	0.878198
1	0	-1.977354	-3.759841	-0.878198
1	0	2.643263	4.380334	0.000000
1	0	-0.224864	5.486480	0.000000
1	0	1.363783	6.440033	0.000000

Frequencies

37.3530	59.4502	71.1221
175.7068	182.7313	196.7812
289.6946	333.7955	383.1536
395.7752	410.7592	475.5495
503.5157	557.6953	613.0435
628.7753	691.8118	694.4499
714.7585	747.9352	758.4873
833.3893	850.3109	886.9347

903.9531	936.6605	939.8884
955.5093	963.8808	969.3097
988.0660	1006.8252	1087.6981
1101.8110	1142.8521	1147.9026
1177.0535	1210.6716	1245.4469
1288.7333	1309.7203	1319.5006
1340.1434	1366.4855	1435.7678
1443.8591	1460.9537	1498.7601
1593.9406	1622.9650	1648.3173
1665.3601	2297.3347	3013.9340
3036.1722	3127.7758	3145.4338
3162.7170	3182.7178	3191.6089
3191.9518	3214.5280	3234.7356

Transition states

[i0a] → [i1] $C_{13}H_{11}$, C_1, ^2A

6	0	-1.918514	-0.642900	0.070680
6	0	-1.979738	0.760619	-0.063750
6	0	-0.824051	1.520545	-0.173108
6	0	0.424365	0.874266	-0.149989
6	0	0.429304	-0.496655	-0.015786
6	0	-0.681733	-1.303241	0.096457
6	0	-3.288523	-1.155824	0.162890
6	0	-4.159607	-0.134482	0.090540
6	0	-3.431685	1.179814	-0.059479
6	0	3.653398	-0.736593	-0.560766
6	0	2.818305	-1.551049	0.115993
6	0	4.944715	1.297650	0.477036
6	0	4.343685	0.358145	0.016883
1	0	-0.871830	2.600587	-0.276071
1	0	1.345882	1.439590	-0.232932
1	0	-0.616620	-2.381591	0.200760
1	0	-3.542160	-2.202708	0.272511
1	0	-5.237998	-0.214250	0.131616
1	0	-3.662058	1.867507	0.763976
1	0	-3.716249	1.698239	-0.983774
1	0	3.805176	-0.890670	-1.625858
1	0	2.680924	-1.457307	1.185256
1	0	2.362088	-2.400450	-0.374923
1	0	5.473311	2.119284	0.893837

Frequencies

-109.6636	15.2019	29.2603
40.5122	81.0842	170.6361
195.0712	226.2267	231.5991
360.5137	391.7154	392.1893
420.3817	529.0208	550.7939
558.7483	593.4891	627.1295
676.4546	697.0965	716.9915
736.8666	740.3857	795.7224
814.0946	858.7222	861.5499
894.8322	920.1694	932.4135
956.0537	958.2670	963.7489
982.8647	1040.0645	1086.7855
1112.7856	1127.8259	1148.4564
1168.6988	1207.3232	1239.8583
1288.5305	1305.4199	1323.7831
1375.9126	1417.5433	1435.8496
1438.1322	1460.7758	1565.7523
1607.2372	1620.3709	1632.5060
2183.4535	3014.7392	3037.3693
3140.4843	3151.1902	3155.6490
3156.2324	3174.3537	3189.4352
3212.5363	3248.9910	3476.3532

[i1] → [P4] $C_{13}H_{11}$, C_1, ^2A

6	0	1.686442	-0.680660	-0.004812
6	0	2.081387	0.671087	-0.016296
6	0	1.126626	1.676784	0.040374
6	0	-0.222118	1.332433	0.102107
6	0	-0.635524	-0.012187	0.103672
6	0	0.339688	-1.022499	0.059095
6	0	2.893875	-1.509784	-0.064915
6	0	3.981614	-0.721559	-0.111096
6	0	3.587721	0.736294	-0.085083
6	0	-3.117917	0.387790	-0.127201
6	0	-2.049861	-0.408998	0.145737
6	0	-5.602515	-0.436095	-0.186966
6	0	-4.452029	-0.072849	-0.154735
1	0	1.417086	2.722299	0.044049
1	0	0.033863	-2.063734	0.071129
1	0	2.891619	-2.592428	-0.070084

1	0	5.009017	-1.057209	-0.159997
1	0	3.938510	1.270120	-0.977473
1	0	4.019319	1.260490	0.777025
1	0	-2.973051	1.444969	-0.329088
1	0	-2.235063	-1.473401	0.252181
1	0	-2.231605	-0.506665	2.238469
1	0	-6.612290	-0.764464	-0.212435
1	0	-0.961744	2.121492	0.166942

Frequencies

-538.5765	44.0429	77.4099
88.1213	159.3538	195.1057
217.9353	253.6778	299.1060
332.2775	354.6217	392.0713
397.0214	425.5673	466.1593
509.0859	568.4400	617.0577
624.2837	641.2482	678.7256
714.3188	747.6876	757.5920
799.1498	823.3815	849.3989
858.4636	901.7426	937.3464
947.9218	959.8336	962.6260
967.2444	987.9288	1042.7024
1091.2570	1137.9889	1147.4307
1174.6545	1205.5228	1239.0032
1255.8334	1296.6812	1307.4904
1324.9283	1349.6044	1381.3411
1435.4606	1457.0248	1500.4902
1599.5349	1610.2254	1630.6342
1651.5953	2181.8667	3014.1504
3036.4826	3146.7262	3158.0723
3160.8743	3163.5316	3184.5352
3191.3738	3214.5962	3476.6721

[i1] → **[i3]** $C_{13}H_{11}$, C_1, ^2A

6	0	1.140650	-0.598237	-0.096614
6	0	2.080590	0.439259	0.124588
6	0	1.672301	1.762066	0.233801
6	0	0.313890	2.083666	0.126956
6	0	-0.627191	1.071815	-0.088985
6	0	-0.188845	-0.239760	-0.193369
6	0	1.864121	-1.869682	-0.169445

6	0	3.179754	-1.648928	-0.004059
6	0	3.458234	-0.178760	0.198511
6	0	-2.132678	1.213347	-0.210347
6	0	-2.636938	-0.179661	-0.650159
6	0	-3.713635	-0.774432	0.070793
6	0	-4.601176	-1.298814	0.699059
1	0	2.400167	2.549706	0.399877
1	0	-0.004511	3.118277	0.210374
1	0	1.390805	-2.829202	-0.331064
1	0	3.955394	-2.403283	-0.009591
1	0	4.130634	0.217819	-0.572810
1	0	3.945645	0.013140	1.162823
1	0	-2.575081	1.489168	0.751011
1	0	-2.421438	1.985341	-0.930043
1	0	-2.750806	-0.275601	-1.731796
1	0	-1.537385	-0.801906	-0.441086
1	0	-5.387893	-1.754722	1.247936

Frequencies

-1645.5757	43.9178	92.2740
130.3900	184.5110	215.7462
246.3150	284.2900	375.8955
394.2850	421.4506	451.4411
485.3748	522.0465	550.6351
585.0681	602.6033	620.2243
666.0268	698.6040	751.7665
754.9918	807.6594	810.2291
848.6737	856.3503	930.8772
932.0978	954.4627	958.3130
963.4025	990.6142	1021.7421
1070.5103	1082.3830	1133.7964
1145.5522	1162.5318	1186.7676
1216.5669	1231.1964	1256.7963
1291.4096	1297.1294	1335.9358
1359.2127	1376.0061	1434.8172
1448.9873	1453.6786	1485.4127
1584.5872	1616.7976	1642.3407
1660.9132	2167.5609	3013.2733
3036.4271	3036.4499	3065.9734
3083.2292	3150.3559	3168.5322
3195.3308	3217.1730	3475.7960

[i3] → [i4] $C_{13}H_{11}$, C_1, ^2A

6	0	1.013715	-0.479919	-0.154852
6	0	1.766222	0.699026	0.076662
6	0	1.133123	1.928566	0.152531
6	0	-0.255738	1.994371	-0.004871
6	0	-1.026959	0.843734	-0.241344
6	0	-0.350398	-0.367976	-0.315195
6	0	1.941913	-1.615604	-0.172815
6	0	3.196632	-1.180741	0.032965
6	0	3.222933	0.319039	0.210969
6	0	-2.527071	0.941929	-0.442552
6	0	-3.346645	-0.029898	0.452576
6	0	-2.804553	-1.376847	0.298782
6	0	-1.885057	-2.129032	0.015546
1	0	1.698522	2.836331	0.336174
1	0	-0.753576	2.958079	0.052011
1	0	1.644054	-2.643772	-0.332512
1	0	4.084841	-1.797608	0.069107
1	0	3.848828	0.807618	-0.546642
1	0	3.636004	0.606448	1.186186
1	0	-2.860891	1.965613	-0.252692
1	0	-2.766682	0.712258	-1.486245
1	0	-3.279994	0.270775	1.504144
1	0	-4.403599	0.017597	0.172796
1	0	-1.316202	-3.013225	-0.152738

Frequencies

-372.3832	64.8145	90.2484
154.3351	194.0543	206.4422
301.2222	336.5116	359.7025
399.5989	439.3819	463.3781
468.9763	545.2956	585.2869
626.6863	651.3271	699.6645
705.0301	738.0138	749.6857
765.4171	814.6094	848.2439
851.5552	896.7419	928.7326
951.7592	954.0504	958.1540
987.0845	992.5472	1024.0618
1072.9425	1133.5981	1145.7804
1158.6694	1186.0144	1211.0169

1222.2206	1245.3887	1270.8859
1325.5325	1332.2820	1349.5683
1380.0249	1434.2532	1441.0575
1449.2882	1476.0405	1483.8427
1571.3105	1615.9357	1640.6549
2061.7093	3012.3629	3024.3397
3026.1075	3035.2018	3058.7386
3074.2120	3144.5102	3167.3217
3191.7733	3214.5129	3437.9273

[i4] → **[i5]** $C_{13}H_{11}$, C_1, ^2A

6	0	0.933942	-0.465560	-0.054102
6	0	1.687952	0.716748	0.042150
6	0	1.062600	1.953365	0.084993
6	0	-0.337702	2.006576	0.014344
6	0	-1.104412	0.853193	-0.090538
6	0	-0.480368	-0.430295	-0.119078
6	0	1.858967	-1.598018	-0.051869
6	0	3.126203	-1.149923	0.028696
6	0	3.153415	0.356407	0.096671
6	0	-2.610228	0.925795	-0.278128
6	0	-3.282142	-0.316953	0.261399
6	0	-2.679644	-1.586654	0.175319
6	0	-1.303989	-1.598622	-0.217844
1	0	1.637176	2.869840	0.167841
1	0	-0.833864	2.971896	0.027255
1	0	1.560897	-2.636733	-0.101554
1	0	4.017352	-1.763143	0.046770
1	0	3.718336	0.792799	-0.736865
1	0	3.633639	0.714273	1.016093
1	0	-3.018823	1.830248	0.180888
1	0	-2.835209	0.995258	-1.354533
1	0	-2.862492	-1.005324	1.312077
1	0	-4.304007	-0.229323	0.626408
1	0	-0.860571	-2.536139	-0.536452

Frequencies

-1514.2831	100.1474	110.4142
175.9726	233.3435	240.9282
308.8017	396.8593	421.4278
448.8008	464.9229	490.8814

522.6268	578.8461	609.9493
645.5944	692.1086	705.2015
724.0592	753.9355	796.9331
810.2492	831.7762	846.8874
916.5329	929.0883	946.8859
952.3852	960.9619	963.2822
965.8487	1031.1185	1070.1074
1124.7195	1146.0882	1162.0074
1185.6736	1217.2956	1220.3829
1230.3427	1258.4891	1268.3912
1293.8213	1327.6876	1351.1999
1369.9172	1397.7749	1425.8317
1434.3814	1442.0820	1456.4663
1468.9804	1586.3516	1609.7172
1612.3574	2126.0567	2960.4640
3014.8127	3037.5939	3058.8806
3117.9504	3153.4676	3155.7566
3172.0785	3197.1533	3218.6736

[i5] → **[P1]** $C_{13}H_{11}$, C_1, ^2A

6	0	-0.935347	-0.472794	0.008611
6	0	-1.685509	0.699979	-0.018330
6	0	-1.065217	1.957974	-0.054203
6	0	0.312547	2.028530	-0.058312
6	0	1.109540	0.857891	-0.031405
6	0	0.485653	-0.431156	-0.001753
6	0	-1.859707	-1.610251	0.041566
6	0	-3.128201	-1.162103	0.036110
6	0	-3.151307	0.344732	-0.002699
6	0	2.539016	0.926755	-0.020114
6	0	1.303767	-1.591066	-0.004095
6	0	2.677199	-1.492006	-0.056023
6	0	3.300481	-0.231769	-0.086590
1	0	-1.659288	2.865650	-0.076053
1	0	0.808393	2.993136	-0.075588
1	0	-1.562141	-2.650159	0.068020
1	0	-4.020614	-1.773079	0.057042
1	0	-3.669342	0.768259	0.867319
1	0	-3.677224	0.723072	-0.888666
1	0	3.010526	1.893275	-0.155857
1	0	2.851658	1.353839	1.880958

1	0	0.835702	-2.568323	0.018081
1	0	3.283722	-2.390324	-0.079474
1	0	4.381137	-0.163638	-0.132365

Frequencies

-638.3681	111.7084	128.7348
220.7028	241.5701	260.6962
277.6307	356.6917	393.2974
434.4268	457.8514	465.6427
514.4098	524.2491	565.6011
612.8697	666.2526	681.5059
725.9719	749.6764	751.3412
805.6751	825.5235	840.7263
880.4402	889.6009	933.4111
952.1503	955.3874	964.0990
968.9362	971.7986	999.0330
1045.3904	1069.7533	1126.4368
1142.6721	1161.0960	1177.9509
1190.5181	1217.7385	1233.6712
1277.9198	1293.0191	1350.8478
1370.0866	1387.0355	1427.1455
1431.3550	1462.6158	1479.7315
1546.5258	1583.4545	1607.7160
1622.4911	1650.4731	3014.2766
3037.1585	3158.0279	3163.3691
3170.2041	3175.8388	3181.2758
3190.5777	3196.3336	3218.1406

[i1] → **[i6]** $C_{13}H_{11}$, C_1, ^2A

6	0	-1.764769	-0.649610	0.074878
6	0	-1.787172	0.759443	-0.036527
6	0	-0.608915	1.481249	-0.210839
6	0	0.555124	0.733591	-0.259952
6	0	0.620556	-0.648582	-0.156376
6	0	-0.567281	-1.364985	0.015928
6	0	-3.145996	-1.110546	0.245080
6	0	-3.983391	-0.059413	0.241825
6	0	-3.219965	1.231284	0.065053
6	0	2.034902	-1.191619	-0.228670
6	0	2.912861	0.014837	-0.630442
6	0	4.081168	0.293625	0.138545

6	0	5.051817	0.556033	0.806513
1	0	-0.609095	2.562949	-0.299554
1	0	-0.560617	-2.447965	0.100325
1	0	-3.431113	-2.149308	0.355971
1	0	-5.059278	-0.101951	0.349193
1	0	-3.370728	1.913329	0.911275
1	0	-3.540594	1.775508	-0.832176
1	0	2.350369	-1.582414	0.742842
1	0	2.129414	-2.009424	-0.949576
1	0	3.091911	0.078725	-1.705580
1	0	2.015898	0.908553	-0.453251
1	0	5.910203	0.780154	1.390434

Frequencies

-1641.9172	37.1080	99.1695
123.3936	189.8635	230.2908
265.0044	282.7198	359.1145
392.6566	405.4631	420.4879
438.8542	537.1487	591.9319
597.7084	620.0044	646.8268
666.5604	701.7290	747.4383
748.6446	764.1438	841.8613
852.9783	862.4447	886.8031
922.6386	948.9750	953.1576
957.5425	962.3462	1022.4307
1074.3851	1091.2221	1132.2117
1146.5602	1167.7923	1187.0943
1232.0243	1245.0308	1253.8627
1289.2680	1297.1907	1327.0767
1359.0459	1372.3163	1436.3107
1440.5920	1462.4025	1484.2928
1579.3244	1616.9007	1637.7405
1665.9693	2168.6747	3014.9151
3035.8618	3037.6959	3065.4666
3083.1672	3149.8473	3158.2135
3188.4667	3212.1821	3475.9045

[i6] → **[i7]** $C_{13}H_{11}$, C_1, ^2A

6	0	1.514095	-0.692155	-0.006639
6	0	1.578512	0.713566	-0.066340
6	0	0.415053	1.462997	-0.230257

6	0	-0.768805	0.760069	-0.345418
6	0	-0.891090	-0.623796	-0.287331
6	0	0.292852	-1.358573	-0.112975
6	0	2.876690	-1.201416	0.177391
6	0	3.744502	-0.176213	0.228841
6	0	3.020839	1.141909	0.080551
6	0	-2.228232	-1.322654	-0.443015
6	0	-3.338326	-0.779666	0.500303
6	0	-3.399484	0.673010	0.364024
6	0	-2.878747	1.738212	0.073834
1	0	0.442275	2.548334	-0.268117
1	0	0.251539	-2.443608	-0.067017
1	0	3.129504	-2.251442	0.257596
1	0	4.816106	-0.253863	0.356980
1	0	3.374949	1.706155	-0.791447
1	0	3.172321	1.791414	0.951951
1	0	-2.580344	-1.201486	-1.472963
1	0	-2.107643	-2.395254	-0.267908
1	0	-4.293512	-1.252510	0.251983
1	0	-3.114855	-1.037557	1.541565
1	0	-2.717496	2.778071	-0.090444

Frequencies

-370.4211	58.6623	97.7936
163.0988	196.4580	223.8368
293.7441	337.7523	349.4061
404.8583	411.7495	427.5795
498.3770	519.6255	586.0164
650.5126	655.4083	705.3961
721.6923	737.5220	745.5357
757.3256	849.6264	850.9347
854.4660	881.1555	886.2157
944.2673	946.8017	954.6839
959.5082	995.0562	1025.4245
1089.9494	1137.2587	1145.1529
1172.5261	1185.0150	1209.9712
1233.8840	1254.9061	1272.0687
1322.0755	1326.7896	1348.8996
1372.2422	1424.5750	1436.8734
1463.3758	1476.4795	1483.4579
1567.8202	1610.9074	1637.5400

2065.2732	3014.0397	3024.2521
3025.9979	3036.6838	3058.6611
3073.3324	3141.4262	3143.6684
3187.0481	3211.5512	3435.1164

[i7] → [i8] $C_{13}H_{11}$, C_1, ^2A

6	0	1.467699	-0.724873	0.013931
6	0	1.504350	0.690596	-0.017421
6	0	0.338962	1.416894	-0.082956
6	0	-0.914252	0.747208	-0.119007
6	0	-0.939041	-0.681494	-0.109649
6	0	0.245587	-1.402156	-0.037866
6	0	2.837774	-1.215468	0.089976
6	0	3.695243	-0.175482	0.104882
6	0	2.948417	1.135076	0.038182
6	0	-2.274780	-1.381668	-0.275083
6	0	-3.412263	-0.536921	0.256455
6	0	-3.405789	0.871717	0.203756
6	0	-2.148908	1.463385	-0.159813
1	0	0.350927	2.502614	-0.095977
1	0	0.219274	-2.487813	-0.036080
1	0	3.110902	-2.262612	0.127181
1	0	4.773896	-0.242433	0.156284
1	0	3.234833	1.722706	-0.842983
1	0	3.154620	1.766678	0.911217
1	0	-2.456261	-1.559025	-1.347435
1	0	-2.259951	-2.368039	0.197654
1	0	-4.317385	-1.054876	0.570585
1	0	-3.346527	0.219188	1.327076
1	0	-2.122326	2.522710	-0.399848

Frequencies

-1486.0331	79.6620	125.0895
152.6728	254.8706	260.8908
309.0523	390.7747	406.0754
419.9931	431.5895	478.4532
536.9844	566.1964	631.0846
703.7422	714.4554	723.4795
740.0566	755.0323	777.3139
790.9513	838.2072	862.2334
886.4839	893.5882	935.3381

952.4739	954.7196	960.2392
963.9352	1042.1518	1091.3783
1117.4094	1149.4421	1165.0706
1182.1277	1223.9093	1231.5165
1236.2206	1254.4142	1271.7909
1298.8792	1318.4409	1347.2174
1354.6686	1389.6225	1435.0051
1439.0749	1454.6281	1463.2424
1492.7071	1552.8453	1606.4407
1628.2968	2122.1677	2959.5309
3016.0159	3038.6245	3053.5199
3111.9196	3138.2947	3152.9454
3156.5882	3190.3441	3213.9244

[i8] → [P2] $C_{13}H_{11}$, C_1, ^2A

6	0	1.468605	0.727764	-0.031980
6	0	1.493551	-0.700491	0.016830
6	0	0.330917	-1.418806	0.039745
6	0	-0.921017	-0.740248	0.013507
6	0	-0.944290	0.691736	-0.028803
6	0	0.274285	1.411934	-0.052512
6	0	2.853567	1.198674	-0.048135
6	0	3.694665	0.150804	-0.011748
6	0	2.936254	-1.155439	0.033522
6	0	-2.212306	1.354964	-0.032287
6	0	-2.151442	-1.446108	0.008930
6	0	-3.390628	0.623504	-0.100282
6	0	-3.357146	-0.781185	-0.057065
1	0	0.338154	-2.504159	0.074617
1	0	0.249857	2.496575	-0.079291
1	0	3.140971	2.241934	-0.083278
1	0	4.775450	0.206365	-0.012763
1	0	3.176502	-1.735315	0.933382
1	0	3.178238	-1.797808	-0.822354
1	0	-2.321931	1.892227	1.866414
1	0	-2.232596	2.428904	-0.177762
1	0	-2.128367	-2.530540	0.041468
1	0	-4.341433	1.140585	-0.157070
1	0	-4.284946	-1.341385	-0.081696

Frequencies

-627.4394	100.7808	131.0957
234.6061	261.0698	273.5486
284.1626	355.4229	403.4864
407.7691	419.4678	428.1362
513.3206	559.8521	576.1645
626.5006	686.0140	732.2410
743.6832	751.6836	760.4405
792.0909	804.8092	858.0692
870.4064	890.1291	902.3627
914.3136	955.8485	957.9191
968.2727	972.8020	997.4677
1044.8681	1074.7111	1119.2089
1154.7801	1163.4725	1173.0817
1179.1870	1242.9325	1250.0622
1267.0137	1280.1541	1346.8745
1373.4261	1376.4289	1429.2370
1444.8037	1471.7435	1476.4855
1532.7180	1597.5965	1621.0673
1633.4966	1673.3742	3013.9616
3035.7807	3153.7969	3158.6335
3162.2506	3167.2946	3176.6528
3189.3852	3190.1128	3212.5394

[i0b] → **[i2]** $C_{13}H_{11}$, C_1, ^2A

6	0	-1.359446	-0.600415	-0.064351
6	0	-2.303288	0.443957	0.044322
6	0	-1.899826	1.770202	0.084064
6	0	-0.527021	2.068224	0.013203
6	0	0.354875	1.013906	-0.095380
6	0	0.011189	-0.318971	-0.135650
6	0	-2.085480	-1.873874	-0.080096
6	0	-3.406553	-1.643566	0.013212
6	0	-3.686526	-0.162278	0.101565
6	0	2.832144	1.507995	-0.271753
6	0	3.465357	0.533497	0.078402
6	0	4.111904	-0.635052	0.544172
6	0	4.525880	-1.643513	-0.238200
1	0	-2.624699	2.574379	0.170201
1	0	-0.189011	3.098850	0.047493
1	0	0.755077	-1.104428	-0.216537
1	0	-1.611988	-2.844623	-0.156034

1	0	-4.184224	-2.395986	0.025698
1	0	-4.214613	0.096246	1.028087
1	0	-4.324016	0.180085	-0.723393
1	0	2.514314	2.456888	-0.629300
1	0	4.277517	-0.689472	1.617755
1	0	4.383432	-1.623675	-1.312055
1	0	5.018953	-2.508929	0.187011

Frequencies

-190.8335	5.3959	28.7760
39.6296	69.3194	103.7902
192.9840	225.9433	229.6048
334.7460	391.4330	393.1097
421.0761	519.0059	551.5487
559.8212	583.2630	658.3132
669.7645	697.4687	700.3741
739.1137	740.5447	783.0903
821.4257	864.4816	871.1003
898.5864	925.3887	937.7404
954.8031	955.7543	963.2090
1002.5038	1036.9013	1086.1928
1111.8592	1127.5547	1148.2636
1169.3740	1206.6557	1239.0846
1287.8493	1315.4003	1325.1144
1374.7508	1419.2408	1438.8378
1440.8139	1461.8532	1565.3108
1622.1436	1633.1857	1640.8633
2121.7774	3013.9677	3036.4350
3132.5889	3146.0660	3146.3877
3162.0270	3164.6801	3189.2702
3212.1837	3236.8509	3459.2868

[i2] → **[P5]** $C_{13}H_{11}$, C_1, ^2A

6	0	1.677947	-0.657222	-0.027726
6	0	2.194552	0.651939	0.056560
6	0	1.341732	1.745362	0.029479
6	0	-0.031430	1.533619	-0.082835
6	0	-0.558571	0.231632	-0.161778
6	0	0.309362	-0.875130	-0.137437
6	0	2.802785	-1.595939	0.023072
6	0	3.956016	-0.914515	0.132493

6	0	3.698196	0.573214	0.165049
6	0	-1.973182	0.017716	-0.248942
6	0	-3.127944	-0.341177	-0.084829
6	0	-4.485451	-0.717395	0.001483
6	0	-5.473280	0.081205	0.435455
1	0	1.727870	2.757416	0.091323
1	0	-0.711702	2.375436	-0.114240
1	0	-0.098269	-1.876945	-0.202162
1	0	2.701146	-2.672811	-0.022312
1	0	4.946593	-1.345797	0.190642
1	0	4.199848	1.092888	-0.661093
1	0	4.070583	1.032496	1.089522
1	0	-2.322759	1.143620	-1.887654
1	0	-4.720689	-1.731525	-0.313883
1	0	-5.280578	1.097298	0.757847
1	0	-6.496435	-0.271920	0.471745

Frequencies

-607.9652	32.8488	51.5546
83.8286	109.0690	166.3211
196.0397	203.8607	286.9496
329.3804	391.3791	395.2754
406.1319	442.4512	491.7515
503.8083	563.3899	608.3488
628.9138	688.4372	700.2949
714.8900	747.7058	759.4217
832.7415	850.7859	889.8314
904.6011	936.5387	939.7764
955.6944	963.9269	970.0030
988.7578	1000.1553	1087.4808
1101.3764	1143.2807	1148.1227
1177.7283	1210.5434	1245.2036
1284.0755	1307.0361	1316.2202
1340.7236	1367.6190	1435.4342
1442.8143	1458.7687	1496.9076
1596.1920	1623.2266	1641.4159
1651.7229	2223.1136	3014.5180
3036.9335	3129.5829	3147.1712
3164.0776	3184.0143	3191.8229
3194.3548	3214.7395	3237.9366

Optimized Cartesian Coordinates (Å) and Calculated Vibrational Frequencies (cm^{-1}) for the 6-Indenyl + Vinylacetylene System

Reactants

Vinylacetylene C_4H_4, C_s, $^1A'$

6	0	0.735441	0.110182	0.00000
6	0	1.906556	-0.171715	0.00000
6	0	-0.635858	0.488606	0.00000
6	0	-1.659532	-0.371423	0.00000
1	0	2.936402	-0.432190	0.00000
1	0	-0.832528	1.558030	0.00000
1	0	-1.500612	-1.443195	0.00000
1	0	-2.682903	-0.016548	0.00000

Frequencies

224.3116	316.4854	557.7241
647.7553	680.3933	703.5142
892.2781	954.7667	1010.0968
1111.4928	1320.9953	1443.5247
1668.6181	2205.5842	3136.2470
3147.5999	3236.4714	3476.1732

6-indenyl C_9H_7**,** C_s, $^2A'$

6	0	-2.128299	0.813777	0.0000
6	0	-2.288651	-0.552933	0.0000
6	0	-1.125228	-1.337803	0.0000
6	0	0.116811	-0.702180	0.0000
6	0	0.214843	0.706135	0.0000
6	0	-0.932098	1.499536	0.0000
6	0	1.477466	-1.249417	0.0000
6	0	2.373217	-0.247733	0.0000
6	0	1.676289	1.092217	0.0000
1	0	-3.269711	-1.014887	0.0000
1	0	-1.198460	-2.420689	0.0000
1	0	-0.881655	2.583568	0.0000
1	0	1.707588	-2.307447	0.0000
1	0	3.449841	-0.355555	0.0000
1	0	1.942889	1.690960	0.880331
1	0	1.943405	1.694453	-0.876938

Frequencies

203.9833	207.9492	390.3342
399.5867	416.9998	533.6907
533.9369	602.1477	696.7671
737.6841	738.2471	804.6383
831.2133	849.7065	861.1688
941.2000	947.5813	955.4983
963.0625	1040.9162	1086.2879
1126.9877	1146.6321	1164.3760
1211.2079	1239.6846	1283.5058
1323.0788	1377.0933	1415.6713
1435.8132	1459.8382	1572.5637
1607.7744	1638.4690	3017.0930
3040.3913	3157.9721	3160.4538
3175.1085	3190.5542	3214.0340

Intermediates

[i'0a] $C_{13}H_{11}$, C_1, ^2A

6	0	2.744945	1.626041	-0.622564
6	0	3.232709	1.267410	0.613511
6	0	2.728734	0.089942	1.187473
6	0	1.773391	-0.646654	0.486497
6	0	1.313441	-0.226226	-0.780414
6	0	1.804385	0.941779	-1.363680
6	0	1.076564	-1.890666	0.829480
6	0	0.232043	-2.228886	-0.160282
6	0	0.289992	-1.218916	-1.281400
1	0	3.976458	1.862678	1.131464
1	0	3.081102	-0.235381	2.161111
1	0	1.465313	1.284903	-2.335657
1	0	1.232380	-2.442365	1.748105
1	0	-0.411669	-3.098249	-0.179531
1	0	0.592332	-1.678666	-2.230560
1	0	-0.685327	-0.749301	-1.458471
6	0	-4.260561	0.401183	0.111168
6	0	-5.158042	-0.399914	0.046951
6	0	-3.227887	1.378843	0.163494
6	0	-2.019672	1.178022	0.701076
1	0	-5.943641	-1.113219	-0.001585

1	0	-3.469009	2.345826	-0.271551
1	0	-1.743423	0.228020	1.142936
1	0	-1.274766	1.964000	0.705878

Frequencies

5.2705	8.8041	12.6339
14.8985	35.1801	58.4345
203.8553	213.2776	225.5546
320.4522	390.3562	400.7407
417.8551	533.9341	534.5839
558.5229	602.7212	645.5557
678.6387	698.0419	705.5244
737.8413	738.0640	804.0267
831.2553	849.6365	861.3244
890.9760	940.1905	948.3580
956.0632	963.8471	967.2626
1011.0912	1039.7825	1085.8749
1110.2121	1126.5417	1150.9256
1164.6425	1210.4702	1240.6720
1284.1193	1320.6098	1323.0283
1377.0490	1415.3917	1435.5743
1445.3289	1458.9868	1571.7576
1606.3040	1637.2110	1666.5173
2204.4138	3019.5875	3044.4094
3135.9639	3149.3887	3157.9740
3161.2903	3175.4084	3190.8802
3214.5692	3239.2806	3477.0804

[i'0b] $C_{13}H_{11}$, C_1, ^2A

6	0	0.480082	1.174534	-1.006946
6	0	0.945590	2.061147	-0.062555
6	0	2.059456	1.666345	0.694582
6	0	2.630693	0.416664	0.452890
6	0	2.106325	-0.446602	-0.533489
6	0	1.000597	-0.070100	-1.294874
6	0	2.929827	-1.713424	-0.559235
6	0	3.778139	-0.251858	1.074360
6	0	3.962001	-1.459060	0.513429
1	0	0.479132	3.026677	0.097837

1	0	2.464098	2.328795	1.452916
1	0	0.580686	-0.715192	-2.059615
1	0	3.391554	-1.884564	-1.539657
1	0	2.324022	-2.602032	-0.342385
1	0	4.377018	0.178363	1.867133
1	0	4.733650	-2.171489	0.773373
6	0	-4.301008	0.076774	-0.134725
6	0	-3.128791	0.338025	-0.233197
6	0	-5.693033	-0.205055	-0.056273
6	0	-6.260173	-0.981924	0.872644
1	0	-2.091074	0.563197	-0.313018
1	0	-6.314534	0.258289	-0.819004
1	0	-5.673323	-1.459696	1.648118
1	0	-7.329458	-1.155141	0.874636

Frequencies

4.7957	10.3917	23.4269
26.8851	38.7854	45.7249
204.9249	209.9256	227.8717
319.4738	390.8357	399.9875
417.4479	532.4227	533.9520
557.4302	602.7955	685.7646
697.0593	707.7880	711.2152
737.1602	737.8890	805.1172
831.0875	850.3346	861.4806
892.8139	941.4296	948.1416
950.8394	955.4319	964.3578
1010.9656	1040.4816	1087.6101
1112.1895	1127.8530	1147.9292
1164.7131	1211.4775	1240.2545
1284.3417	1321.6397	1323.6159
1377.8444	1415.8392	1436.0538
1443.7181	1459.7364	1571.7985
1607.7415	1637.8788	1668.5122
2201.2739	3018.3592	3041.8088
3134.0508	3146.6616	3160.0672
3163.5759	3176.8744	3192.3610
3215.6521	3235.4416	3440.0874

[i'1] $C_{13}H_{11}$, C_1, ^2A

6	0	-0.638895	0.793055	0.329057
6	0	0.159078	1.907800	0.051368
6	0	1.531535	1.786684	-0.172985
6	0	2.110861	0.522116	-0.117005
6	0	1.314622	-0.608545	0.161403
6	0	-0.045440	-0.479299	0.379477
6	0	3.493671	0.073585	-0.299016
6	0	3.562486	-1.260065	-0.143958
6	0	2.199364	-1.833845	0.163172
1	0	-0.301616	2.889894	0.014452
1	0	2.130437	2.666159	-0.384262
1	0	-0.660741	-1.349421	0.588545
1	0	4.324206	0.730878	-0.524336
1	0	4.456491	-1.864593	-0.222286
1	0	1.887221	-2.570176	-0.588064
1	0	2.183635	-2.353117	1.129677
6	0	-3.938089	-0.601289	-0.336426
6	0	-4.809479	-1.435514	-0.141030
6	0	-2.957242	0.334894	-0.543104
6	0	-2.134164	0.942773	0.562788
1	0	-5.570077	-2.158258	0.023321
1	0	-2.751176	0.656834	-1.559609
1	0	-2.416410	0.486271	1.515537
1	0	-2.371815	2.011423	0.644577

Frequencies

23.6445	23.8233	94.5785
168.3237	203.5572	213.9530
276.2101	316.5430	388.6711
418.5183	424.2851	433.5893
438.2408	482.4253	544.0570
597.8043	603.4986	641.5882
645.6714	708.5937	748.4552
759.8523	782.7126	840.6684
861.2846	878.5015	895.0264
935.3559	952.2138	954.4476
958.4002	965.3205	1024.5447
1090.2584	1134.9266	1143.9661
1148.2151	1149.4065	1187.8073
1217.5877	1241.4358	1251.3015

1292.6574	1313.4736	1341.5832
1390.5438	1400.8730	1437.3998
1459.3096	1475.1130	1501.9624
1596.5743	1635.0247	1655.6407
2013.3248	2999.5471	3015.9488
3038.5915	3064.8789	3151.1323
3154.1947	3155.5427	3173.2923
3189.6919	3213.3833	3468.1783

[i'2] $C_{13}H_{11}$, C_1, ^2A

6	0	-0.589723	-0.414471	-0.102889
6	0	-0.454919	0.983694	-0.162366
6	0	0.793392	1.592725	-0.123566
6	0	1.934917	0.794590	-0.023301
6	0	1.811908	-0.606951	0.037806
6	0	0.566043	-1.208797	-0.000896
6	0	-1.910233	-1.074338	-0.145881
6	0	-3.079634	-0.498238	-0.251908
6	0	-4.297447	0.068779	-0.372655
6	0	-5.115066	0.477825	0.679419
6	0	3.193776	-1.209348	0.142146
6	0	3.357638	1.133029	0.037730
6	0	4.088255	0.007665	0.131634
1	0	-1.349414	1.591978	-0.238697
1	0	0.873888	2.673580	-0.170158
1	0	0.468558	-2.289589	0.045396
1	0	-1.882723	-2.165330	-0.080966
1	0	-4.667609	0.218270	-1.387832
1	0	-4.804841	0.357340	1.709425
1	0	-6.080002	0.926396	0.483829
1	0	3.319560	-1.799472	1.058670
1	0	5.167087	-0.048127	0.192447
1	0	3.747077	2.143081	0.009854
1	0	3.414969	-1.885112	-0.693611

Frequencies

31.9882	54.6577	117.2573
154.0167	210.8505	226.6823
230.7652	319.3666	353.9436

405.7995	428.2069	436.6876
521.0910	551.0885	577.0795
589.1075	642.3180	705.8815
746.1904	754.8140	757.7987
761.8484	814.0805	850.6277
862.0220	896.0742	900.9807
938.8955	952.5244	953.8104
960.2115	966.2129	970.5335
1080.5592	1094.3078	1136.8253
1148.1659	1163.3470	1191.0530
1216.0221	1242.9464	1249.8832
1292.1893	1312.9005	1341.5538
1388.4105	1405.0701	1436.4361
1468.7124	1490.4305	1504.5509
1588.6987	1631.8635	1650.1515
1886.0799	3015.7372	3038.6180
3055.3633	3093.4399	3149.6803
3151.5406	3162.2827	3179.1096
3190.2459	3214.0194	3250.3651

[i'3] $C_{13}H_{11}$, C_1, ^2A

6	0	-0.615405	0.427330	0.390174
6	0	-0.004591	1.665464	0.115389
6	0	1.365584	1.772737	-0.129996
6	0	2.157621	0.626583	-0.107124
6	0	1.574265	-0.639494	0.164105
6	0	0.230824	-0.669198	0.394043
6	0	-2.101782	0.307552	0.638726
6	0	-2.849535	-0.324399	-0.562548
6	0	-4.286118	-0.446892	-0.334583
6	0	-5.465858	-0.534877	-0.122651
6	0	2.655463	-1.693456	0.129566
6	0	3.592654	0.419244	-0.317986
6	0	3.890888	-0.884981	-0.188188
1	0	-0.623019	2.558304	0.102798
1	0	1.804637	2.743293	-0.333259
1	0	-2.523949	1.294705	0.841724
1	0	-2.284484	-0.307178	1.524218
1	0	-2.424787	-1.312748	-0.767993

1	0	-2.671488	0.280526	-1.458278
1	0	-6.509517	-0.617695	0.056439
1	0	2.743476	-2.221217	1.086817
1	0	4.294008	1.212690	-0.544275
1	0	4.873746	-1.325249	-0.291592
1	0	2.457311	-2.459108	-0.630169

Frequencies

31.9384	60.1176	60.9704
150.3215	190.8421	207.9293
271.2505	315.6089	352.9353
409.3885	428.5989	441.1015
467.7241	546.5038	596.6534
615.9279	664.2990	674.9666
698.7931	739.8925	749.9524
770.1786	781.7585	829.5392
864.1248	936.1354	936.2343
942.3440	955.4232	960.5673
972.0895	1010.6958	1025.9925
1080.4498	1135.8307	1145.2354
1157.8669	1180.9622	1231.9352
1246.1061	1270.0616	1291.8041
1300.7239	1325.1323	1367.6936
1381.5240	1431.9733	1442.7619
1453.8008	1477.3817	1498.3153
1559.0903	1621.5515	1646.9214
2220.4737	3023.0232	3024.1811
3046.8028	3046.9628	3052.9629
3090.9981	3149.4133	3175.7474
3190.3127	3214.5109	3477.8598

[i'4] $C_{13}H_{11}$, C_1, ^2A

6	0	-1.105284	0.826312	0.103122
6	0	-0.366487	2.004448	0.012188
6	0	1.028870	1.992792	-0.060194
6	0	1.685086	0.766371	-0.036668
6	0	0.951896	-0.434941	0.050664
6	0	-0.437632	-0.423841	0.118043
6	0	1.921656	-1.594876	0.037054

6	0	3.109313	0.428357	-0.100122
6	0	3.262415	-0.906059	-0.057938
6	0	-2.612415	0.852463	0.274413
6	0	-3.320892	-0.353332	-0.395587
6	0	-2.543131	-1.572760	-0.080261
6	0	-1.248794	-1.662650	0.167089
1	0	-0.892073	2.954341	0.002165
1	0	1.582328	2.922455	-0.134245
1	0	1.749737	-2.268238	-0.812522
1	0	1.846650	-2.214025	0.940479
1	0	3.906169	1.158257	-0.170114
1	0	4.202420	-1.441208	-0.085645
1	0	-3.027351	1.788024	-0.110807
1	0	-2.840175	0.821658	1.348297
1	0	-3.367513	-0.225167	-1.485651
1	0	-4.353775	-0.419874	-0.041280
1	0	-0.754018	-2.609927	0.358505

Frequencies

98.8177	128.7097	190.5629
228.7212	233.2451	306.7168
367.6071	411.5570	424.2886
465.9665	486.1856	516.8100
560.4868	619.3816	630.6970
711.7920	715.6887	744.1591
770.0540	826.9381	833.7547
838.0439	863.8812	902.2676
943.4000	945.5059	954.4662
962.2105	972.3019	974.9567
1019.7509	1039.4270	1114.2120
1147.0753	1159.8280	1175.7902
1197.7037	1215.5080	1241.9594
1246.7396	1258.2967	1290.5740
1320.3742	1327.6739	1364.2490
1396.2555	1436.6032	1450.9033
1466.0018	1475.7394	1482.6522
1600.0623	1633.7190	1637.1772
1685.2989	2993.4583	3002.3948
3009.8781	3031.6508	3056.2825
3064.2787	3151.5606	3153.2098
3175.7776	3189.6038	3213.6517

[i'5] $C_{13}H_{11}$, C_s, $^2A''$

6	0	-1.082887	0.886308	0.000097
6	0	-0.299492	2.040466	-0.000059
6	0	1.094027	1.988497	-0.000146
6	0	1.713264	0.736865	-0.000077
6	0	0.945043	-0.435712	0.000051
6	0	-0.460343	-0.395133	0.000113
6	0	1.877074	-1.624496	-0.000051
6	0	3.130285	0.360469	-0.000025
6	0	3.242014	-0.978607	0.000115
6	0	-2.594920	1.002139	0.000222
1	0	-0.793733	3.007714	-0.000087
1	0	1.678427	2.901986	-0.000285
1	0	1.731525	-2.267502	0.877847
1	0	3.949753	1.068350	-0.000009
1	0	4.165453	-1.542576	0.000413
1	0	-2.915612	1.600324	-0.867813
1	0	-2.915609	1.599603	0.868769
6	0	-3.326804	-0.303940	-0.000135
6	0	-2.669768	-1.504206	-0.000188
6	0	-1.266611	-1.581590	0.000093
1	0	-4.410951	-0.272645	-0.000250
1	0	-0.781413	-2.549819	0.000100
1	0	-3.244786	-2.424905	-0.000340
1	0	1.731645	-2.266890	-0.878407

Frequencies

82.9856	108.4550	178.8092
233.4622	239.3658	293.3270
419.0093	421.0676	452.8672
463.3513	496.9249	519.2376
603.3887	613.7911	660.3440
662.0740	704.9687	728.8582
737.4980	780.6106	824.3068
833.3454	861.7936	927.0441
937.4934	941.1819	953.4729
955.6621	960.7784	964.7030
976.6067	1028.6003	1098.3921

1124.8098	1145.2385	1167.1394
1176.7355	1199.7010	1221.9212
1246.9332	1252.5082	1270.2439
1301.0872	1346.9644	1381.4239
1398.4420	1431.7417	1437.0816
1442.2514	1446.9794	1494.0362
1557.2710	1592.6302	1618.2668
1633.2851	2951.2607	2951.6549
3008.6595	3030.0161	3148.0728
3152.0162	3172.3823	3174.8543
3189.4499	3190.2378	3213.3358

[i'6] $C_{13}H_{11}$, C_1, ^2A

6	0	0.617913	0.200906	0.450625
6	0	-0.299833	-0.866500	0.354095
6	0	-1.640138	-0.610328	0.105265
6	0	-2.115019	0.707876	-0.055848
6	0	-1.229196	1.791959	0.032537
6	0	0.081490	1.462419	0.277738
6	0	2.091091	-0.033103	0.695663
6	0	2.922379	0.040692	-0.610519
6	0	-3.558814	0.652346	-0.298263
6	0	-2.807741	-1.559786	-0.034503
6	0	-3.968368	-0.628167	-0.290123
1	0	0.057085	-1.885049	0.485106
1	0	-1.563728	2.817420	-0.083205
1	0	2.239071	-1.013629	1.155420
1	0	2.476193	0.711384	1.396705
1	0	2.538783	-0.695084	-1.325745
1	0	-4.185050	1.520932	-0.457613
1	0	-2.962223	-2.161735	0.869800
1	0	-4.982805	-0.972537	-0.442222
6	0	4.346603	-0.191308	-0.389601
6	0	5.513925	-0.386718	-0.180785
1	0	6.547687	-0.556490	-0.005627
1	0	2.777427	1.023467	-1.071509
1	0	-2.668195	-2.270402	-0.858800

Frequencies

25.8431	57.3841	61.2326
150.4037	193.6023	221.0979
264.8165	310.7814	351.9270
405.7647	420.1755	426.8974
458.5394	541.3332	604.9030
632.1354	664.0326	674.8147
700.5551	736.1332	745.7583
769.1288	774.9769	856.1377
863.5578	878.8840	914.5507
948.7008	956.2888	962.3493
967.4658	1010.8347	1017.1614
1087.5626	1137.1018	1148.3659
1163.3402	1187.1676	1238.0468
1251.3096	1271.9201	1287.9306
1298.1511	1325.6616	1365.8980
1377.1622	1418.0305	1436.6072
1462.4677	1475.9026	1496.2747
1558.8046	1620.6860	1637.1746
2220.4503	3016.2355	3024.2577
3039.1109	3047.9661	3053.1029
3091.9113	3141.1791	3164.8304
3192.4204	3215.0765	3477.5654

[i'7] $C_{13}H_{11}$, C_1, ^2A

6	0	-0.324347	1.452644	-0.059578
6	0	2.278400	-1.330190	-0.290050
6	0	-0.251294	-1.358528	-0.065929
6	0	-1.466325	-0.689906	-0.005539
6	0	-1.505571	0.716234	-0.006791
6	0	0.901756	0.780699	-0.113598
6	0	2.184269	1.522661	-0.125391
6	0	3.299427	0.860106	0.120893
6	0	3.445346	-0.585219	0.407887
6	0	0.941008	-0.633429	-0.123782
6	0	-2.880814	-1.215180	0.065399
6	0	-2.908913	1.134676	0.058801
6	0	-3.703659	0.051224	0.099442
1	0	-0.343339	2.537963	-0.050478
1	0	2.507952	-1.383374	-1.362757

1	0	2.223626	-2.360133	0.073725
1	0	-0.217430	-2.444482	-0.074358
1	0	2.160235	2.596784	-0.287215
1	0	4.401181	-0.982718	0.054197
1	0	3.418473	-0.744104	1.494683
1	0	-3.048976	-1.832398	0.957021
1	0	-3.238627	2.166045	0.072021
1	0	-4.784471	0.055667	0.150003
1	0	-3.134324	-1.843990	-0.797429

Frequencies

92.0760	124.7938	185.4197
255.5855	260.2380	307.5575
374.9967	397.1141	411.6938
422.1987	444.8280	522.6197
559.9496	638.6087	702.9477
719.7022	732.2053	754.3984
764.2783	779.5866	827.2894
864.3767	888.2202	892.8556
901.4110	929.7722	950.3812
955.3634	961.1661	974.2373
1021.0479	1065.6523	1112.8233
1146.5939	1172.0623	1178.7444
1196.6383	1212.2832	1236.4590
1244.3973	1275.1210	1297.0727
1320.2537	1328.4259	1361.1778
1376.1516	1436.7478	1453.8789
1467.7899	1477.0521	1499.9975
1578.1871	1625.3395	1650.3908
1688.1367	2992.2147	3001.2099
3014.4879	3036.6303	3055.9846
3063.3621	3142.8713	3147.9092
3159.9683	3189.3827	3213.5981

[i'8] $C_{13}H_{11}$, C_s, $^2A''$

6	0	0.311771	1.436537	0.000032
6	0	-2.222472	-1.452586	0.000091
6	0	0.297226	-1.374786	0.000061
6	0	1.496646	-0.681711	0.000159

6	0	1.503174	0.731145	0.000127
6	0	-0.918988	0.740838	0.000027
6	0	-2.166527	1.449208	-0.000045
6	0	-3.392867	0.764534	-0.000116
6	0	-3.455434	-0.602561	-0.000071
6	0	-0.916824	-0.681417	0.000053
6	0	2.924304	-1.174419	-0.000139
6	0	2.899469	1.177861	0.000080
6	0	3.717954	0.111866	-0.000153
1	0	0.305668	2.522023	-0.000014
1	0	-2.245192	-2.130912	0.868530
1	0	-2.245109	-2.131161	-0.868152
1	0	0.288880	-2.461783	0.000035
1	0	-2.149113	2.532982	-0.000078
1	0	-4.313885	1.339026	-0.000208
1	0	-4.414914	-1.108170	-0.000116
1	0	3.150385	-1.792416	-0.878675
1	0	3.150936	-1.792860	0.877913
1	0	4.799669	0.140480	-0.000119
1	0	3.208075	2.215751	0.000243

Frequencies

72.2141	116.5805	165.3467
254.3218	259.6955	310.1044
400.6193	405.7825	419.8417
425.5202	492.3428	559.5826
585.4616	635.3246	661.3105
709.3075	723.3503	746.6234
749.2109	776.8984	784.8426
859.9822	882.2178	890.5191
899.0744	938.0228	950.3026
955.7335	955.7675	963.1191
964.5835	1046.5286	1103.5171
1127.9455	1147.8607	1169.3633
1180.2847	1200.9499	1222.6510
1242.0134	1256.7794	1269.3929
1312.4356	1346.6626	1357.8798
1390.6820	1437.0080	1438.9281
1445.9265	1460.3952	1499.6899
1555.2448	1581.1370	1622.4995

1646.3857	2945.9360	2947.5565
3010.6828	3031.8721	3142.1595
3151.5327	3159.7944	3170.7215
3182.0276	3189.4014	3213.1242

Products

1*H*-cyclopenta-[*b*]naphthalene [P2] $C_{13}H_{10}$, C_s, $^1A'$

6	0	-3.4297275383	0.6926828295	0.0039083678
6	0	0.2561865651	-1.4034018581	-0.0085023831
6	0	-3.4192071452	-0.7206557811	-6.487593E-4
6	0	1.4301622887	-0.6884204437	-0.0080385742
6	0	0.2375332283	1.4304945887	5.892895E-4
6	0	1.4176697405	0.7420283073	-0.0034772169
6	0	-2.2463676634	1.3923572342	0.0043120379
6	0	-2.2271153712	-1.4039826096	-0.0046946993
6	0	-0.9977522925	0.720531113	2.165193E-4
6	0	-0.9860464949	-0.7144502301	-0.0044032352
6	0	2.8281081359	-1.1220833093	-0.0116269207
6	0	2.8483269174	1.2348432817	-0.004056437
6	0	3.6409965108	-0.0519460444	-0.0095010525
1	0	-4.3754448604	1.222915632	0.0070883174
1	0	0.2599391198	-2.4888289276	-0.0119952953
1	0	-4.3573702871	-1.2643043552	-9.374379E-4
1	0	0.217623734	2.5163608324	0.0041197655
1	0	-2.2529829395	2.477688416	0.0078122976
1	0	-2.2185160279	-2.4892073171	-0.0081914894
1	0	3.1434835396	-2.157922306	-0.0153885217
1	0	3.0748527551	1.8496933954	0.8759822814
1	0	3.072160391	1.8553276045	-0.8808330576
1	0	4.7229266941	-0.0789710526	-0.0107867963

Frequencies

102.2294	134.8645	251.8437
263.5800	278.6570	394.6986
405.8898	417.1671	426.3605
487.3719	559.6989	578.1974
628.8197	686.4746	732.6775
738.6653	751.4693	764.7804
783.4099	806.1723	857.4753
858.7720	890.3014	902.4118

913.7707	955.6878	957.5792
963.1137	970.5211	991.6628
1043.4534	1077.4282	1121.2771
1155.6730	1169.2853	1174.4788
1180.6497	1244.5385	1251.5039
1268.6960	1282.1901	1347.9739
1373.3697	1387.7710	1434.9787
1446.5223	1470.3410	1486.9167
1537.3526	1611.9868	1627.0456
1655.0763	1677.6805	3013.8854
3035.4208	3153.1920	3155.6051
3159.0651	3162.4123	3173.3962
3186.6618	3189.2638	3212.1926

1*H*-cyclopenta[*a*]naphthalene [P3] $C_{13}H_{10}$, C_s, $^1A'$

6	0	3.3589805782	-0.1589532841	-0.0052741521
6	0	-0.8626124942	-0.4592216299	0.0061451685
6	0	2.7512244302	-1.4362419127	-0.0057558711
6	0	-1.6304316353	0.7002778521	0.0104255245
6	0	0.3504445096	2.0582620245	0.0073112859
6	0	-1.0208972146	1.9753841923	0.0110703316
6	0	2.58240266	0.9743296087	-0.0010636067
6	0	1.3828455855	-1.5556845697	-0.0020600345
6	0	1.1658232353	0.8928735063	0.0028576508
6	0	0.5497812064	-0.4047593755	0.0022898527
6	0	-3.0471181043	0.3231433831	0.013518318
6	0	-1.786615793	-1.65287093	0.0068930735
6	0	-3.1559300206	-1.0165005908	0.0115352725
1	0	4.4401442599	-0.0787740034	-0.00823888
1	0	3.372925776	-2.3247255603	-0.0090822067
1	0	0.8378607683	3.0277237362	0.0077226495
1	0	-1.6280620211	2.8741736402	0.0144845493
1	0	3.0467756867	1.9552584003	-6.703734E-4
1	0	0.9246806356	-2.5385591873	-0.0024656456
1	0	-3.8673579721	1.0301984874	0.0178637838
1	0	-1.6405804813	-2.2929696258	-0.8725833972
1	0	-1.6357579267	-2.2952054346	0.8839587431
1	0	-4.0761106684	-1.5851637269	0.0138329637

Frequencies

111.6057	140.7443	235.7064
237.2840	257.3698	398.3460
432.9203	435.8184	465.2515
517.6631	520.4055	551.8391
616.8391	670.8841	681.8888
717.6433	751.4780	760.5919
787.6060	828.8756	839.7089
870.5955	872.9566	937.1401
954.7419	955.4339	959.8592
969.6851	982.2343	991.7663
1043.6091	1060.8926	1117.9424
1144.2864	1166.9366	1179.2631
1185.6203	1233.5150	1244.7639
1263.9305	1288.3090	1363.9889
1378.3244	1398.4726	1416.6215
1434.3888	1470.0882	1487.4172
1552.8699	1587.7715	1621.6410
1637.3459	1664.1362	3014.2828
3037.1636	3156.0941	3158.7295
3163.7980	3176.1937	3177.0078
3187.4191	3190.5460	3215.9190

***(E)*-6-(but-1-en-3-yn-1-yl)-1*H*-indene [P6]** $C_{13}H_{10}$, C_s, $^1A'$

6	0	0.658422	0.002137	-0.000145
6	0	-0.333062	-1.001011	-0.000143
6	0	-1.671187	-0.654180	-0.000142
6	0	-2.061256	0.699443	-0.000058
6	0	-1.092378	1.705594	-0.000073
6	0	0.250089	1.351307	-0.000143
6	0	2.059853	-0.409915	-0.000089
6	0	3.149735	0.385262	0.000017
6	0	4.478748	-0.104334	0.000114
6	0	5.622901	-0.486474	0.000202
6	0	-2.913241	-1.514276	-0.000025
6	0	-3.522593	0.756479	0.000219
6	0	-4.024269	-0.491967	0.000230
1	0	-0.030281	-2.043898	-0.000161
1	0	-1.378963	2.751727	-0.000027
1	0	0.996816	2.136433	-0.000181

1	0	2.226999	-1.483733	-0.000084
1	0	3.044791	1.466577	0.000039
1	0	6.626958	-0.832507	0.000178
1	0	-2.962498	-2.169866	-0.878511
1	0	-5.073510	-0.755979	0.000486
1	0	-4.098727	1.673175	0.000358
1	0	-2.962149	-2.170312	0.878117

Frequencies

42.9157	81.1724	90.2873
164.2416	209.8993	219.8334
298.4934	310.0383	394.9551
409.1366	428.1513	468.5369
508.4610	571.6992	601.4583
614.5102	640.2369	679.4867
706.5788	755.5357	762.8297
800.5242	835.2791	859.1374
866.5909	897.7669	942.0719
951.5885	955.8052	958.4509
966.9996	991.1371	1038.9222
1087.9708	1136.8482	1148.3601
1171.7773	1223.1273	1248.5745
1253.0242	1296.5698	1319.7943
1331.0501	1349.6969	1394.3906
1434.8369	1461.0457	1502.5962
1585.2607	1629.4557	1645.8185
1667.2320	2192.8918	3016.8829
3039.8340	3142.1278	3150.1471
3155.8150	3165.8536	3186.5309
3191.6192	3214.8150	3477.4300

6-(but-3-ene-1-yn-1-yl)-1*H*-indene [**P7**] $C_{13}H_{10}$, C_s, $^1A'$

6	0	0.000000	0.596652	0.000000
6	0	-1.403233	0.458704	0.000000
6	0	-2.003296	-0.794917	0.000000
6	0	-1.194987	-1.932143	0.000000
6	0	0.210395	-1.804947	0.000000
6	0	0.809532	-0.560823	0.000000
6	0	-1.525249	-3.356975	0.000000

6	0	-0.393951	-4.084901	0.000000
6	0	0.820091	-3.187491	0.000000
6	0	0.594552	1.887587	0.000000
6	0	1.093335	2.992125	0.000000
6	0	1.716364	4.264321	0.000000
6	0	1.069568	5.437977	0.000000
1	0	-2.012758	1.354195	0.000000
1	0	-3.084455	-0.880668	0.000000
1	0	1.888285	-0.452540	0.000000
1	0	-2.534048	-3.750159	0.000000
1	0	-0.333014	-5.165156	0.000000
1	0	1.454615	-3.359469	0.878356
1	0	1.454615	-3.359469	-0.878356
1	0	2.804309	4.259342	0.000000
1	0	1.616405	6.372836	0.000000
1	0	-0.012673	5.490068	0.000000

Frequencies

49.4975	61.8250	99.5978
166.9944	179.4692	210.0654
265.5520	339.4232	382.5588
384.4054	413.2267	450.3929
504.8386	549.3600	601.3854
609.9153	666.9862	688.8452
734.2738	755.7113	765.9189
844.7839	850.7163	885.5887
910.3171	955.6141	958.1626
971.7304	974.9741	990.9467
1004.3592	1014.1815	1082.8126
1106.8265	1151.4599	1160.9645
1175.0731	1254.4709	1258.8153
1305.8460	1308.0270	1321.0875
1354.1131	1400.9547	1417.5866
1440.9764	1480.3506	1494.9988
1529.5659	1543.8819	1589.7353
1656.5463	2203.1157	3028.2172
3053.4078	3154.9652	3159.7361
3195.6641	3199.6786	3210.9945
3213.9335	3230.7234	3256.3990

Transition states

[i'0a] → [i'1] $C_{13}H_{11}$, C_1, ^2A

6	0	0.406341	1.019195	-0.020563
6	0	-0.456152	2.089097	-0.125601
6	0	-1.832856	1.818014	-0.143156
6	0	-2.259093	0.492997	-0.053191
6	0	-1.329257	-0.563798	0.054075
6	0	0.040491	-0.308296	0.073048
6	0	-2.086074	-1.869930	0.133793
6	0	-3.605883	-0.086464	-0.046042
6	0	-3.527338	-1.423922	0.059296
1	0	-0.096695	3.110389	-0.195005
1	0	-2.547796	2.630664	-0.225168
1	0	0.775565	-1.102683	0.153826
1	0	-1.873220	-2.412988	1.063119
1	0	-1.824156	-2.548237	-0.687832
1	0	-4.518183	0.492660	-0.116202
1	0	-4.362864	-2.110797	0.089118
6	0	2.995815	1.386340	-0.100857
6	0	3.559567	0.371230	0.584905
6	0	3.929718	-0.871260	0.012075
6	0	4.254174	-1.940356	-0.443456
1	0	2.782223	2.327664	0.387904
1	0	2.857549	1.336403	-1.172951
1	0	3.728126	0.475393	1.653518
1	0	4.542729	-2.875549	-0.856289

Frequencies

-113.3941	18.4857	27.5133
40.3811	82.1787	170.5188
208.3829	213.6230	228.6298
360.2825	392.8758	401.5502
419.1716	528.7428	538.8661
558.6717	596.4474	627.2607
676.7173	697.9841	716.5019
738.3783	739.1932	805.4931
816.8815	859.2324	865.8132
894.5821	919.7666	937.1123
949.6328	955.1935	962.7010
983.0918	1038.9387	1086.5286

1112.3847	1128.7959	1147.1311
1163.7998	1212.7900	1240.5866
1286.1258	1305.7734	1323.4779
1379.3522	1416.7530	1435.6563
1435.8432	1462.6200	1572.0874
1607.1395	1609.6393	1638.7644
2183.5377	3017.2211	3040.1994
3141.5758	3153.4599	3157.0484
3161.1594	3169.2609	3189.6384
3213.3975	3249.8688	3476.1110

[i'1] → [P6] $C_{13}H_{11}$, C_1, ^2A

6	0	0.630327	0.006657	0.088311
6	0	-0.357166	-0.997610	0.049038
6	0	-1.694077	-0.650586	-0.006263
6	0	-2.084393	0.703159	-0.015663
6	0	-1.117594	1.709238	0.034456
6	0	0.224502	1.354294	0.087696
6	0	2.038555	-0.402613	0.125053
6	0	3.120020	0.392649	-0.103709
6	0	4.447378	-0.084608	-0.140595
6	0	5.593204	-0.462435	-0.178999
6	0	-2.934426	-1.511101	-0.060781
6	0	-3.544784	0.759510	-0.075011
6	0	-4.045078	-0.489103	-0.102092
1	0	-0.054313	-2.040322	0.060517
1	0	-1.404250	2.755283	0.037923
1	0	0.970538	2.138173	0.142845
1	0	2.212739	-1.472504	0.186381
1	0	2.991793	1.460044	-0.257026
1	0	6.598650	-0.803297	-0.210455
1	0	2.206555	-0.590582	2.201397
1	0	-2.947367	-2.163923	-0.942532
1	0	-5.093240	-0.753672	-0.146477
1	0	-4.120934	1.675976	-0.093807
1	0	-3.018986	-2.169875	0.812582

Frequencies

-550.8601	44.7638	76.7265

88.3748	154.3240	209.4789
218.4651	246.7741	300.1233
326.2414	350.6162	395.0462
414.8763	427.8223	464.8793
509.2824	571.5536	602.8318
614.7294	639.9177	678.3105
707.1886	755.7185	763.8421
799.2602	835.0222	847.3893
866.2537	893.4282	941.0866
951.6845	956.7442	958.4368
967.4268	989.0394	1043.1460
1088.2101	1136.3718	1148.4223
1170.2539	1220.5100	1245.7586
1251.7061	1293.4800	1309.7227
1320.4497	1343.9226	1393.9498
1434.8190	1458.5413	1501.1457
1584.3468	1611.8045	1630.8272
1651.1334	2180.1707	3017.2296
3040.2281	3147.3651	3154.1508
3160.4300	3166.3092	3185.6363
3191.9592	3215.1432	3476.2192

[i'1] → **[i'3]** $C_{13}H_{11}$, C_1, ^2A

6	0	0.617962	1.086964	0.085449
6	0	-0.319592	2.102321	-0.127175
6	0	-1.677078	1.790198	-0.233984
6	0	-2.091788	0.461194	-0.127309
6	0	-1.151990	-0.577908	0.090861
6	0	0.170024	-0.225525	0.186256
6	0	2.123797	1.218604	0.207476
6	0	2.619194	-0.176987	0.649011
6	0	3.694456	-0.778401	-0.068155
6	0	4.580515	-1.309000	-0.693383
1	0	0.004424	3.135631	-0.207546
1	0	2.418006	1.989319	0.926494
1	0	2.569986	1.489985	-0.753599
1	0	2.728201	-0.274009	1.731075
1	0	5.366502	-1.769621	-1.239402
6	0	-1.887614	-1.894209	0.163315
6	0	-3.422747	-0.148896	-0.198176

6	0	-3.326397	-1.479759	-0.035706
1	0	-1.549845	-2.594507	-0.610340
1	0	-4.338225	0.406997	-0.359000
1	0	-4.148881	-2.182625	-0.042313
1	0	1.514847	-0.793382	0.435508
1	0	-2.403714	2.578852	-0.397120
1	0	-1.733746	-2.398214	1.125365

Frequencies

-1655.8707	43.5849	92.3763
127.0059	191.8201	221.8022
244.8249	268.6024	376.8399
412.9522	417.8839	448.6821
477.6263	523.1360	552.1824
579.4151	606.5165	619.6509
666.2445	698.7910	740.9696
753.0693	797.5705	823.8335
849.5110	878.4443	926.3330
936.5521	947.8141	952.7900
961.3806	979.6255	1022.2011
1071.5288	1080.8521	1132.6694
1145.1457	1162.3032	1186.0599
1222.6447	1233.4991	1257.5861
1286.9638	1296.2665	1328.1858
1359.4360	1386.8449	1432.7136
1446.5877	1453.8015	1484.5675
1579.1141	1623.1824	1642.8757
1658.2534	2167.3807	3020.7595
3035.5741	3044.1915	3064.8050
3083.3695	3151.6279	3173.4396
3188.9584	3214.2651	3474.9971

[i'3] → [i'4] $C_{13}H_{11}$, C_1, ^2A

6	0	-1.025413	0.852585	0.240589
6	0	-0.266797	2.011048	0.003195
6	0	1.119690	1.963485	-0.155694
6	0	1.768299	0.733536	-0.081382
6	0	1.024974	-0.451838	0.150222
6	0	-0.330573	-0.353195	0.312223

6	0	1.978462	-1.625175	0.167990
6	0	3.179282	0.361818	-0.211921
6	0	3.317113	-0.968213	-0.073416
6	0	-2.525567	0.930062	0.443928
6	0	-3.333030	-0.052345	-0.451502
6	0	-2.772502	-1.392089	-0.299804
6	0	-1.843352	-2.132237	-0.015749
1	0	-0.776745	2.968647	-0.052840
1	0	1.677533	2.875276	-0.339329
1	0	1.738684	-2.360533	-0.610435
1	0	1.951897	-2.162298	1.124164
1	0	3.980449	1.067572	-0.394276
1	0	4.246646	-1.519829	-0.123855
1	0	-2.873642	1.949224	0.255309
1	0	-2.762286	0.696176	1.487603
1	0	-3.271694	0.250576	-1.502695
1	0	-4.390305	-0.020150	-0.170616
1	0	-1.264053	-3.009327	0.154908

Frequencies

-373.7169	67.7407	87.6671
154.1190	194.0981	213.3771
292.3277	333.4670	356.6857
417.0651	441.7102	456.2145
466.9709	540.7529	590.2310
622.1669	654.0723	700.0999
705.1641	732.4491	749.9930
764.7393	827.6891	840.9211
868.3238	888.9210	937.8949
940.1318	952.3074	959.5071
978.8036	990.6930	1022.8894
1075.1608	1132.1344	1142.8863
1157.0764	1186.4386	1211.6879
1235.5455	1239.3208	1272.0639
1312.0145	1325.8333	1366.5078
1384.9988	1431.1158	1439.4519
1450.1166	1474.9854	1483.2586
1564.1641	1621.2159	1640.0736
2060.6455	3015.0372	3023.1789
3026.4607	3038.9392	3059.5241
3074.5486	3144.4834	3173.4392

3186.7479	3212.1283	3436.5647

[i'4] → [i'5] $C_{13}H_{11}$, C_1, ^2A

6	0	-1.098967	0.852862	0.102409
6	0	-0.347331	2.020315	0.000228
6	0	1.048312	1.989629	-0.072644
6	0	1.690183	0.753356	-0.039360
6	0	0.943925	-0.435594	0.051944
6	0	-0.452033	-0.415838	0.122794
6	0	1.895913	-1.607333	0.039637
6	0	3.110942	0.398280	-0.101641
6	0	3.246266	-0.938120	-0.057199
6	0	-2.613207	0.905424	0.275546
6	0	-3.243995	-0.316917	-0.364097
6	0	-2.542192	-1.540345	-0.313141
6	0	-1.281570	-1.611268	0.225851
1	0	-0.859320	2.977628	-0.013162
1	0	1.613131	2.911807	-0.153495
1	0	1.811639	-2.224605	0.943778
1	0	1.708610	-2.279640	-0.807339
1	0	3.916930	1.117846	-0.174090
1	0	4.179127	-1.485669	-0.084550
1	0	-3.025262	1.821693	-0.155776
1	0	-2.853123	0.937136	1.348366
1	0	-4.067448	-0.202934	-1.065467
1	0	-3.691495	-1.370558	0.309788
1	0	-0.870262	-2.529408	0.629981

Frequencies

-1702.0983	102.1524	114.6402
189.2373	233.2466	245.3597
297.9707	404.5305	422.7118
449.2976	465.5399	477.5297
534.4221	598.6358	618.4442
639.8195	685.3965	713.0623
733.7070	743.8985	785.3794
818.6939	830.9579	840.7420
912.9372	931.3530	940.3265
946.1616	953.9384	961.3533
987.2645	1027.9886	1083.7413

1115.9028	1143.7859	1159.6523
1184.3475	1200.6438	1218.6546
1240.7777	1245.7015	1265.3637
1287.2341	1315.0646	1346.3750
1374.9890	1397.5565	1430.0217
1437.9586	1448.1227	1461.0650
1491.3126	1593.6316	1620.3219
1633.5640	2086.2271	2977.3810
3010.2040	3032.5131	3062.1033
3128.6210	3152.4791	3165.0551
3176.1361	3189.4268	3213.4805

[i'5] → [P3] $C_{13}H_{11}$, C_1, ^2A

6	0	-1.108136	0.863708	-0.032745
6	0	-0.323453	2.043966	-0.058341
6	0	1.051515	1.992333	-0.053534
6	0	1.688986	0.733356	-0.018241
6	0	0.946190	-0.443031	0.006933
6	0	-0.466228	-0.418204	-0.003164
6	0	1.896012	-1.615880	0.040033
6	0	3.113512	0.387086	-0.001936
6	0	3.250721	-0.949416	0.031917
6	0	-2.537559	0.914776	-0.020457
1	0	-0.831911	3.002222	-0.075332
1	0	1.637232	2.904890	-0.074129
1	0	1.756640	-2.239570	0.932275
1	0	3.918238	1.111393	-0.014922
1	0	4.182925	-1.497686	0.051515
1	0	-3.021132	1.875378	-0.156652
1	0	-2.855940	1.334971	1.877631
6	0	-3.285494	-0.253078	-0.085654
6	0	-2.645950	-1.506126	-0.054974
6	0	-1.272415	-1.589590	-0.004438
1	0	-4.366871	-0.198399	-0.130114
1	0	-0.790481	-2.560608	0.018444
1	0	-3.242225	-2.411444	-0.077290
1	0	1.767322	-2.280555	-0.823823

Frequencies

-649.8645	109.0848	136.2622
226.7618	236.0127	252.1176
276.0125	352.0434	408.5551
434.3317	450.0075	465.9904
518.3310	537.6427	551.7296
616.6457	667.7983	681.4303
717.0251	749.0600	764.9057
795.8234	832.6098	839.5166
869.0842	883.0763	938.0351
955.7167	955.9607	964.9243
973.6390	981.1450	998.9466
1045.3275	1057.6205	1116.7689
1144.4799	1160.5928	1178.5283
1184.2764	1229.6508	1245.0675
1263.1922	1282.9418	1362.0693
1370.8056	1396.0496	1413.1785
1433.7977	1463.4314	1481.1701
1543.8592	1584.0924	1609.9530
1626.5058	1652.1148	3014.2360
3037.1605	3160.2662	3162.8406
3169.3373	3178.4429	3180.1201
3190.9237	3192.3202	3217.1715

[i'1] → **[i'6]** $C_{13}H_{11}$, C_1, ^2A

6	0	0.615207	-0.631116	-0.161097
6	0	-0.583236	-1.336860	0.009724
6	0	-1.768505	-0.616654	0.070487
6	0	-1.781923	0.792915	-0.036868
6	0	-0.591000	1.510180	-0.209544
6	0	0.561613	0.751736	-0.260407
6	0	2.023357	-1.188302	-0.236209
6	0	2.913465	0.011714	-0.631061
6	0	4.082140	0.276540	0.142024
6	0	5.053246	0.527422	0.813794
6	0	-3.190712	-1.096673	0.246416
6	0	-3.172267	1.245951	0.064150
6	0	-3.984941	0.187391	0.224741
1	0	-0.582576	-2.420681	0.090450
1	0	-0.585383	2.591749	-0.293812

1	0	2.110357	-2.002524	-0.962422
1	0	2.336202	-1.588790	0.732441
1	0	3.095403	0.078748	-1.705487
1	0	5.911959	0.741571	1.400984
1	0	-3.327959	-1.643747	1.187713
1	0	-3.479842	2.282998	0.014429
1	0	-5.061664	0.220955	0.326557
1	0	2.023493	0.913648	-0.452225
1	0	-3.498657	-1.779392	-0.555524

Frequencies

-1648.8339	37.1813	99.5563
120.4714	192.8081	242.3887
261.1453	269.8259	357.6819
405.1807	406.7156	416.8302
437.7187	537.5411	590.6784
595.2044	619.0683	650.5508
666.3570	700.5708	741.8589
748.2476	763.1976	840.7919
861.2056	869.9739	880.9881
916.2022	950.7165	953.2179
959.0968	961.9232	1022.2984
1074.4359	1085.5542	1129.1109
1150.1364	1177.9794	1186.9236
1234.4315	1242.5718	1264.3713
1279.9205	1299.2946	1324.9840
1360.5340	1376.1166	1434.6317
1438.3183	1464.4948	1484.3004
1573.6403	1625.2815	1633.0300
1666.1448	2168.7638	3015.5854
3034.1725	3038.1856	3063.8142
3083.9765	3144.9524	3164.7618
3189.7879	3213.3134	3475.0806

[i'6] → [i'7] $C_{13}H_{11}$, C_1, ^2A

6	0	0.882775	-0.611385	-0.286359
6	0	-0.314563	-1.331619	-0.114147
6	0	-1.522006	-0.656073	-0.008759

6	0	-1.572641	0.750346	-0.066247
6	0	-0.393859	1.491420	-0.227504
6	0	0.777213	0.774001	-0.340091
6	0	2.209504	-1.327681	-0.445691
6	0	3.329254	-0.802183	0.496532
6	0	3.409517	0.649866	0.363318
6	0	2.900545	1.721836	0.076764
6	0	-2.926896	-1.181240	0.178637
6	0	-2.970780	1.166446	0.076307
6	0	-3.753680	0.082411	0.216000
1	0	-0.282655	-2.417615	-0.070838
1	0	-0.411942	2.576606	-0.262238
1	0	2.562490	-1.208900	-1.475830
1	0	2.075255	-2.399201	-0.273225
1	0	3.104445	-1.059306	1.537689
1	0	4.277335	-1.287435	0.244833
1	0	2.751637	2.764121	-0.084054
1	0	-3.235466	-1.844087	-0.639708
1	0	-4.828714	0.084827	0.339389
1	0	-3.305546	2.196266	0.067812
1	0	-3.033138	-1.762143	1.103611

Frequencies

-371.1766	58.7457	95.2251
161.4240	199.4533	230.9795
285.8891	331.5506	344.9162
411.6843	419.7120	425.4316
496.9919	520.6460	588.1381
645.5849	654.9161	702.5513
719.6811	734.7236	748.2708
756.3946	846.6244	863.3109
865.0956	872.4077	880.9606
942.9689	949.4356	955.2494
960.0361	994.5564	1024.4209
1086.1181	1133.9804	1147.6143
1178.9876	1184.9164	1211.2631
1241.5694	1250.0753	1275.5114
1309.2303	1325.8932	1358.7606
1374.2458	1418.5436	1438.1731
1464.6137	1476.0175	1482.5991
1560.5585	1622.7017	1630.7185

2064.4971	3014.1004	3023.2278
3026.1145	3036.3787	3059.1801
3072.7530	3137.2304	3149.1335
3188.7764	3212.6303	3434.3959

[i'7] → [i'8] $C_{13}H_{11}$, C_1, ^2A

6	0	0.311260	1.446584	0.062741
6	0	-2.263707	-1.380652	0.290440
6	0	0.266822	-1.368928	0.058743
6	0	1.473723	-0.685349	-0.001306
6	0	1.496638	0.724263	0.008201
6	0	-0.917709	0.764568	0.118871
6	0	-2.196676	1.461516	0.184739
6	0	-3.288784	0.828010	-0.357712
6	0	-3.368901	-0.581613	-0.373886
6	0	-0.931674	-0.657294	0.125719
6	0	2.893494	-1.194202	-0.076901
6	0	2.896068	1.156762	-0.054800
6	0	3.701989	0.082171	-0.102920
1	0	0.317599	2.531880	0.055297
1	0	-2.475713	-1.505469	1.362533
1	0	-2.214343	-2.389848	-0.128012
1	0	0.246998	-2.455297	0.065621
1	0	-2.236571	2.479331	0.557794
1	0	-4.048016	-1.068690	-1.070170
1	0	-4.246243	0.173313	0.272252
1	0	3.067284	-1.803904	-0.972914
1	0	3.155894	-1.826240	0.781214
1	0	4.782702	0.098405	-0.153699
1	0	3.215157	2.191512	-0.061483

Frequencies

-1698.5896	87.4406	124.5489
180.0663	257.6109	264.0195
315.3241	389.8565	405.3956
420.9263	432.8105	474.2866
539.3852	581.3885	639.7339
695.7748	716.0506	726.1078
746.9276	753.5358	764.9202

794.6612	819.2762	863.3797
886.2314	897.3286	923.5662
950.2851	953.5942	962.2635
983.7204	1049.2621	1093.9787
1114.3151	1147.0502	1171.4577
1183.2557	1205.3236	1212.4667
1241.7652	1256.1860	1263.3152
1297.2202	1311.5154	1341.8216
1356.7053	1393.2140	1437.1287
1439.5055	1456.3033	1462.3975
1499.6460	1572.9985	1622.3062
1643.0072	2086.7235	2975.2679
3011.6965	3033.1724	3058.8066
3126.5124	3146.8734	3159.2539
3163.3609	3189.5857	3213.5459

[i'8] → [P2] $C_{13}H_{11}$, C_1, ^2A

6	0	0.306443	-1.447926	0.038574
6	0	-2.189494	1.363598	-0.029912
6	0	0.298743	1.383293	-0.051854
6	0	1.477741	0.689375	-0.032034
6	0	1.484610	-0.738771	0.016763
6	0	-0.931161	-0.752378	0.012451
6	0	-2.175382	-1.438557	0.008344
6	0	-3.368997	-0.753684	-0.056331
6	0	-3.380829	0.651541	-0.098810
6	0	-0.934298	0.679357	-0.029098
6	0	2.909397	1.176694	-0.047917
6	0	2.880673	-1.178386	0.034894
6	0	3.697434	-0.111871	-0.000432
1	0	0.304139	-2.532695	0.072808
1	0	-2.191834	2.437422	-0.178423
1	0	-2.290047	1.901264	1.856005
1	0	0.283795	2.468731	-0.077864
1	0	-2.169830	-2.523139	0.040272
1	0	-4.305860	-1.298773	-0.080866
1	0	-4.323117	1.183893	-0.155058
1	0	3.135542	1.825931	0.807069
1	0	3.137134	1.760619	-0.948552

1	0	3.191588	-2.214453	0.072225
1	0	4.779215	-0.142502	0.004550

Frequencies

-645.0918	101.2422	130.2764
245.6886	254.3178	260.9959
299.4987	354.7090	405.6628
406.9748	422.3041	426.1855
514.8715	561.6630	576.5665
626.5405	685.1844	732.1514
737.3089	752.2663	769.2219
789.0469	805.1457	857.4916
871.7685	889.7710	903.5553
914.3863	955.6264	957.3250
968.9253	974.2894	998.3680
1044.6468	1074.4091	1118.8989
1155.3329	1163.4957	1174.1717
1178.6142	1241.9891	1250.3140
1267.3796	1279.2591	1347.7605
1371.2412	1378.2204	1428.5712
1444.0594	1471.3515	1477.4004
1531.9252	1601.6605	1616.0670
1635.5296	1673.3176	3014.5358
3036.4261	3156.7875	3159.3180
3163.2972	3168.0065	3177.4607
3190.5855	3192.3979	3214.4504

[i'0b] → [i'2] $C_{13}H_{11}$, C_1, ^2A

6	0	0.400138	0.673747	-0.443520
6	0	-0.162512	1.799852	0.119935
6	0	-1.512743	1.743678	0.495318
6	0	-2.220037	0.559256	0.288357
6	0	-1.595374	-0.568008	-0.287218
6	0	-0.254428	-0.523165	-0.663119
6	0	-2.605978	-1.688872	-0.379347
6	0	-3.613793	0.206720	0.576159
6	0	-3.850651	-1.063057	0.205029
1	0	0.414825	2.705315	0.273608
1	0	-1.992758	2.609364	0.941081

1	0	0.246581	-1.379902	-1.102588
1	0	-2.290185	-2.575453	0.184730
1	0	-2.761675	-2.019458	-1.413981
1	0	-4.332808	0.882109	1.022943
1	0	-4.791093	-1.589814	0.299385
6	0	3.515031	0.344272	-0.362586
6	0	2.784601	0.837461	-1.198468
6	0	4.287520	-0.211396	0.683131
6	0	4.649735	-1.500375	0.764635
1	0	2.373108	1.303814	-2.060300
1	0	4.599477	0.481204	1.461401
1	0	4.359654	-2.220193	0.008721
1	0	5.245824	-1.857666	1.595162

Frequencies

-203.5712	7.3180	22.5071
42.5542	70.9564	94.0173
207.6720	212.0170	230.2228
327.0747	390.7843	401.9622
416.3824	514.9294	542.3213
560.6472	581.6200	655.2967
670.0161	695.6261	698.8091
739.5462	740.2313	810.0079
825.4836	858.4625	860.0148
898.2581	936.6737	940.5438
948.5848	954.4234	962.3420
1001.2358	1036.8395	1086.2055
1111.4508	1128.5597	1146.2689
1162.6472	1212.0909	1240.3110
1284.9521	1315.3752	1323.1054
1379.5263	1414.9446	1436.2530
1440.9206	1461.8999	1573.2990
1607.9560	1638.0638	1642.0100
2114.6607	3016.0327	3038.8642
3134.7230	3147.9290	3153.4457
3157.1970	3169.8613	3188.6101
3212.7845	3238.0522	3458.1101

[i'2] → [P7] $C_{13}H_{11}$, C_1, ^2A

6	0	0.550161	0.289052	0.152209
6	0	0.001253	1.581664	0.047246
6	0	-1.371703	1.772490	-0.064810
6	0	-2.210453	0.658196	-0.070332
6	0	-1.667999	-0.640016	0.038288
6	0	-0.305264	-0.831844	0.152346
6	0	1.969962	0.130976	0.239251
6	0	3.178543	0.171262	0.070421
6	0	4.586512	0.178545	-0.019651
6	0	5.334072	-0.871190	-0.396168
6	0	-2.799910	-1.640110	0.008724
6	0	-3.665124	0.539047	-0.170694
6	0	-4.017633	-0.758344	-0.127661
1	0	0.670573	2.433266	0.053039
1	0	-1.776486	2.775364	-0.145541
1	0	0.120675	-1.824112	0.245528
1	0	5.076504	1.113755	0.242380
1	0	4.884996	-1.819759	-0.664626
1	0	6.413672	-0.796641	-0.438032
1	0	2.029886	-1.002366	1.905683
1	0	-5.026745	-1.145064	-0.180901
1	0	-4.341517	1.379214	-0.264513
1	0	-2.836687	-2.248921	0.920724
1	0	-2.709366	-2.343096	-0.828753

Frequencies

-605.8972	35.6488	51.7989
81.5356	111.3311	166.0192
206.2708	212.0337	273.7931
323.1901	377.5899	392.0719
423.4483	442.3074	493.2497
518.4797	578.9379	602.5160
611.0373	688.3089	695.7077
708.8680	756.8853	764.6486
844.0301	858.4447	882.4161
895.1164	934.8838	953.5361
955.9479	960.7000	969.2156
985.9091	999.2884	1085.1686
1101.8650	1145.1500	1149.2547
1167.7527	1224.6463	1250.7957
1285.2932	1312.6973	1315.3150

1316.2182	1386.0351	1434.7910
1443.8598	1458.8433	1500.3501
1581.4227	1627.8658	1640.1227
1652.5376	2218.0056	3017.8049
3040.9107	3130.2133	3147.8757
3169.3382	3180.7336	3191.9565
3192.7422	3215.5611	3238.6665

References

1. R. B. Miller and J. M. Frincke, *J. Org. Chem.*, 1980, **45**, 5312-5315.
2. A. Hasan Howlader, K. Diaz, A. M. Mebel, R. I. Kaiser and S. F. Wnuk, *Tetrahedron Lett.*, 2020, DOI: https://doi.org/10.1016/j.tetlet.2020.152427, 152427.